Docket No.: 20523 US (C038435/0120240)

IN THE UNITED STATES PATENT AND TRADEMARK OFFICE

In re Application of:)

Chyi-Cheng CHEN and Bruno LEUENBERGER) Examiner: L. Channavajjala

Serial No.: 09/726,880) Art Unit: 1615

Filed: November 30, 2000)

For: **A VITAMIN POWDER COMPOSITION AND METHOD OF MAKING**)

DECLARATION OF MR. HERMANN STEIN UNDER 37 C.F.R. §1.132

Commissioner for Patents
P.O. Box 1450
Alexandria, VA 22313-1450

Sir:

I, Hermann Stein, a citizen and resident of Switzerland, hereby declare as follows:

1. From April 1958 until September 1961 I studied chemical laboratory assistant at Farbwerke Hoechst AG, Frankfurt/Main Hoechst, Germany. From April 1963 until March 1966 I studied chemical engineering at Paul-Ehrlich-Schule, Frankfurt/Main, Germany.

2. Employment history:

- April 1958 - March 1963 chemical laboratory assistant at Farbwerke Hoechst AG
- April 1963 – March 1968 chemical laboratory assistant and chemical engineer at Battelle-Institut e.V., Frankfurt/Main, Germany. Development of new high temperature polymers and new resins for cosmetic applications.

- April 1968 – November 1982 at F. Hoffmann La Roche AG, Basle Switzerland, development of new cosmetic products, starting as head of development laboratory and finally chief of cosmetic development department.

- December 1982 – January 1984 at Vick International Paris, development of new cosmetic products and know how transfer cosmetic department Hoffmann La Roche to Vick International.

- February 1984 – January 2002 at F. Hoffmann La Roche AG, Basle, Switzerland and later on Roche Vitamins AG, Basle Switzerland: Development of new vitamin product formulations, improvement of existing vitamin product formulations and development of new production processes for vitamin product formulations. Position: Head of development laboratory and mini plant, process engineer for pilot plant production trials.

- Since March 2002, I have been a technical consultant for Roche Vitamins AG and DSM.

3. The present application discloses and claims powder compositions containing at least one fat-soluble vitamin dispersed in a matrix consisting of an emulsion-forming composition selected from the group consisting of a natural polysaccharide gum, a mixture of polysaccharide gums, a protein, a mixture of proteins, and mixtures thereof, wherein the fat-soluble vitamin is present in the powder composition in the form of solid droplets having an average diameter of about 80 to about 120 nanometers (nm).

4. I am aware that a Final Office Action issued in the above-identified application on February 23, 2004. I understand that claims 1 and 3-15 were rejected under 35 USC § 103 over Stein *et al.*, EP 0 937 412 ("Stein") or Stein in view of Ford *et al.*, 5,607,707 ("Ford"). (Paper No. 02122004 at 2.) I further understand that claim 17 was rejected under 35 USC § 103 over Stein alone or Tritsch *et al.*, EP 0 841 010 ("Tritsch '010") alone or in combination with Ford in view of Finnan *et al.*, U.S. Patent No. 4,830,859 ("Finnan"). (Paper No. 02122004 at 5.)

5. I am a co-inventor of the subject matter described and claimed in the Stein document relied upon by the Examiner in rejecting the claims of the above-captioned application. Stein is entitled "PREPARATION OF A FINELY DIVIDED PULVEROUS CAROTENOID PREPARATION" and discloses "a continuous process for converting carotenoids, retinoids or natural colourants into finely divided pulverous forms which are particular[ly] required for colouring foodstuff[s] and animal feeds." (Col. 1, paragraph 0001.) In particular, Stein discloses a five step process:

> a) forming a suspension of the active ingredient in a water-immiscible organic solvent optionally containing an antioxidant and/or an oil,
> b) feeding the suspension of step a) to a heat exchanger and heating said suspension to 100-250°C, whereby the residence time in the heat exchanger is less than 5 sec,
> c) rapidly mixing the solution of step b) at a temperature in the range of 20-100°C with an aqueous solution of a swellable colloid optionally containing a stabilizer,
> d) removing the organic solvent and
> e) converting the dispersion of step d) into a pulverous preparation. (Abstract and col. 1-2, paragraph 0008.)

6. During the research that lead to the invention disclosed in Stein, my co-inventors and I, using the knowledge available at the time, attempted to produce the smallest

possible particle size. In particular, Example 5 was included with a view toward optimizing the process by producing the smallest possible particle size. Example 5 is reproduced below:

> Solvent: methylene chloride, direct heat transfer (steam).
>
> 9.25 kg Fish Gelatin, 18.5 kg of sugar and 2.5 kg of Ascorbyl palmitate were dissolved in 30.25 kg of water in Kettle 1. The pH-value of this matrix was adjusted with NaOH (20%) to 7.2 - 7.6.
>
> 6.0 kg of β-Carotene, 0.75 kg of dl-α-tocopherol and 3.0 kg of corn oil were dispersed in 30.0 kg of methylene chloride in Kettle 2.
>
> The β-carotene suspension was fed by pump 6 with a flow rate of 20 kg/h to the heat exchanger 4 where it was mixed with steam to reach an outlet temperature of 145°C. The residence time in the heat exchanger 4 was 1.3 sec. The matrix was pumped by pump 7 with a flow rate of 30.4 kg/h to the Kettle 3 where the solved β-carotene was mixed with the matrix and emulsified in it. The emulsion was cooled down to 35°C in heat exchanger 5.
>
> Methylene chloride was removed from the emulsion by using a vertical evaporator. The resulting emulsion showed a particle size of the inner phase of 196 nm and was spray dried.
>
> The final product has a β-carotene content of 9.9%, E1/1: 1120, λ_{max}: 440-460 nm. The powder was well soluble in water, the solution has a very intensive yellow color. (Col. 6, paragraph 0054-0058.)

Figure I is reproduced for clarity:

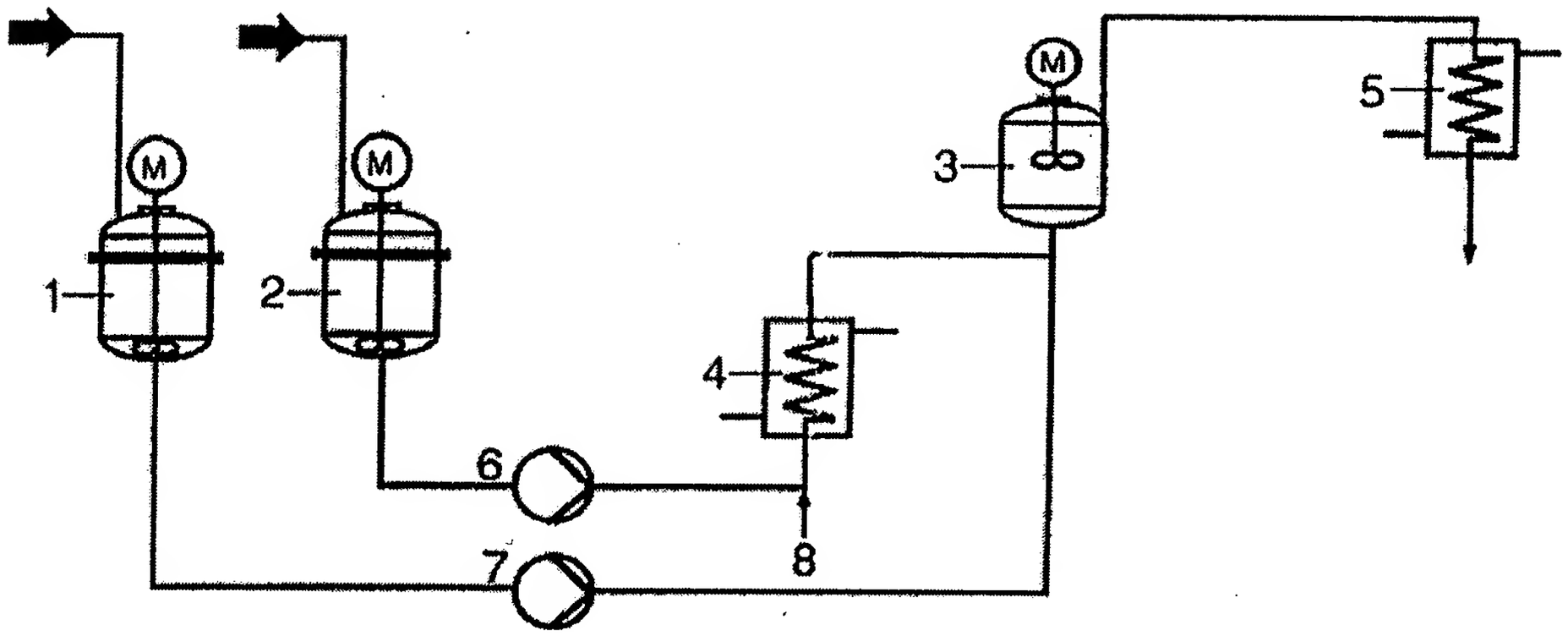

7. As Example 5 shows, at that time, at best we could produce particles sizes of about 196 nm. Based on my unique knowledge of the methods and compositions of Stein, and my long experience in the area of the production carbohydrate matrices, it is my opinion that one of skill in the art at the time of the above-captioned invention familiar with the disclosure of Stein could not have produced particles of the presently claimed size.

8. Moreover, it is also my opinion that one could not have predicted that the process of the present invention would produce significantly smaller particle sizes than the methods of Stein.

I declare further that all statements made herein of my own knowledge are true and that all statements made on information and belief are believed to be true, and further that these statements were made with the knowledge that willful false statements and the like so made are punishable by fine or imprisonment, or both, under Section 1001 of

Title 18 of the United States Code and that such willful false statements may jeopardize the validity of the application or any patent issuing thereon.

Dated: March 16, 2005

Hermann Stein

THE MERCK INDEX

AN ENCYCLOPEDIA OF
CHEMICALS, DRUGS, AND BIOLOGICALS

FOURTEENTH EDITION

Maryadele J. O'Neil, *Editor*
Patricia E. Heckelman, *Senior Associate Editor*
Cherie B. Koch, *Associate Editor*
Kristin J. Roman, *Assistant Editor*

Catherine M. Kenny, *Editorial Assistant*
Maryann R. D'Arecca, *Administrative Associate*

Published by
Merck Research Laboratories
Division of
MERCK & CO., INC.
Whitehouse Station, NJ, USA

2006

thesis: M. Tomita, Y. Sendju, Z. *Physiol. Chem.* 169, 263 (1927); R. Voeffray *et al., Helv. Chim. Acta* 70, 2058 (1987). Enantioselective synthesis from glycerol: M. Marzi *et al., J. Org. Chem.* 65, 6766 (2000). Biosynthesis: G. Wolf, C. R. A. Berger, *Arch. Biochem. Biophys.* 92, 360 (1961). Absolute configuration: T. Kaneko, R. Yoshida, *Bull. Chem. Soc. Jpn.* 35, 1153 (1962). Metabolism in humans: M. E. Mitchell, *Am. J. Clin. Nutr.* 31, 293 (1978). Historical review: G. Fraenkel, S. Friedman, *Vitam. Horm.* XV, 73-118 (1957). Review of physiological significance and deficiency syndromes: C. J. Rebouche, D. J. Paulson, *Annu. Rev. Nutr.* 6, 41-66 (1986); of clinical pharmacology: J. J. Bahl, R. Bressler, *Annu. Rev. Pharmacol. Toxicol.* 27, 257-277 (1987); of biosynthesis in mammals: F. M. Vaz, R. J. A. Wanders, *Biochem. J.* 361, 417-429 (2002). Review of effect on myocardial metabolism and clinical experience in ischemic heart disease: R. Lango *et al., Cardiovasc. Res.* 51, 21-29 (2001); of use as dietary supplement in athletes: H. Karlic, A. Lohninger, *Nutrition* 20, 709-715 (2004). Symposium on physiology, pharmacology and therapeutic potential: *Ann. N.Y. Acad. Sci.* 1033, 1-197 (2004).

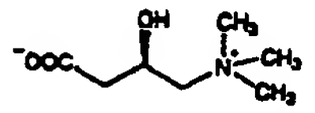

Crystals from anhydrous ethanol + acetone, dec 196-198° (Carter, Bhattacharyya); also reported as crystals from isopropanol, mp 200° (dec) (Marzi). Very hygroscopic solid. $[\alpha]_D^{25}$ −31.3° (c = 10 in water); $[\alpha]_{546}^{25}$ −37.0° (c = 10 in water). Sol in water, hot alcohol. Practically insol in acetone, ether, benzene.

Hydrochloride. [6645-46-1] Levocarnitine chloride; Flatistine. $C_7H_{15}NO_3.HCl$; mol wt 197.66. Crystals, dec 142°.

DL-Form. [406-76-8] γ-Amino-β-hydroxybutyric acid trimethylbetaine; γ-trimethyl-β-hydroxybutyrobetaine. Synthesis: B. Strack *et al., Ber.* 86, 525 (1953); H. E. Carter, P. K. Bhattacharyya, *J. Am. Chem. Soc.* 75, 2503 (1953). Hygroscopic crystalline solid, dec 195-197°. Sol in water, ethanol.

DL-Form hydrochloride. [461-05-2] Needles from ethanol, mp 196° (dec). Very sol in water; sol in hot ethanol; slightly sol in cold ethanol. Practically insol in acetone, ether.

D-Form. [541-14-0] Prepn: S. Friedman *et al., Arch. Biochem. Biophys.* 66, 10 (1957). Crystals, dec 210-212°. $[\alpha]_D$ +30.9°. Very sol in water and alcohol. Practically insol in acetone and ether.

D-Form hydrochloride. [10017-44-4] Crystals, dec 142°.

THERAP CAT: Vitamin (enzyme cofactor).

1850. Carnosine. [305-84-0] β-Alanyl-L-histidine; Ignotine. $C_9H_{14}N_4O_3$; mol wt 226.23. C 47.78%, H 6.24%, N 24.77%, O 21.22%. Naturally occurring dipeptide found in large amounts in skeletal muscle. Also present in other tissues such as brain, cardiac muscle, kidney. Water soluble antioxidant; functions as a free-radical scavenger. Isoln: Gulewitsch, Amiradzibi, *Ber.* 33, 1902 (1900); Wolff, Wilson, *J. Biol. Chem.* 95, 495 (1932); 109, 565 (1935). Synthesis from histidine and β-iodo- or β-nitropropionyl chloride: Baumann, Ingvaldsen, *Ibid.* 35, 271 (1918); Barger, Tutin, *Biochem. J.* 12, 406 (1918). Later syntheses: Sifford, du Vigneaud, *J. Biol. Chem.* 108, 753 (1935); R. A. Turner, *J. Am. Chem. Soc.* 75, 2388 (1953); F. J. Vinick, S. Jung, *J. Org. Chem.* 48, 392 (1983). Crystal structure: H. Itoh *et al., Acta Crystallogr.* 33B, 2959 (1977). Possible role in wound healing: D. E. Fischer *et al., Proc. Soc. Exp. Biol. Med.* 158, 402 (1978). Review of physiological properties and therapeutic potential: S. E. Gariballa, A. J. Sinclair, *Age Ageing* 29, 207-210 (2000).

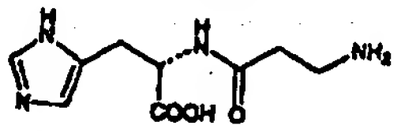

Crystals from aqueous ethanol, mp 262° (dec) (Vinick, Jung); also reported as mp 260° (capillary tube) and as mp 308-309° (Dennis bar) (Sifford, du Vigneaud). $[\alpha]_D^{25}$ +21.0° (c = 1.5 in water). pK_1 2.64; pK_2 6.83; pK_3 9.51. Alkaline reaction. One gram dissolves in 3.1 ml water at 25°.

Nitrate. [5852-98-2] $C_9H_{15}N_5O_6$. Crystals, dec 222°. $[\alpha]_D^{20}$ +24.1° (c = 1.5 in water). Very sol in water.

Hydrochloride. [5852-99-3] $C_9H_{15}ClN_4O_3$. Crystals, dec 245°. Very sol in water.

D-Form. [5853-00-9] Crystals, mp 260°. $[\alpha]_D^{28}$ −20.4° (c = 1.5).

1851. Caro's Acid. [7722-86-3] Peroxymonosulfuric acid; sulfomonoperacid; persulfuric acid. H_2O_5S; mol wt 114.08. H 1.77%, O 70.12%, S 28.11%. Dry reagent is prepd by stirring 10 g potassium persulfate into 11 g concd H_2SO_4 for 10 min and adding 30 g finely powdered potassium sulfate; liquid reagent is obtained by triturating potassium persulfate with three times as much (by weight) of H_2SO_4; dil reagent is prepd by stirring 10 g potassium persulfate into 11 g concd H_2SO_4 and adding 50 cc ice: Baeyer, Villiger, *Ber.* 32, 3625 (1899); another prepn by reacting 90% H_2O_2 with chlorosulfonic acid at −40 to −50°: Ball, Edwards, *J. Am. Chem. Soc.* 78, 1125 (1956).

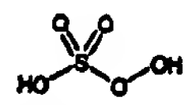

The product is a sirupy liquid consisting of about equal amounts of Caro's acid and H_2SO_4. pK_2 of Caro's acid 9.4 ± 0.1. Oxygen is evolved at room temp; should be stored at dry ice temp.

Caution: Can be dangerously unstable, like most peroxides. Description of explosion at Brown University: J. O. Edwards, *Chem. Eng. News* 33, 3336 (1955). Explosion at Sun Oil, *Ibid.* 38, 59 (Nov. 21, 1960). May be highly irritating to skin, eyes, mucous membranes.

USE: In prepn of dyes; oxidation of olefins to α-glycols; oxidation of ketones to lactones or esters; treating woolens to prevent felting and shrinking; in bleaching compositions.

1852. α-Carotene. [7488-99-5] $C_{40}H_{56}$; mol wt 536.87. C 89.49%, H 10.51%. About as widely distributed as its β-isomer, but in smaller amounts. Best sources for both the α- and β-isomers are carrots, palm-oil, and green leaves of various species. As a provitamin A it is half as active as β-carotene. Found in the mother liquors after crystallizing β-carotene. Isoln by chromatography: Karrer, Walker, *Helv. Chim. Acta* 16, 641 (1933). Structure: Kuhn, Lederer, *Ber.* 64, 1349 (1931); Karrer *et al., Helv. Chim. Acta* 14, 614 (1931); 16, 975 (1933). Natural (+)-α-carotene has 6'*R* configuration: Eugster *et al., Ibid.* 52, 1729 (1969). Synthesis of *dl*-α-carotene: Eugster, Karrer, *Ibid.* 38, 610 (1955); Tschamer *et al., Ibid.* 40, 1676 (1957); Ruegg *et al., Ibid.* 44, 985 (1961).

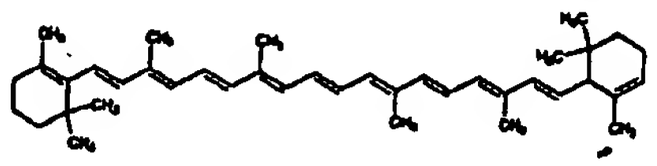

Deep purple prisms, polyhedra from petr ether or from benzene + methanol, mp 187.5° (evacuated tube). $[\alpha]_{443}^{12}$ +385° (c = 0.08 in benzene). Absorption max ($CHCl_3$): 485, 454 nm. More sol than β-carotene. Freely sol in carbon disulfide, chloroform; sol in ether, benzene. Slightly sol in petr ether, alcohol. 100 ml hexane dissolves 294 mg at 0°. Practically insol in water, acids, alkalies. Absorbs oxygen from the air, giving rise to inactive colorless oxidation products. The oxidation in light is autocatalytic. *Store in darkness in sealed ampoules and at low temp (−20°C).*

THERAP CAT: Vitamin A precursor.

THERAP CAT (VET): Vitamin A precursor for all species except cats.

1853. β-Carotene. [7235-40-7] β,β-Carotene; Carotaben; Provatene; Solatene. $C_{40}H_{56}$; mol wt 536.87. C 89.49%, H 10.51%. Most important of the provitamins A. Widely distributed in the plant and animal kingdom. In plants it occurs almost always together with chlorophyll. Isoln from carrots: Willstätter, Escher, *Z. Physiol. Chem.* 64, 47 (1910); Kuhn, Lederer, *Ber.* 64, 1349 (1931); Barnett *et al.*, US 2848508 (1958). Chromatography: Karrer, Walker, *Helv. Chim. Acta* 16, 641 (1933). Structure: Willstätter, Mieg, *Ann.* 355, 1 (1907); Zechmeister *et al., Ber.* 61, 566 (1928); 66, 123 (1933); Karrer *et al., Helv. Chim. Acta* 12, 1142 (1929); 13, 1084 (1930); 14, 1033 (1931); Kuhn, Brockmann, *Ber.* 65, 894 (1932); 66, 1319 (1933); 67, 1408 (1934); *Ann.* 516, 95 (1935). Crystal structure: Sterling, *Acta Crystallogr.* 17, 1224 (1964). Synthesis: Milas *et al., J. Am. Chem. Soc.* 72, 4844

(1950); Karrer, Eugster, *Compt. Rend.* 250, 1920 (1950); Inhoffen *et al., Chem. Zig.* 74, 285, 309 (1950); Surmatis, Ofner, *J. Org. Chem.* 26, 1171 (1961); Rüegg *et al., Helv. Chim. Acta* 44, 985 (1961); Bestmann *et al., Ann.* 1973, 760; Fischli, Mayer, *Helv. Chim. Acta* 58, 1584 (1975). Industrial mfg procedure: Isler *et al., Helv. Chim. Acta* 39, 249 (1956); Isler *et al.*, US 2917539 (1959 to Hoffmann-La Roche). Microbial production by *Choanephora trispora:* Zajic, US 2959521; US 2959522 and US 3128236 (1960, 1960 and 1964, all to Grain Processing); Miescher, US 3001912 (1961 to C.S.C.). *Review:* Fleming, *Selected Organic Syntheses* (John Wiley, London, 1973) pp 70-74.

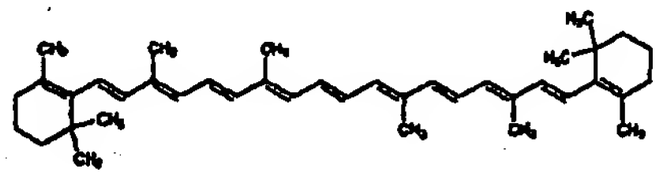

Deep-purple, hexagonal prisms from benzene + methanol. Red, rhombic, almost square leaflets from petr ether. mp 183° (evacuated tube). Absorption max (chloroform): 497, 466 nm. Less sol than α-carotene. Sol in CS_2, benzene, chloroform. Moderately sol in ether, petr ether, oils. 100 ml hexane dissolve 109 mg at 0°. Very sparingly sol in methanol and ethanol. Practically insol in water, acids, alkalies. Dil solns are yellow. Absorbs oxygen from the air giving rise to inactive, colorless oxidation products. *Keep tightly closed and protected from light. Store at low temp (−20°C).* Commercial crystalline β-carotene has a vitamin A activity of 1.67 million U.S.P. units per gram. The I.U. of 0.6 μg β-carotene is almost exactly equivalent to 0.3 μg vitamin A.

USE: Yellow coloring agent for foods.

THERAP CAT: Vitamin A precursor. Ultraviolet screen.

THERAP CAT (VET): Vitamin A precursor for all species except cats.

1854. γ-Carotene. [472-93-5] $C_{40}H_{56}$; mol wt 536.87. C 89.49%, H 10.51%. A rare carotenoid. Has provitamin A activity. Best source is *Penicillium sclerotiorum:* Mase *et al., Arch. Biochem. Biophys.* 68, 150 (1957). Also present in small proportions in many plant materials, esp fruits containing β-carotene. Chromatographic isoln from crude carotenes: Kuhn, Brockmann, *Ber.* 66, 407 (1933); Winterstein, *Z. Physiol. Chem.* 219, 249 (1933). Structure: Kuhn, Brockmann, *loc. cit.; Naturwissenschaften* 21, 44 (1933). Synthesis: Garbers *et al., Helv. Chim. Acta* 36, 1783 (1953); Ruegg *et al., ibid.* 44, 985 (1961).

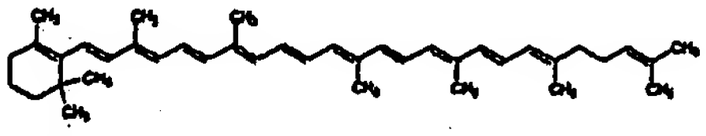

Probably crystallizes in polymorphous forms. Synthetic form: red plates, mp 152-153.5°. Absorption max (petr ether): 437, 462, 494 nm ($E^{1\%}_{1cm}$ 2055, 3100, 2720). Natural form: minute, deep-red prisms with bluish luster from benzene + methanol. mp 177.5°. Absorption max (chloroform): 508.5, 475, 446 nm. Somewhat less sol than β-carotene. *Store in darkness in sealed ampoules at low temps (0°C).*

THERAP CAT: Vitamin A precursor.

THERAP CAT (VET): Vitamin A precursor for all species except cats.

1855. δ-Carotene. [472-92-4] ε,ψ-Carotene. $C_{40}H_{56}$; mol wt 536.87. C 89.49%, H 10.51%. Extracted from the fruit of *Gonocaryum pyriforme* Mig., *Icacinaceae:* Winterstein, *Z. Physiol. Chem.* 219, 249 (1933). Occurs also in carrots and certain varieties of tomatoes. Isoln from tomato mutants: Porter, Murphey, *Arch. Biochem. Biophys.* 32, 21 (1951). Structure: Karrer, Quackenbush, *ibid.* 88, 59 (1960). Synthesis: Manchand *et al., J. Chem. Soc.* 1965, 2019. Absolute configuration: Buchecker, Eugster, *Helv. Chim. Acta* 54, 327 (1971).

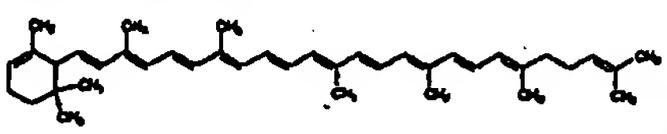

Long orange-red needles from CS_2 + hexane. mp 140.5°. $[\alpha]_{Cd}$ +317°; $[\alpha]_D^{25}$ +352° ±16% (hexane). uv spectrum: Karrer, Quackenbush, *loc. cit.*

1856. β-Carotol. [465-28-1] (3*R*-(3α,3aα,8aα)-1,2,3,3a,4,5,6,8a-Hexahydro-6,8a-dimethyl-3-(1-methylethyl)-3a(1*H*)-azulenol; 4,5,8,8a-hexahydro-3-isopropyl-6,8a-dimethyl-3a(1*H*)-azulenol. $C_{15}H_{24}O$; mol wt 222.37. C 81.02%, H 11.79%, O 7.19%. Occurs in oil of carrot seeds, *Daucus carota* L., *Umbelliferae:* Tsukamoto, *J. Pharm. Soc. Jpn.* 525, 961 (1925); C. (1926); Sorm *et al., Collect. Czech. Chem. Commun.* Pigulevskii, Kovaleva, *Zh. Prikl. Khim.* 32, 2703 (19 Sykora *et al., Collect. Czech. Chem. Commun.* 26 Zalkow *et al., J. Org. Chem.* 26, 981 (1961). Ste Levisalles, Rudler, *Bull. Soc. Chim. Fr.* 1964, 202 Synthesis of (+)-form: DeBraissia *et al., ibid.* 1972 *Chem. Commun.* 1972, 855.

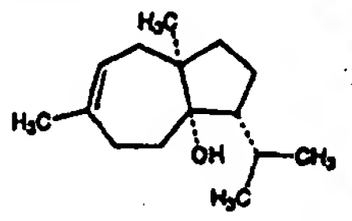

(+) - Carotol

Liquid. $bp_{2.5}$ 126°. $[\alpha]_D^{20}$ +30.4°. n_D^{20} 1.4964. d^{20} 0.

1857. Caroverine. [23465-76-1] 1-[2-(Die yl]-3-[(4-methoxyphenyl)methyl]-2(1*H*)-quinoxalinone aminoethyl)-3-(*p*-methoxybenzyl)dihydro-2-quinoxa mium. $C_{32}H_{37}N_5O_2$; mol wt 365.47. C 72.30%, 11.50%, O 8.76%. Prepn: Zellner *et al.*, US 302 Donau-Pharm.). Polarographic study: P. Pflegel, 667 (1969). Pharmacological study: P. Hahn *et al., Pharmacodyn. Ther.* 199, 108 (1972).

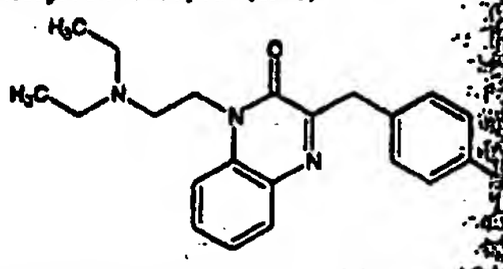

Crystals from isopropyl alcohol. mp 69°. $bp_{0.01}$ 202 Hydrochloride. Doc 188°.

THERAP CAT: Antispasmodic.

1858. Carpaine. [3463-92-1] $C_{28}H_{50}N_2O_4$; mo C 70.25%, H 10.53%, N 5.85%, O 13.37%. Fou *papaya* L. and in *Vasconcellosia hastata* Caruel, *Carica* from papaya leaves: Greshoff, *Mededeel. uit 's Land tenzorg.* No. 7, 5 (1890); Rapoport, Baldridge, *J. Am. C* 343 (1951). Reportedly causes bradycardia, CNS de kowski, *Arch. Int. Pharm.* 15, 84 (1905). Structure an istry: Govindachari *et al., Tetrahedron Lett.* 1965, configuration: Coke, Rice, *J. Org. Chem.* 30, 3420 (1 of structural studies: Govindachari, *J. Indian Chem.* (1968).

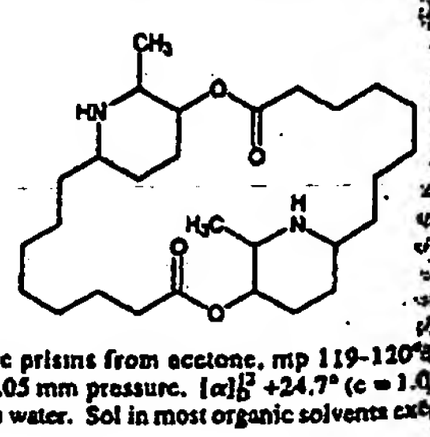

Monoclinic prisms from acetone, mp 119-120° a 120° under 0.05 mm pressure. $[\alpha]_D^{32}$ +24.7° (c = 1.0 Slightly sol in water. Sol in most organic solvents exc

1859. Carpetimycins. Carba ...mycin and olivanic acids, *q.v.* ...re known. Prodn of A and B b; ...193, now named *Streptomyces g.* ...bacterial properties: NL 80(...18529 (1980, 1985 to Takeda): A ...17 (1980); by *Streptomyces* strain ...2. 1388. Structure and abs confg ...1425 (1980); M. Nakayama *et al.* ...ino study: Y. Nozaki *et al., ibid.* ...metimycin A: H. Natsugari *et al.* ...813, 403; M. Ihara *et al., Heterc* ...ymak, M. N. Rao, *J. Org. Chem.* ...-carpetimycin A: T. Iimori *et a* ...813); M. Aratani *et al., Tetrahe* ...abashi *et al., ibid.* 2217.

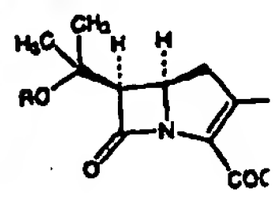

Carpetimycin A: Carpetimycin B

(Carpetimycin A. [76025-73- ...lpino)ethenyl]sulfinyl]-6-(1-h ...bicyclo[3.2.0]hept-2-ene-2-c ...tibiotic C-19393-H_2; antibioti ...$_{16}N_2O_4S$; mol wt 342.37. Col ...27° (c = 1.7 in water). uv ma ...00) (Nakayama, 1980).

(Carpetimycin B. [76094-36- ...e KA-6643-B; C-19393-S_2. ...olorless solid melting above ...ater). uv max (water): 240, 2 ...280).

1860. Carphenazine. [2(...inyl)-1-piperazinyl]propyl]-10 ...10-[3-[4-(2-hydroxyethyl)-1- ...phenothiazine; 2-propionyl-10 ...propyl]phenothiazine; Prok ...35.59. C 67.73%, H 7.34%, ... H. Sherlock, N. Sperber, U ...low *et al.*, US 3023146 (19(

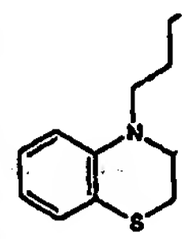

...maleate. [2975-34-0] ...lts from isopropanol, ...ystals from methanol, m ...UTIC CAT: Antipsycho ...

(1861. Carpipramine. ...benz[*b,f*]azepin-5-yl) ...-[4-(4-piperidino-4 ...-dibenz[*b,f*]azepi ...C; mol wt 446.63. C ...1984; Nakanishi, T. ...*et al.*, US 33296

mechanism of action: H. Ito, *Expert Opin. Ther. Targets* 8, 287-294 (2004).

THERAPCAT: Anti-inflammatory.

9494. Tocol. [119-98-2] 3,4-Dihydro-2-methyl-2-(4,8,12-trimethyltridecyl)-2*H*-1-benzopyran-6-ol; 2-methyl-2-(4,8,12-trimethyltridecyl)-6-chromanol; 2-methyl-2-phytyl-6-chromanol; 6-hydroxy-2-methyl-2-phytylchroman; 2-methyl-2-phytyl-6-hydroxychroman. $C_{26}H_{44}O_2$; mol wt 388.63. C 80.35%, H 11.41%, O 8.23%. Synthesis by the condensation of hydroquinone and phytol in the presence of anhydr formic acid: Pendse, Karrer, *Helv. Chim. Acta* 40, 1837 (1957). Antioxidant activity of tocol and its methyl derivs: Olcott, van der Veen, *Lipids* 3, 331 (1968).

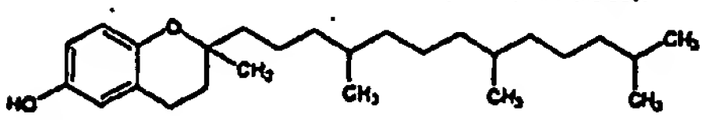

Colorless, viscous oil. $bp_{0.001}$ 165-175°.
Acetate. $C_{28}H_{46}O_3$. Viscous oil. $bp_{0.001}$ 180-185°.
USE: Antioxidant.

9495. α-Tocopherol. [59-02-9] (2*R*)-3,4-Dihydro-2,5,7,8-tetramethyl-2-[(4*R*,8*R*)-4,8,12-trimethyltridecyl]-2*H*-1-benzopyran-6-ol; (+)-2,5,7,8-tetramethyl-2-(4',8',12'-trimethyltridecyl)-6-chromanol; *R,R,R*-α-tocopherol; *d*-α-tocopherol; 5,7,8-trimethyltocol; Optovit; Tocovital. $C_{29}H_{50}O_2$; mol wt 430.71. C 80.87%, H 11.70%, O 7.43%. Most bioactive of the naturally occurring forms of vitamin E, *q.v.* Richest sources are green vegetables, grains, and oils, particularly palm, safflower and sunflower oils. Isoln from wheat germ: H. M. Evans *et al., J. Biol. Chem.* 113, 319 (1936). Structure: E. Fernholz, *J. Am. Chem. Soc.* 59, 1154 (1937); 60, 700 (1938). Synthesis of *dl*-form: P. Karrer *et al., Helv. Chim. Acta* 21, 520, 820 (1938); F. Bergel *et al., J. Chem. Soc.* 1938, 1382. Distillation from vegetable oils and prepn of esters: J. G. Baxter *et al., J. Am. Chem. Soc.* 918 (1943). Prepn of crystalline natural form: C. D. Robeson, *ibid.* 1660; of crystalline acetate: *idem, ibid.* 64, 1487 (1942). Abs config of natural α-tocopherol: H. Mayer *et al., Helv. Chim. Acta* 46, 963 (1963). Stereoselective synthesis: K.-K. Chan *et al., J. Org. Chem.* 43, 3435 (1978). Total synthesis of all 8 stereoisomers: N. Cohen *et al., Helv. Chim. Acta* 64, 1158 (1981). Clinical trial in Alzheimer's disease: M. Sano *et al., N. Engl. J. Med.* 336, 1216 (1997); to improve immune function in healthy elderly: S. N. Meydani *et al., J. Am. Med. Assoc.* 277, 1380 (1997). Review of bioavailability from vitamin E supplements: M. G. Traber, *BioFactors* 10, 115-120 (1999). Review of clinical trials in heart disease: W. A. Pryor, *Free Radical Biol. Med.* 28, 141-164 (2000).

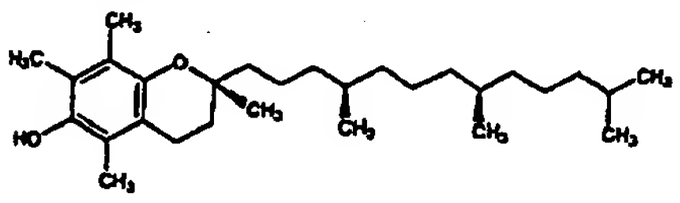

Transparent needles, mp 2.5-3.5°. $[\alpha]_{546.1}^{25}$ −3.0° (benzene); $[\alpha]_{546.1}^{25}$ +0.32° (ethanol).
Acetate. [58-95-7] Spondyvit. $C_{31}H_{52}O_3$; mol wt 472.74. Light yellow oil. Crystallized at −30° as needle-like crystals, mp 26.5-27.5°. $[\alpha]_D^{25}$ +0.25° (c = 10 in chloroform); $[\alpha]_D^{25}$ +3.2° (in ethanol).
Succinate. [4345-03-3] *d*-α-Tocopheryl acid succinate; Tocovite. Needles from peur ether, mp 76-77°. uv max (ethanol): 286 nm ($E_{1cm}^{1\%}$ 38.5). Practically insol in water.
dl-α-Tocopherol. [10191-41-0] *all-rac*-α-Tocopherol. Equimolar mixture of all four racemates. Slightly viscous, pale yellow oil. d_4^{23} 0.950; $bp_{0.1}$ 200-220°; n_D^{23} 1.5045. uv max: 294 nm ($E_{1cm}^{1\%}$ 71). Practically insol in water. Freely sol in oils, fats, acetone, alcohol, chloroform, ether, other fat solvents. Stable to heat and alkalies in the absence of oxygen. Not affected by acids up to 100°. Slowly oxidized by atm oxygen, rapidly by ferric and silver salts. Gradually darkens on exposure to light.
dl-α-Tocopherol acetate. [52225-20-4] *dl*-α-Tocopheryl acetate; Detulin; Ephynal; Eusovit; Evion. Comprehensive description: B. C. Rudy, B. Z. Senkowski, *Anal. Profiles Drug Subs.* 111-126 (1974). Pale yellow, viscous liquid. mp −27.5°; 0.9533. $bp_{0.01}$ 184°; $bp_{0.015}$ 194°; $bp_{0.3}$ 224°. n_D^{20} 1.4950-1.49 uv max (cyclohexane): 285.5 nm. Practically insol in wa Freely sol in acetone, chloroform, ether. Less readily sol in alc.
USE: As an antioxidant in vegetable oils and shortening.
THERAPCAT: Vitamin E supplement.
THERAPCAT (VET): Vitamin E supplement.

9496. β-Tocopherol. [16698-35-4]; [148-03-8] (*dl*-fo (2*R*)-3,4-Dihydro-2,5,8-trimethyl-2-[(4*R*,8*R*)-4,8,12-trimethyl decyl]-2*H*-1-benzopyran-6-ol; (+)-2,5,8-trimethyl-2-(4,8,1 methyltridecyl)-6-chromanol; 5,8-dimethyltocol; cumotocoph neotocopherol; *p*-xylotocopherol. $C_{28}H_{48}O_2$; mol wt 416.68 80.71%, H 11.61%, O 7.68%. One of the naturally occurring f of vitamin E, *q.v.* Is biologically less active than α-toocoph May be separated by fractional crystn: Emerson *et al., Sc* 83, 421 (1936); *J. Biol. Chem.* 113, 319 (1936); Baxter *et al., J Chem. Soc.* 65, 918 (1943).

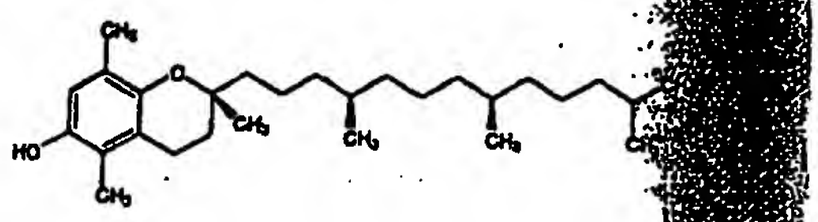

Pale yellow, viscous oil. $bp_{0.1}$ 200-210°. $[\alpha]_{546.1}^{25}$ +2.9° (c= in ethanol). uv max: 297 nm ($E_{1cm}^{1\%}$ 87.6). Insol in water. F sol in oils, fats, acetone, alcohol, chloroform, ether, other fat vents. Very stable to heat and alkalies. Slowly oxidized by at pheric oxygen, rapidly by ferric and silver salts. Gradually dar on exposure to light.

9497. γ-Tocopherol. [54-28-4]; [7616-22-0] (*dl*-form (2*R*)-3,4-Dihydro-2,7,8-trimethyl-2-[(4*R*,8*R*)-4,8,12-trimethyltridecyl]-2*H*-1-benzopyran-6-ol; (+)-2,7,8-trimethyl-2-(4,8,12-trimethyltridecyl)-6-chromanol; (*R,R,R*)-γ-tocopherol; 7,8-dimethyltocol; α-xylotocopherol. $C_{28}H_{48}O_2$; mol wt 416.68. C 80.7 H 11.61%, O 7.68%. One of the naturally occurring for vitamin E, *q.v.* Most abundant tocopherol in soybean a oils. Isoln by fractional crystn: Emerson *et al., Science* (1936); *J. Biol. Chem.* 113, 319 (1936); J. G. Baxter *et al.*, *Chem. Soc.* 65, 918 (1943). Prepn of crystalline natural D. Robeson, *J. Am. Chem. Soc.* 65, 1660 (1943). Comp bioactivity with α-tocopherol, *q.v.*: J. O. Bieri, R. P. Evarts, 104, 850 (1974). Protective effects vs reactive nitrogen ox cies: R. V. Cooney *et al., Proc. Natl. Acad. Sci. USA* (1993); S. Christen *et al., ibid.* 94, 3217 (1997). HPLC de serum: A. Sobczak *et al., J. Chromatogr. B* 730, 265 Review of bioavailability, metabolism, and activity: Q. *al., Am. J. Clin. Nutr.* 74, 714-722 (2001).

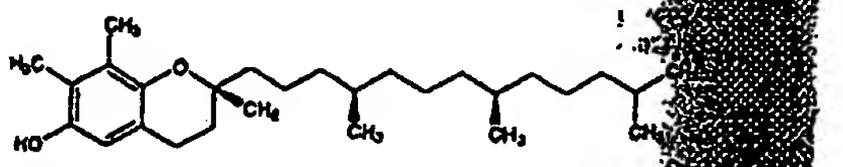

Pale yellow, viscous oil. Has been crystallized as trans needles, mp −3 to −2°. $bp_{0.1}$ 200-210°. $[\alpha]_{546.1}^{25}$ −2.4° (c in benzene); $[\alpha]_{546.1}^{25}$ +2.2° (c = 9.32 in ethanol). uv max: 2 ($E_{1cm}^{1\%}$ 92.8). Insol in water. Freely sol in oils, fats, aceton hol, chloroform, ether, other fat solvents. Very stable to h alkalies. Slowly oxidized by atmospheric oxygen, rapidly b and silver salts. Gradually darkens on exposure to light.

9498. δ-Tocopherol. [119-13-1] (2*R*)-3,4-Dihydr methyl-2-[(4*R*,8*R*)-4,8,12-trimethyltridecyl]-2*H*-1-benzop ol; 8-methyltocol. $C_{27}H_{46}O_2$; mol wt 402.65. C 8 11.52%, O 7.95%. One of the naturally occurring forms E, *q.v.* Isoln from soybean oil: Stern *et al., J. Am. Chem* 869 (1947). Synthesis: Green *et al., J. Chem. Soc.* 1959, 3 900085 (1961 to Hoffmann-La Roche).

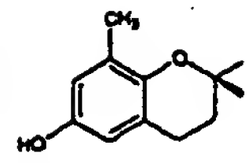

Pale yellow, viscou +1.1° (c = 10.9 in benz

9499. Tocoretin 3,4-dihydro-2,5,7,8-t tridecyl]-2*H*-1-benzop yl-2-[(4*R**,8*R**)-4,8,1 tretinoin tocoferil; DL- non. $C_{49}H_{76}O_3$; mol Wound healing agent fibroblasts. Prepn: H. *idem*, US 3878202 (19 Pharmacology: K. Sal 116, 228223z (1992). 205, *C.A.* 117, 19823 Kawamura *et al., Dig.* tion in skin ulcers: T. *et al., ibid.* 209. Acute 43, 227 (1992). *C.A.* 11

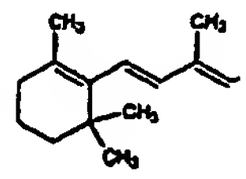

Light yellow oil. u in mice (mg/kg): >100 THERAPCAT: Vulne

9500. α-Tocotrie stereo). (2*R*)-3,4-Dihy trimethyl-3,7,11-tride tetramethyl-2-(4,8,12-t ζ1-tocopherol. $C_{29}H_{44}$ O 7.54%. One of the Isoln from wheat bran (1955); Green *et al.*, Green *et al., J. Chem* McHale *et al., ibid.* 19 icochemical Propertie Harris, I. G. Wood, *Vi* of all-*trans*-form: Schu

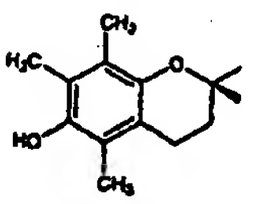

uv max (ethanol): 29

9501. β-Tocotrie trimethyl-2-[(3*E*,7*E*)-4, benzopyran-6-ol; 2,5,8 trienyl)chroman-6-ol; 5 wt 410.63. C 81.90%, occurring forms of vita from bran: Eggitt, War Norris, *Ibid.* 6, 689 (19 *J. Chem. Soc.* 1959, 33 *al., J. Chem. Soc.* 1963, *Acta* 46, 2517 (1963).

receptor kinase. Orthovanadate activates insulin receptor kinase by inhibiting the activity of a protein tyrosine phosphatase in the cells. Cephalochromin is a polyphenolic compound that has been observed to activate the IRTK activity (unpublished observation). Compound A is a small molecule that has been shown to enhance IRTK in these cells (21, 22). As shown in Fig. 2C, insulin receptor isolated from cells that have been treated with these agents showed a higher IRTK activity than the untreated cells. Moreover, this activity was similar to what has been observed for these compounds using the radioactive version of IRTK assay (date not shown). Taken together, these data demonstrate the usefulness of this assay for measuring the kinase activity of the insulin receptor that has been treated with diverse kinds of activators.

In summary, we have presented a significant improvement in the method to measure insulin receptor tyrosine kinase activity. This has been accomplished by developing a FRET-based assay, which utilizes a biotinylated substrate peptide from a natural substrate site of the IRTK, a Eu-labeled pT66, an antiphosphotyrosine antibody that specifically recognizes the phosphorylated peptide, and XL665-labeled streptavidin. Utilizing these reagents, we have demonstrated that this detection method yields results similar to what would be expected with the radioactive version of this type of assay. We have also shown that this assay is not only able to detect insulin-stimulated activation of the receptor kinase activity, but is also able to measure increases in the kinase activity of the insulin receptor that has been stimulated with compounds known to enhance insulin receptor kinase activity in cells. In contrast to other formats this assay is performed in a single plate without various washing steps which are often necessary to remove unincorporated ATP from the reaction. Due to this feature of the assay we have been able to process more than twenty-five 96-well plates per day. In short, this assay is a very robust and efficient method of determining the status of insulin receptor kinase isolated from cells *in vitro* without the use of radioactive materials.

Acknowledgments. We thank Debbie Szalkowski for help with the radioactive IRTK assay and Alice Marcy for help during the development of this assay.

REFERENCES

1. White, M. F., and Kahn, C. R. (1994) *J. Biol. Chem.* **269,** 1–4.
2. Parham, P. (1990) *Nature* **345,** 662–664.
3. Turner, R. C., Hattersley, A. T., Shaw, J. T. E., and Levy, J. C. (1995) *Diabetes* **44,** 1–10.
4. Taylor, S. I. (1999) *Cell* **97,** 9–12.
5. Pilch, P. F., and Czech, M. P. (1980) *J. Biol. Chem.* **255,** 1722–1731.
6. Rosen, O. M. (1989) *Diabetes* **38,** 1508–1511.
7. Perlman, R., Bottaro, D. P., White, M. F., and Kahn, C. R. (1989) *J. Biol. Chem.* **264,** 8946–8950.
8. Baron, V., Gautier, N., Komoriya, A., Hainaut, P., Scimeca, J. C., Mervie, M., Lavielle, S., Dolais-Kitabgi, J., and Van Obberghen, E. (1990) *Biochemistry* **29,** 4634–4641.
9. Luo, R. Z., Beniac, D. R., Fernandes, A., Yip, C. C., and Ottensmeyer, F. P. (1999) *Science* **285,** 1077–1080.
10. Kasuga, M., Fujita-Yamaguchi, Y., Blithe, D. L., and Kahn, C. R. (1983) *Proc. Natl. Acad. Sci. USA* **80,** 2137–2141.
11. Yu, K. T., and Czech, M. P. (1984) *J. Biol. Chem.* **259,** 5277–5286.
12. Ellis, L., Morgan, D. O., Clauser, E., Roth, R. A., and Rutter, W. J. (1987) *Mol. Endocrinol.* **1,** 15–24.
13. Wilden, P. A., Kahn, C. R., Siddle, K., and White, M. F. (1992) *J. Biol. Chem.* **267,** 16660–16668.
14. Boge, A., and Roth, R. A. (1995) *Anal. Biochem.* **231,** 323–332.
15. Ozawa, T., Sato, M., Sugawara, M., and Umezawa, Y. (1998) *Anal. Chem.* **70,** 2345–2352.
16. Cummings, R. T., McGovern, H. M., Zheng, S., Park, Y. W., and Hermes, J. D. (1999) *Anal. Biochem.* **269,** 79–93.
17. Shoelson, S. E., Chatterjee, S., Chaudhuri, M., and White, M. F. (1992) *Proc. Natl. Acad. Sci. USA* **89,** 2027–2031.
18. Zhang, B., Salituro, G., Szalkowski, D., Li, Z., Zhang, Y., Royo, I., Vilella, D., Diez, M. T., Pelaez, F., Ruby, C., Kendall, R. L., Mao, X., Griffin, P., Calaycay, J., Zierath, J. R., Heck, J. V., Smith, R. G., and Moller, D. E. (1999) *Science* **284,** 974–977.
19. Kolb, A. J., Kaplita, P. V., Hayes, D. J., Park, Y.-W., Pernell, C., Major, J. S., and Mathis, G. (1998) *Drug Discovery Today* **3,** 333–342.
20. Park, Y.-W., Cummings, R. T., Wu, L., Zheng, S., Cameron, P. M., Woods, A., Zaller, D. M., Marcy, A. I., and Hermes, J. D. (1999) *Anal. Biochem.* **269,** 94–104.
21. Liu, K., Xu, L., Szalkowski, D., Li, Z., Ding, V., Kwei, G., Huskey, S., Moller, D. E., Heck, J. V., Zhang, B. B., and Jones, A. B. (2000) *J. Med. Chem.* **43,** 3487–3494.
22. Qureshi, S. A., Ding, V., Li, Z., Szalkowski, D., Biazzo-Ashnault, D., Xie, D., Saperstein, R., Brady, E., Huskey, S., Shen, X., Liu, K., Xu, L., Salituro, G. M., Heck, J. V., Moller, D. E., Jones, A. B., and Zhang, B. B. (2000) *J. Biol. Chem.* **275,** 36590–36595.
23. Park, Y.-W. (1999) IBC's 8th Annual International Conference, Berkeley, CA, (March 1–3, 1999).

Relationship between Turbidity of Lipid Vesicle Suspensions and Particle Size

Edwin V. Pozharski,[1] Leon McWilliams, and Robert C. MacDonald
Department of Biochemistry, Molecular Biology and Cell Biology, Northwestern University, Evanston, Illinois 60208

Received September 15, 2000; published online March 7, 2001

Various physical methods exist for determining the distribution of sizes of micron and submicron particles in suspension. Light and electron microscopy, viscosimetry, sedimentation techniques, the electrical sens-

[1] To whom correspondence should be addressed at current address: Rosenstiel Basic Medical Sciences Research Center, Brandeis University, 415 South St., Waltham, MA 02254.

Analytical Biochemistry **291,** 158–162 (2001)
doi:10.1006/abio.2001.5012
0003-2697/01 $35.00

ing zone method (Coulter technique), various scattering techniques (static and dynamic light scattering, X-ray and neutron diffraction), chromatography, electrophoresis, and some other more exotic methods have been used for sizing. In liposome applications, the most common in recent years has been the dynamic light scattering technique. The method is relatively fast and easily applied to normal samples without special preparation. Also, it can be extended to assess the shape and size distributions. Electron microscopy, although more complicated, invasive, and time-consuming, helps to obtain detailed and reliable information about lipid particles having an extended size range or nonspherical shape.

A rapid and reliable method of estimating particle size is especially useful when dealing with lipid vesicles and, despite the numerous methods mentioned above, none of them combines both speed and ready availability of the required experimental equipment. In this paper we describe a method for estimating an average size of lipid vesicles with only a spectrophotometer. Theoretical considerations and experimental evidence allow us to propose two possible measurement schemes, both based on calibration with vesicles of known size: (i) fit turbidities measured with more than one vesicle sample of known size to a standard curve; (ii) obtain the turbidity spectrum for a vesicle sample of known size and convert it to the size dependence of turbidity. The vesicle samples of known size can readily be produced by extrusion (1, 2). The details of both approaches are discussed further.

Experimental Approach (Procedure 1)

Figure 1 represents the experimentally obtained relationship between the turbidity of a lipid suspension and the size of the constituent vesicles. Egg L-α-phosphatidylcholine (Avanti) at 1 mg/ml was used, samples of different sizes having been obtained by sonication for different durations of time in a water bath sonicator. The actual diameter of vesicles was measured by dynamic light scattering (Brookhaven Instruments BI-200SM goniometer and BI-9000 digital correlator; correlation curves analyzed by quadratic cumulants (3)). The turbidity was measured as the apparent optical density with a Beckman DU-50 spectrophotometer at 440 nm (upper curve) and 780 nm (lower curve).

The first important observation is the general shape of the curve. The turbidity as a function of vesicle diameter fits two intersecting lines, being linear for small and constant for large sizes. These two lines intersect at some wavelength, λ_i, which is proportional to (although smaller than) the wavelength of the incident light. The plateau value of turbidity depends upon the wavelength of incident light. The turbidity at any wavelength of the sample of any particle size was proportional to the lipid concentration up to 5 mg/ml (data not shown). We conducted similar experiments with egg lecithin and its 7:3 mixture (by weight) with cholesterol and in all cases obtained the same general size-turbidity dependence (data not shown), indicating that such behavior is inherent in the properties of lipid vesicles as light scatterers.

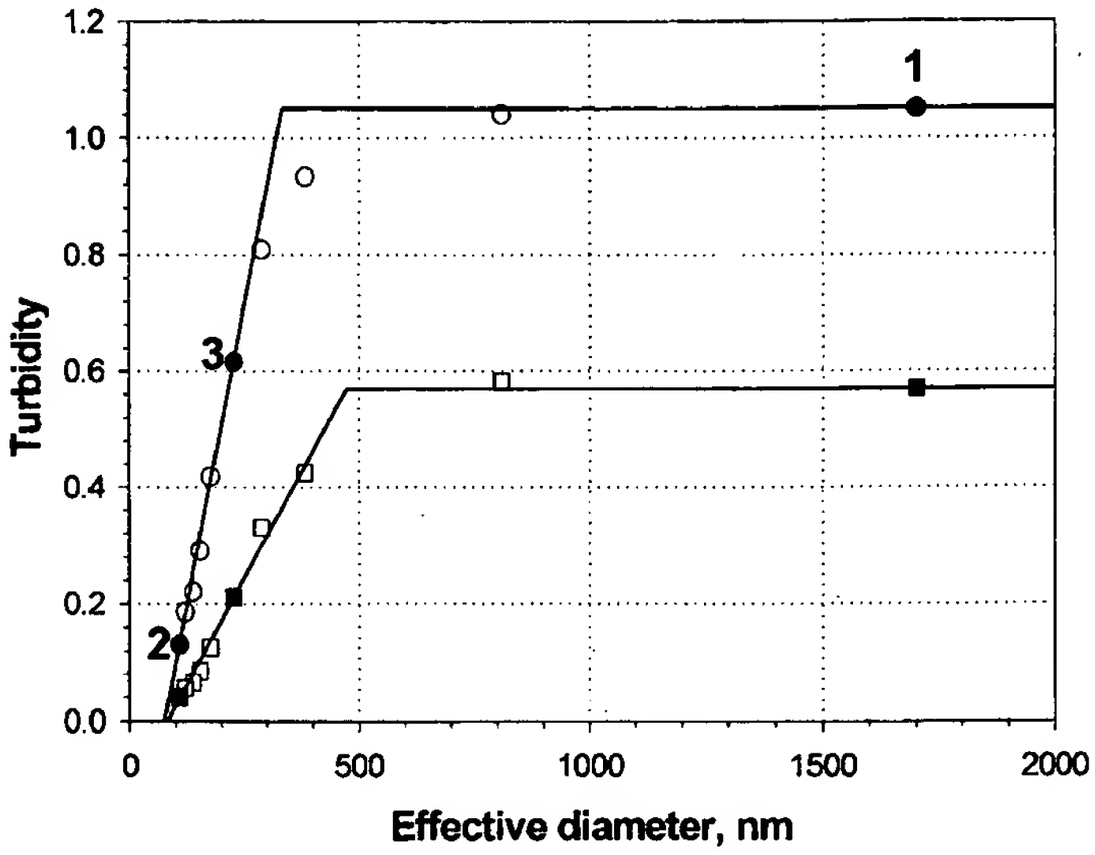

FIG. 1. General shape of the size-turbidity dependence for an egg L-α-phosphatidylcholine vesicle suspension at 1 mg/ml. Turbidity was measured at two wavelengths: λ = 440 nm (circles) and 780 nm (squares). Closed symbols indicate size standards. Lines show the result of fitting by two intersecting lines as described in procedure 1.

The explanation of the experimental size-turbidity dependence is given below in terms of Rayleigh-Debye scattering theory; however, even without a theoretical model, one can propose the following approach based only on the experimental results:

1. Measure the turbidity of a handshaken lipid suspension (in most cases these vesicles are larger than a wavelength, so it allows estimation of the turbidity maximum)—point 1 in Fig. 1.
2. Measure the turbidity of two standards smaller than the chosen wavelength (for instance, obtained by extrusion)—points 2 and 3 in Fig. 1.
3. Fit the above three values with two intersecting lines.

The linear region of the curve can then be used to assess the size of the unknown vesicles. The maximum turbidity, although useless by itself for size estimates, determines the range of sizes where a calibration is applicable.

Theory-Based Approach (Procedure 2)

The overall turbidity of a lipid vesicle suspension can be related to the scattering characteristics of the individual vesicle (4). If we consider a homogeneous ensem-

ble of thin shells as the model, one can show that turbidity, A, is given by[2]

$$A = 0.054 c S_0 N_a l \alpha_S / M \qquad [1]$$

(see footnote for meaning of the symbols). The scattering efficiency, α_S, is the fraction of light scattered by an individual vesicle of given size, and in order to complete the model it is necessary to apply scattering theory to obtain its analytical expression.

As long as a lipid vesicle is considered to be a thin shell or hollow sphere, the scattering efficiency can be determined within Rayleigh-Debye light scattering theory (5, 6). We generally followed this theory to derive an expression (below) for the scattering efficiency. Therefore, we will not present the complete derivation, which is rather straightforward, but limit our discussion to few important considerations.

Rayleigh-Debye theory is applicable to lipid vesicles. The applicability of Rayleigh-Debye theory is limited to the cases when there is no significant change of phase of the incident light when it penetrates the particle. In order to satisfy that condition, the thickness of the bilayer h (or stacked bilayers in multilamellar structure) should obey the condition,

$$h \ll \lambda_0/(4\pi m_0(m-1)) \sim 1.1\lambda_0, \qquad [2]$$

when $m_0 \sim 1.33$—refractive index of water; $m = m_{lipid}/m_0 \sim 1.4/1.33 = 1.05$ and λ_0 is the wavelength of incident light. Since the bilayer thickness is about 5 nm, even highly multilamellar structures obey the above condition, as long as visible or ultraviolet light is used. It is especially important to emphasize that it is the "longest dimension through the particle" (Ref. 7, p. 415), i.e., the bilayer thickness rather than its overall size (vesicle diameter), that is the decisive parameter for Rayleigh-Debye scattering. In the case of lipid vesicles, this means that it is still applicable when the diameter of the vesicle is comparable to or even larger than the wavelength.

Lipid vesicle: Thin shell or hollow sphere? The hollow sphere model of lipid vesicles is clearly closer to reality than that of a thin shell. However, this model leads to undesirable complications of the final equations. We compared the scattering efficiency α_S, calculated for both models, and found that the correction introduced by the hollow sphere model is less than 0.2% in the case of unilamellar vesicles. Even for multilamellar vesicles with as many as 10 bilayers it is less than ~6%. We thus find Rayleigh-Debye scattering by thin shells to be adequate to describe the turbidity of lipid vesicle suspensions. The theory gives the following relationship between the turbidity A and diameter of vesicle D

$$A = 4.82 \frac{c S_0 N_a l m_0^2 h^2 (m^2-1)^2}{M\lambda_0^2 (m^2+2)^2} \int_{\theta_0}^{\pi} \frac{\sin\theta(1+\cos^2\theta)\sin^2(2\pi m_0 D \sin(\theta/2)/\lambda_0)}{\sin^2(\theta/2)}\, d\theta, \qquad [3]$$

where θ_0 is the acceptance angle of the detector (see footnote 2 for the meaning of other symbols). We introduce this parameter in order to indicate the fact that some part of the light scattered into small angles could impinge upon the detector, thus decreasing the apparent turbidity.

Calculations based on Eq. [3] show that, as size increases, turbidity rises to a plateau value, given a finite but small acceptance angle. The physical reason for this behavior is that larger particles scatter more and more light into the small scattering angle domain as diameter increases. As a consequence, experimental readings will strongly depend upon spectrophotometer geometry. We found, for instance, that the turbidity changes dramatically when the sample-detector distance is changed. The calibration procedure 1 (see above) and the experimental measurement must, therefore, be done under the same conditions (including sample concentration, lipid content, and measurement geometry). The problem of sample-detector geometry could be resolved by appropriate correction factors (8) or instrumentally, by using diaphragms (4), but doing so would considerably complicate the procedure.

Equation [3] can be rewritten in the following general form

[2] The intensity of transmitted light, I, is given by

$$I = I_0 \exp(-\alpha_S n \sigma l),$$

where α_S is scattering efficiency, n the concentration of particles, σ is their cross-sectional area, l the optical path length, and I_0 the intensity of the incident light. Turbidity, A, is

$$A = -\log(I/I_0) = 0.43\alpha_S n \sigma l.$$

The concentration, n, of unilamellar vesicles with bilayer thickness h and diameter D (assuming $h \ll D$), is given by

$$n = c/m_0 = cS_0N_A/2\pi MD^2,$$

where c is the weight concentration of lipid, m_0 the mass of individual vesicle, S_0 the area per lipid molecule in the bilayer, and M the molecular weight of lipid. Taking into account that $\sigma = \pi D^2/4$, one can obtain

$$A = 0.43\alpha_S(cS_0N_A/2\pi MD^2)(\pi D^2/4)l = 0.054\alpha_S cS_0N_A l/M.$$

$$A(D, \lambda) = f(D/\lambda)/\lambda^2. \quad [4]$$

The function f in the above equation can be obtained from the turbidity spectrum of a standard sample (known size) and then used to generate the size-turbidity relationship for a fixed wavelength. This consideration makes possible another mode of spectrophotometer calibration, utilizing only a single sample of known size.

1. Measure the turbidity spectrum (turbidity A as a function of wavelength) of a sample having a vesicle population of known size; i.e., obtain the function $A_0(\lambda) = A(D_0, \lambda) = f(D_0/\lambda)/\lambda^2$. As with procedure 1, the calibration sample can be produced by extrusion.
2. Calculate the size dependence of turbidity measured at some fixed wavelength λ_0, using the equation

$$\begin{aligned} A(D, \lambda_0) &= f(D/\lambda_0)/\lambda_0^2 = f(D_0/(\lambda_0 D_0/D))/\lambda_0^2 \\ &= f(D_0/\lambda^*)/\lambda_0^2 = \lambda^{*2} A_0(\lambda^*)/\lambda_0^2 \\ &= D_0^2 A_0(\lambda = \lambda_0 D_0/D)/D^2, \end{aligned} \quad [5]$$

where $\lambda^* = \lambda_0 D_0/D$.

It should be noted that this approach allows calibration only in a limited size range. Let us assume that a D_0 = 100-nm extruded sample is produced and the turbidity spectrum is obtained over the λ = 400–800 nm spectral range. Then, for λ_0 = 400 nm, the calibration can be used for sizes $D = \lambda_0 D_0/\lambda$ = 50–100 nm and, for λ_0 = 800 nm, $D = \lambda_0 D_0/\lambda$ = 100–200 nm. Naturally, this approach would benefit from any extension of spectral range.

Concluding Remarks

Turbidity and turbidity spectra measurements have been successfully used in the past to estimate the average size of dispersed particles (see Ref.7, pp. 325–343; 9, pp. 491–494). Interestingly, specific turbidity (i.e., turbidity normalized to concentration) for solid spheres at first increases with size, reaches a maximum, and then decreases for larger sizes. What accounts for the difference from the case of hollow spheres? If the scattering efficiency has a plateau because of interference of light scattered by different parts of the particle, this would seem to apply to solid spheres as well. Closer analysis reveals that a difference between shells and spheres is, in fact, expected. Equation [1] indicates that the only term which relates turbidity to size is the scattering efficiency of individual vesicles. In fact, turbidity is also proportional to the cross-sectional area of the particle (i.e., to D^2) and to the number of particles in a unit volume, which for vesicles (i.e., thin shells) is inversely proportional to D^2. Since these two dependencies mutually cancel, neither appears in Eq. [1]. The situation is different if particles can be represented as a solid sphere. In that case their cross-sectional area is given by the same expression, but the particle concentration is inversely proportional to D^3 (not D^2), thus causing a decrease of the turbidity as a function of size, as long as the scattering efficiency increase is not so large as to overwhelm the particle concentration effect.

The range of sizes available for the method is limited by the wavelength of incident light, thus giving the maximal measurable size of about 500–600 nm (can be slightly extended if proper equipment is available to take readings in the infrared range). Theory predicts that one can extend this range by reducing the acceptance angle of the light detector; however, even with a zero aperture, the turbidity changes by only about 15% when the vesicle diameter drops from two to one wavelength. The accuracy of the procedure could thus decrease, even with precautions to minimize the acceptance angle.

Chong and Colbow (4) previously described a method to obtain vesicle sizes using the turbidity spectrum. Their method did not involve use of any standards and, as a consequence, required determination of the refractive index spectrum of the lipid. Determination of the refractive index is tedious and requires specialized equipment (10). On the other hand, the introduction of extrusion methods (1, 2) has made it very easy to prepare vesicle dispersions of known size. Turbidity-based vesicle size measurement has thus become eminently practical. Because the method presented here has important advantages of speed, simplicity, and common availability of the necessary equipment, it should be useful in laboratories in which liposome research is done.

Acknowledgments. This work was supported by NIH Grants GM52329 and HL59586. L.M. was supported by the National Science Foundation through the Materials Research Internships for Minority Undergratuates Program, Materials Research Center, Northwestern University (DMR-9632472). We acknowledge the use of dynamic light scattering instrument in the Keck Biophysics Facility at Northwestern University.

REFERENCES

1. Hope, M. J., Bally, M. B., Webb, G., and Cullis, P. R. (1985) Production of large unilamellar vesicles by a rapid extrusion procedure—Characterization of size distribution, trapped volume and ability to maintain a membrane-potential. *Biochim. Biophys. Acta* **812**, 55–65.
2. MacDonald, R. C., MacDonald, R. I., Menco, B. P. M., Takeshita, K., Subbarao, N. K., and Hu, L. R. (1991) Small-volume extrusion apparatus for preparation of large, unilamellar vesicles. *Biochim. Biophys. Acta* **1061**, 297–303.
3. Koppel, D. E. (1972) Analysis of macromolecular polydispersity in intensity correlation spectroscopy: The method of cumulants. *J. Chem. Phys.* **57**, 4814–4820.

4. Chong, C. S., and Colbow, K. (1976) Light scattering and turbidity measurements on lipid vesicles. *Biochim. Biophys. Acta* **436**, 260–282.
5. Lord Rayleigh (1918) On the scattering of light by spherical shells, and by complete spheres of periodic structure, when the refractivity is small. *Proc. R. Soc. A* **94**, 296–300.
6. Tinker, D. O. (1972) Light scattering by phospholipid dispersions: Theory of light scattering by hollow spherical particles. *Chem. Phys. Lipids* **8**, 230–257.
7. Kerker, M. (1969) The Scattering of Light and Other Electromagnetic Radiation, Academic Press, New York.
8. Heirwegh, K. P. M. (1966) Errors in extinction measurements as due to scattering of light by solutions of relatively small particles. *J. Colloid Interface Sci.* **21**, 1–8.
9. Allen, T. (1990) Particle Size Measurement, 4th ed., Chapman & Hall, London.
10. Yi, P. N., and MacDonald, R. C. (1973) Temperature dependence of optical properties of aqueous dispersions of phosphatidylcholine. *Chem. Phys. Lipids* **11**, 114–134.

Concurrent Measurement of Promoter Activity and Transfection Efficiency Using a New Reporter Vector Containing both *Photinus pyralis* and *Renilla reniformis* Luciferase Genes

Jae B. Park[1]

Phytonutrients Laboratory, Building 307, Room 313, Beltsville Human Nutrition Research Center, Agricultural Research Service, USDA, Beltsville, Maryland 20705

Received October 6, 2000; published online February 26, 2001

Reporter vectors are essential for the quantitative analysis of gene elements that potentially regulate mammalian gene expression (1). These gene elements may be *cis*-acting, such as promoters and enhancers, or *trans*-acting, such as various DNA-binding factors (2). Several kinds of reporter vectors have been developed to study the promoter and/or enhancer activities of genes: chloramphenicol acetyltransferase (CAT)[2] reporter vector, β-galactosidase reporter vector, β-glucuronase, alkaline phosphatase reporter vector, green fluorescent protein reporter vector, and luciferase reporter vector (3–7). Currently, reporter vectors using chemiluminescence-based assays (β-galactosidase reporter vector, β-glucuronase, alkaline phosphatase reporter vector, and luciferase reporter vector) are commonly used in many quantitative analyses of gene elements (8), because the sensitivity of the assays is several orders of magnitude greater than that of conventional colorimetric- or fluorometric-based assays. Of them, luciferase reporter vectors are the most favored reporter vectors for functional analysis of promoters and enhancers of genes, due to their rapid, sensitive, and reproducible assay system (9). In the luciferase assay, luciferin and other components are added to cell extracts, and the production of light from both cell extracts expressing the luciferase gene is measured conveniently by a luminometer or scintillation counter (10).

Although luciferase reporter vectors have been commonly employed in numerous studies, the transfection of only luciferase vector cannot provide normalized values of the activities of gene elements without simultaneous transfection of a second reporter vector to measure the efficiency (11). In this paper, a novel report vector ($pJDL_{cmv}$) was constructed to contain two luciferase genes, *Photinus pyralis* and *Renilla reniformis* luciferases, regulated by two different promoters for the first time, in order to measure simultaneously promoter activity and transfection efficiency. Two promoters of human glutaredoxin and ribonucleotide reductase R2 gene were investigated with this novel reporter vector to verify its appropriateness for simultaneous measurement of promoter activity and transfection efficiency.

Materials and Methods

T4 DNA ligase and restriction enzymes were purchased from Promega (Madison, WI), Chameleon double-stranded site directed mutagenesis kit was from Stratagene (La Jolla, CA), and *Taq* polymerase and deoxynucleotides were from Perkin-Elmer (Norwalk, CT). Bio-Rad protein assay kit (Bio-Rad, Hercules, CA) was used to determine the amount of protein.

Cell culture conditions. HeLa and NT cells were cultured in DMEM supplemented with 10% fetal bovine serum. The cells were grown to 60% confluence for the transfection experiments.

PCR cloning of P. pyralis and R. reniformis luciferase genes. *P. pyralis* and *R. reniformis* luciferase genes were amplified from pGL and pRL vectors (Promega), respectively, by PCR using respective forward and backward primers corresponding to two genes: 5′-TGCTTGGCATTCCGGTACTGTTGG-3′ and 5′-TTTACAATTTGGACTTTCCGCCCTTCTT-3′ for the *Photinus* gene; 5′-CTGCAGAAGTTGGTCGTGAGGCAC-3′ and 5′-TTGTTCATTTTTGAGAACAGC-3′ for the *Renilla* gene (12).

PCR cloning of two DNA fragments containing poly(A) signal for P. pyralis and R. reniformis luciferase genes. Two DNA fragments containing SV40 early and late poly(A) signals were respectively amplified from pEGFP (Clontech) and pRL (Promega) by PCR using forward and

[1] Fax: (301) 504-9456. E-mail: Park@307.bhnrc.usda.gov.

[2] Abbreviations used: CAT, chloramphenicol acetyltransferase; DMEM, Dulbecco's modified Eagle's medium; PCR, polymerase chain reaction; CMV, *cytomegalovirus;* poly(A), polyadenylation.

Analytical Biochemistry **291**, 162–166 (2001)
doi:10.1006/abio.2001.5003
0003-2697/01 $35.00

International Journal of Food Science and Technology 2002, 37, 263–269

Formation of sunflower oil emulsions stabilized by whey proteins with high-pressure homogenization (up to 350 MPa): effect of pressure on emulsion characteristics

Anne Desrumaux* & Julie Marcand

Département de Génie des Procédés Alimentaires, ENITIAA GPA, BP82225-44322 Nantes Cedex 03, France

(Received 9 August 2000; Accepted in revised form 6 February 2001)

Summary A new ultra-high-pressure homogenizer was used to make very fine oil in water emulsions. The effect of pressures up to 350 MPa on sunflower oil (20%) in water emulsions was studied. The emulsifier used was whey protein concentrate (1.5%). The properties of the emulsions were characterized by laser light scattering (droplet size distribution) and coaxial cylinders rheometry (rheological behaviour). The protein adsorption fraction was obtained by a spectrophotometric method using bicinchoninic acid reagent.

Significant modifications in the structure and the texture of the emulsions were observed as the pressure increased. No change was revealed by polyacrylamide gel electrophoresis of the whey protein within the pressure range studied. Microdifferential scanning calorimetry scans indicated that the changes of the structural and textural properties may be because of changes in the protein conformation.

Keywords Droplet size, emulsification, microdifferential scanning calorimetry, protein adsorption, viscosity.

Introduction

A large variety of foods are emulsions, from the more natural, e.g. milk, to the more sophisticated, e.g. sausages, mayonnaises. Emulsions are dispersions of liquid droplets in a liquid continuous phase. As the two liquids are immiscible, emulsions are very unstable. In order to stabilize emulsions, there must be surface active molecules at the interface of the droplet to prevent instantaneous coalescence.

Food emulsions are commonly produced in high-pressure homogenizers, in colloid mills or in batch reactors with high-speed blenders. Initially built for the homogenization of milk, high-pressure homogenizers are the most often used, as they give fine emulsions with precise texture properties (creams, ice creams) and higher degrees of stability. The principle of high-pressure homogenization is simple: a coarse emulsion produced with a high-speed blender is forced under pressure through a narrow valve. The combination of the intense shear, cavitation and turbulent flow conditions in this valve leads to the disruption of fat globules (Walstra & Smulders, 1997; McClement, 1999). The decrease of the average size of the fat globules reduces the creaming velocity (Stokes law) and increases the stability of the emulsion. Food homogenizers usually go up to 60 MPa and the gap of the valves is typically between 15 and 300 μm. Increasing the pressure and decreasing the gap size cause a greater degree of breakdown of droplets. Despite the large use of high-pressure homogenizers, few studies deal with the effect of very high pressures on the emulsions properties. Moreover, the studies are limited in the pressure range. According to Mulder & Walstra (1974) and Phipps (1975), the average fat globule diameter (d) decreases with emulsification pressure (P) in a relation $d\alpha P^{-0.6}$, for pressures between 0.25 and 40.5 MPa. Davies (1985) described the breakdown of fat droplets with the Kolmogoroff theory and found a relation between the maximal droplet size

*Correspondent: Fax: +33 251785467;
e-mail: desrumau@enitiaa-nantes.fr

and $P^{0.4}$. According to Tornberg (1980), for pressures over 40 MPa and for a mass oil fraction of 12%, a phenomenon called 'overprocessing' occurs: the average droplet size increases with pressure. Robin *et al.* (1992) processed butter oil in water emulsions, with sodium caseinate as emulsifier, from 7.8 to 76.3 MPa in a microfluidizer. In the microfluidizer, two microsteams were projected under pressure against one another. They showed that the average size of fat globules decreased with pressure and reached a minimum around 60 MPa. Until now, no study has related the effect of 'dynamic' high pressures over 100 MPa on food emulsion formation. The effects of isostatic pressure on emulsions has been studied as a means of preservation. It has been shown that its influence on the already formed emulsions depends on the emulsifiers used (Dumay *et al.*, 1996).

Thus, the purpose of this work was to test the hypothesis that ultra-high-pressure homogenization (from about 50 to 350 MPa) significantly alters properties of oil-in-water emulsions when compared with more traditional pressure treatments.

Material and methods

Ingredients

Whey protein concentrate 'PS85' (85% protein), obtained by ultrafiltration of casein serum, was supplied by Eurial Poitou Touraine (Herbignac, France). The reported composition of this product is: $N \times 6.38$: 85%; fat: 3%; mineral salts: 4%; water content: 4%; pH 6.5 ± 0.2. The proteins are soluble over the complete pH range, and are good emulsifiers at pH < 7.

Sunflower oil was purchased from Lesieur (Neuilly-sur-Seine, France). Distilled water was filtered through a 0.2-μm filter before use. Solutions of whey proteins (1.5%) were prepared using a ultraturrax rotor–stator system (Ika Larbortechnik, Staufen, Germany) and stored at 4 °C.

Ultra-high-pressure homogenizer

Coarse emulsions containing 20%, by mass, of sunflower oil and 80% of the whey protein concentrate aqueous solution were prepared at 4 °C, using an ultraturrax rotor–stator system and then passed through a homogenizer operating from 20 to 350 MPa (Stansted Fluid Power Ltd, Essex, UK). Emulsions were homogenized at different pressures in the range of 50–350 MPa. The homogenizing chamber was cooled with a cooling jacket containing cold water at 5 °C, in order to slow down the rise of temperature. Each emulsion was carefully collected and stored at 4 °C before analysing. This procedure was used to prevent any change in the size distribution of the fat globules because of churning. The experiments were duplicated.

The reproducibility of the high-pressure homogenization was tested by repeating an experimental point (20% oil, 150 MPa) four times.

Light scattering measurements

The size distributions of the oil droplets were determined by the laser light scattering method. The diffractometer model used was the Mastersizer S (Malvern Instruments, Malvern, UK) equipped with a 300 reverse Fourier lens and a He–Ne laser ($\lambda = 633$ nm). The emulsion was measured 5 min after ultra-high-pressure homogenization to cancel any creaming effect, and diluted to about 1/1000 with distilled water in the diffractometer cell, whilst stirring. Size distribution was presented as volume percentage vs. droplet diameter. The volume size distribution was calculated from the intensity of the light diffracted at each angle using Mie theory. The analysis requires a parameter known as the presentation value, a combination of the ratio of the relative refractive indices of the dispersed phase and water and the absorbance of the dispersed phase. The 3NAD presentation was used: oil (1.4564, 0.0000) in water (1.33), for which the absorbance value was selected after consultation with Malvern Instruments and verified using a carefully diluted emulsion of known concentration. The full size distribution was obtained using a polydisperse analysis, which allowed the calculation of the mean droplet diameter d_{32} (Sauter mean diameter) and a dispersion index called 'span', defined as

$$\text{span} = \frac{d[90] - d[10]}{d[50]}$$

where $d[x]$ is the average droplet size in a volume in which $[x]$% of the total sample weight remains constant. Measurements were repeated three times for each sample.

Rheology measurements

Dynamic shear stress measurements were done at 20 °C with an AR 1000 Rheometer (TA Instruments, Waters Corporation, USA), equipped with a coaxial system (medium concentric cylinder with a conical end; R1 = 13.83 mm, R2 = 15.0 mm). Flow curves (shear stress vs. shear rate) were determined at increasing shear rates: 0–1200 s^{-1} in 2 min (up and down flow curves).

Protein surface concentration

Emulsion samples were centrifuged at 13 000 *g* for 30 min to separate the droplets from the aqueous serum phase. The supernatant (the cream) was carefully removed from the aqueous phase using a syringe. The cream layer was resuspended in ultrapure water to wash away any protein trapped between droplets, and the resulting emulsion was centrifuged again at 13 000 *g* for 30 min. The protein concentration of the two serums was determined by the Sigma Pierce spectrophotometric method using bicinchoninic acid reagent (BCA, Sigma procedure TPRO-562). This spectrophotometric method is based on the reduction of Cu^{2+} to Cu^{+} by the proteins (Biuret reaction). Cu^{+} reacts with the BCA and an intense purple complex is formed. This complex produces an absorbance maximum at 562 nm, which is directly proportional to the protein concentration (Smith *et al.*, 1985). A calibration curve was generated using bovine serum albumin (BSA) standard solution (Sigma, St Louis, USA), with a determination coefficient $r^2 = 0.99$ (15 different concentrations used). The quantity of whey proteins absorbed was expressed in equivalent BSA and was calculated from the difference in the serum concentration prior to and after emulsification. The surface concentration of the absorbed protein was calculated from the known surface area per unit volume of emulsion and the difference in the amount of protein measured in the serum phase and the amount used to make the original emulsion, making allowance for any dilution.

Electrophoresis (SDS-PAGE)

The protein fractions were determined by sodium dodecyl sulphate-polyacrylamide gel electrophoresis (SDS-PAGE), following the procedure described by Arrese *et al.* (1991). Gel slabs were fixed and stained simultaneously in aqueous solution containing 40% v/v ethanol, 7% v/v acetic acid and 0.025% coomassie brilliant blue R250. Proteins were denaturated with a treatment buffer containing 0.125 M Tris, 4% SDS v/v Glycerol, 0.2 M dithiotreitol, 0.02% bromophenol blue. About 50 µg of protein was applied to each gel slot. Molecular weights of the protein bands were estimated by means of the SDS-70L kit (Sigma Chemical Co., St Louis, USA).

Microdifferential scanning calorimetry

Microdifferential scanning calorimetry (µDSC) was used to assess the degree of denaturation of the whey protein by the pressure of homogenization. µDSC thermographs of aqueous solutions of whey proteins before and after a single run in the homogenizer were prepared by using a Setaram 3 calorimeter (Calluire, France). Samples (700 mg) of 2% dispersions of whey proteins (pH 6.7) in distilled water were hermetically sealed in hastelloy C276 pans (volume = 1 cm^3). A closed pan filled with distilled water was used as the reference. The heating rate was fixed at 0.5 °C min^{-1} from 20 to 110 °C. Triplicate samples were analysed by µDSC.

Results and discussion

Whey protein composition

Electrophoresis measurements indicated that the whey proteins were mainly composed of β-lactoglobulin (18 600 Da), α-lactalbumin (14 200 Da), and serum albumin (66 000 Da) (Fig. 1). Examination of the µDSC curves showed three endothermic phenomena (Fig. 2): the first around 40–45 °C, the second between 60 and 65 °C and the third between 70 and 75 °C. These endothermic phenomena in whey proteins are explained by the behaviour of β-lactoglobulin and α-lactalbumin, which are the predominant proteins (Paulsson *et al.*, 1985). The dimer form of β-lactoglobulin exits at 5.2 < pH < 7.5 as in our case (pH 6.7). Thus, according to McKenzie (1971) the first endothermic peak could be a dissociation of the dimers of β-lactoglobulin. The

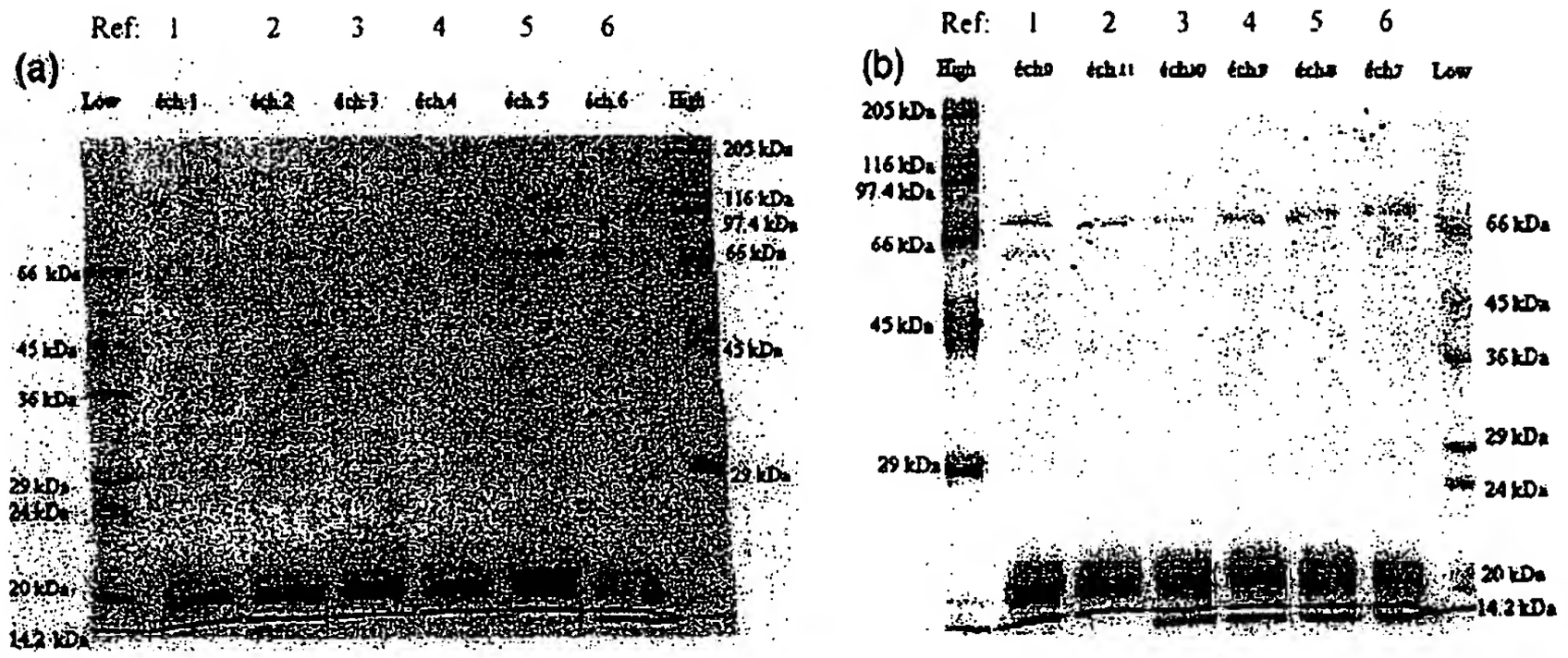

Figure 1 (a) SDS-PAGE of proteins before and after a single run in the homogenizer. Ref: α-lactalbumin (14.2 kDa), tripsin (20 kDa), egg albumin (45 kDa), serum albumin (66 kDa). Column 1: before homogenization. Columns 2–6: after a single run in the homogenizer at 2: 30 MPa; 3: 60 MPa; 4: 90 MPa; 5: 120 MPa; 6: 150 MPa. (b) SDS-PAGE of protein after one run in the homogenizer. Ref: see (a). Column 1: 180 MPa; 2: 210 MPa; 3: 240 MPa; 4: 270 MPa; 5: 300 MPa; 6: 350 MPa.

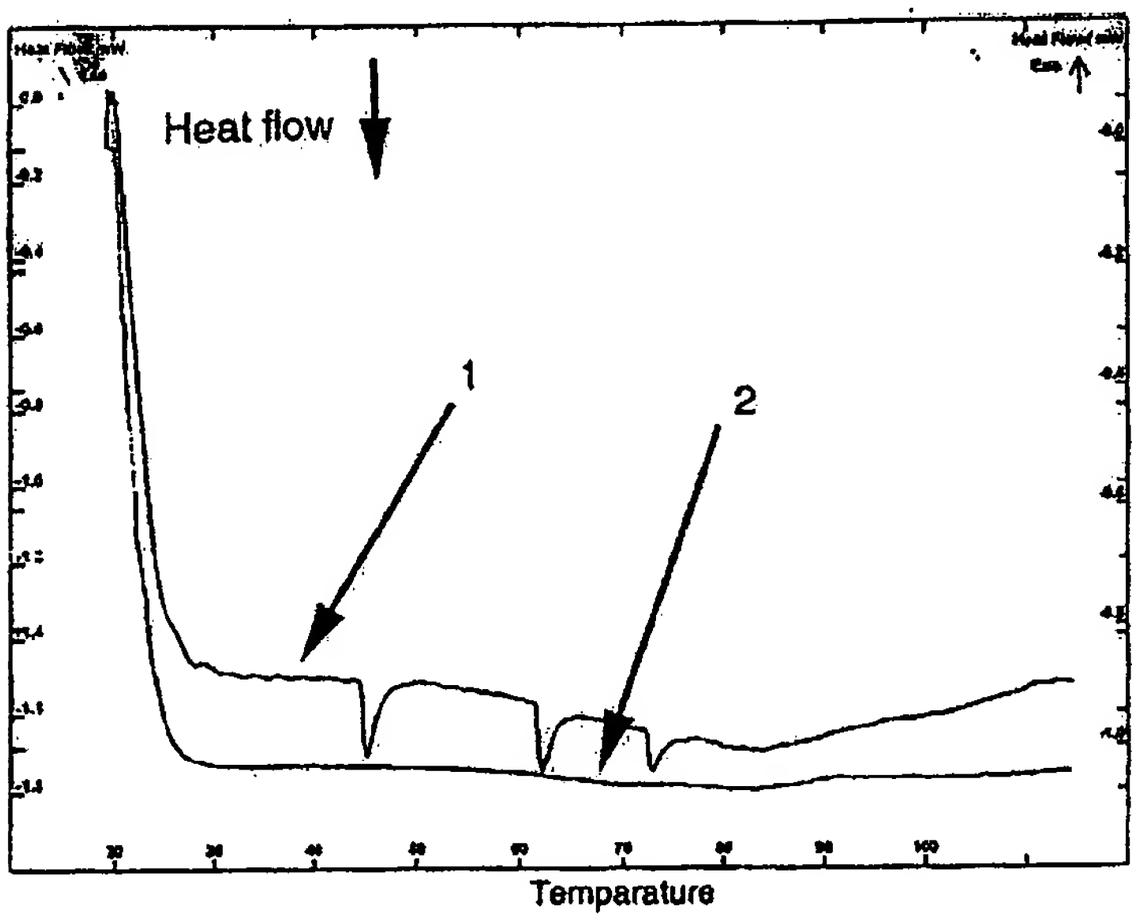

Figure 2 Micro-DSC graph of whey protein aqueous solutions (1.5%) before (1) and after (2) treatment at 300 MPa in the high-pressure homogenizer.

second endothermic peak at 60–65 °C corresponds at pH around 7 to the denaturation of the α-lactalbumin, and the last endothermic peak around 70–75 °C corresponds to the denaturation of the β-lactoglobulin.

Reproducibility of the experiments

The reproducibility of the high-pressure homogenization after testing with an experimental point (20% oil, 150 MPa) and repeated four times on four different days is shown in Table 1. According to the s.d. obtained, the reproducibility was satisfactory.

Evolution of temperature during the experiments

Despite the use of the cooling jacket, the temperature of the emulsion at the exit of the valve increased linearly with the pressure in the valve

Table 1 Reproducibility of the point 150 MPa, 20% oil

Temperature at the exit of the homogenizer	Sauter diameter d_{32} (μm)	Size dispersion coefficient	Viscosity (Pa s)	Fraction of adsorbed proteins (mg m^{-2})
40 °C (1)	0.68 (0.02)	3.75 (0.6)	0.009 (0.001)	0.77 (0.1)

Values within parentheses are standard deviations.

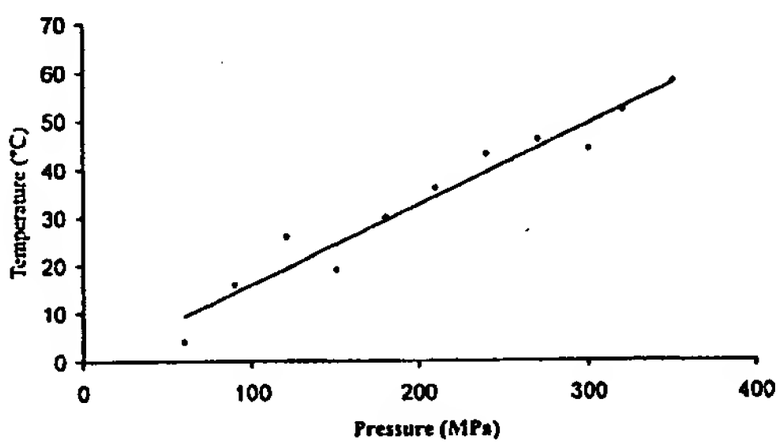

Figure 3 Effect of pressure on the temperature at the exit of the homogenizer.

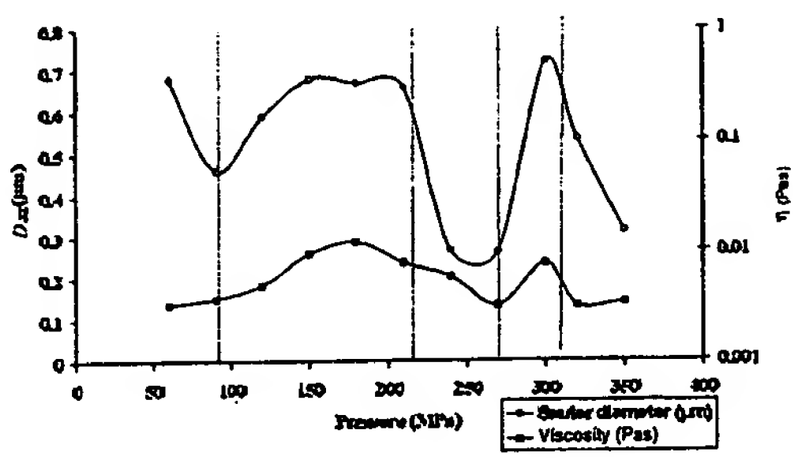

Figure 4 Effect of the pressure of homogenization on the Sauter diameter d_{32} and the viscosity η of the emulsions.

(Fig. 3). Above 300 MPa, the temperature of the emulsion at the exit is close to the temperatures of the peaks observed by μDSC.

Effect of high pressure on emulsion properties

The Sauter diameter before homogenization was around 30 μm. Homogenization reduced the Sauter diameter appreciably, the reduction increasing with treatment pressure from 50 to 90 MPa (Fig. 4). This result agrees with the study of Robin *et al.* (1992), who observed a decrease in the droplet average size between 7.8 and 76.3 MPa. Above 90 MPa, d_{32} increased with pressure (Fig. 4) and then stabilized approaching 200 MPa. Robin *et al.* (1992) observed a similar plateau of the droplet size diameter, but between 60 and 76.3 MPa. This phenomenon can be referred to as 'overprocessing,' as stated by Tornberg (1980): the average droplet size is stable over a certain range of pressure, and increases at higher pressures. The density of energy (up to 10^{12} W m^{-3}) is estimated by knowing the flow rate and the pressure drop inside the valve, and is partially dissipated as heat (Fig. 3), which can lead to an increase of the Sauter diameter: the Brownian motion increases and so also the probability of collision and coalescence.

Above 200 MPa, d_{32} decreased and then increased again at around 250 MPa. However, there was a final decrease of d_{32} above about 300 MPa. This final decrease could be explained by the increased probability of rupture. At this level of pressure, the shear rate inside the valve is enormous, the probability of rupture again becomes higher than the probability of coalescence and d_{32} decreases.

The effects of high-pressure homogenization on the sizes dispersion coefficient are interesting: above 90 MPa, as the pressure increased, the dispersion coefficient strongly decreased (sevenfold) (Fig. 5). Also, the droplet size distribution was bimodal for the lower pressures, but at higher

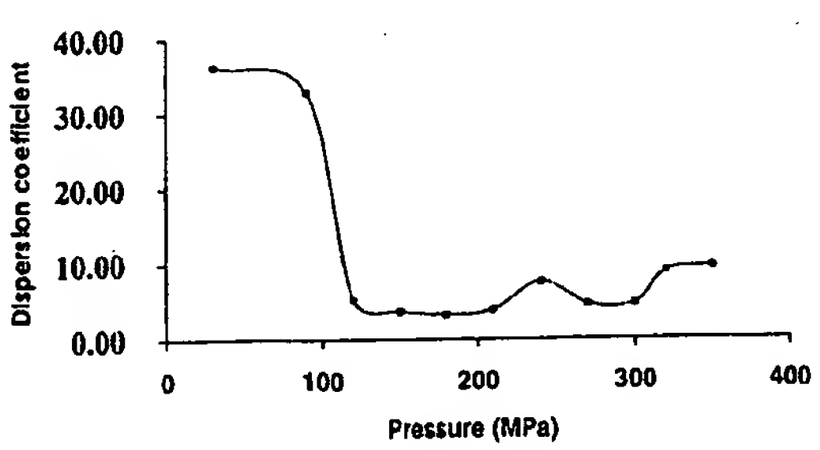

Figure 5 Effect of pressure of homogenization on the size dispersion coefficient of the droplet.

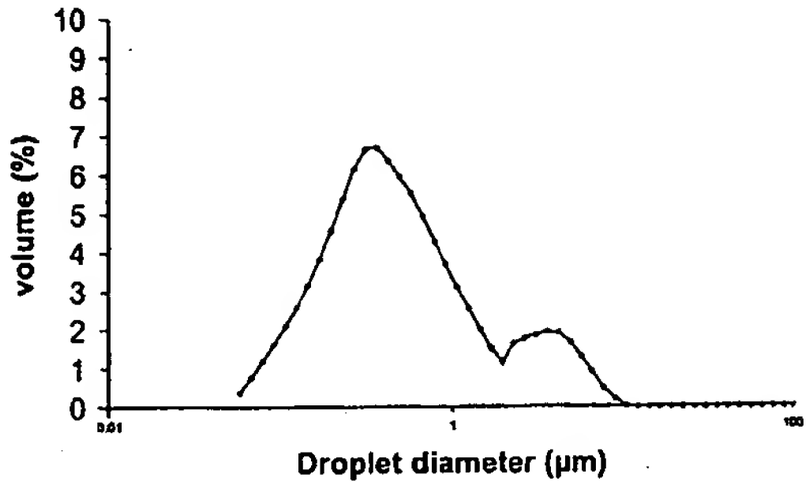

Figure 6 Size distribution of the oil droplet of the emulsion after a single run in the homogenizer at 300 MPa.

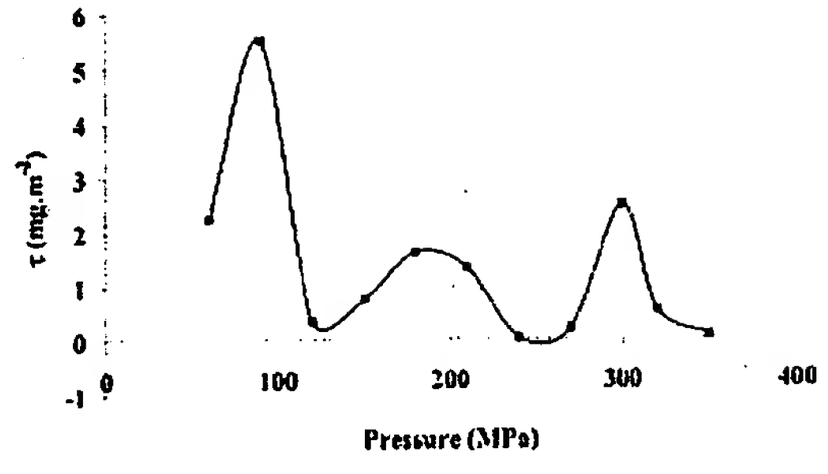

Figure 7 Effect of pressure of homogenization on the fraction of absorbed proteins.

pressures the second peak decreased (Fig. 6). Thus, the coalescence rate of the droplets is reduced because a large dispersion favours rapid coalescence. Above 90 MPa, the main effect of high-pressure homogenization on the size properties is the decrease in the dispersion coefficient of size.

Examination of the rheological properties of the emulsions showed a Newtonian behaviour in all cases, agreeing with previous studies (Desrumaux & Della Valle, 1999). However, the viscosity changed with the pressure in the valve (Fig. 4).

It is interesting to see the similarity of behaviour between the curves for the viscosity η and the Sauter diameter d_{32} (Fig. 4). Both show a complicated behaviour, with four zones, although differences exist in the limits of the zones. In the first zone, up to 90–100 MPa, the Sauter diameter decreased and viscosity increased slowly (Fig. 4). At the same time, the amount of adsorbed protein increased (Fig. 7), as expected, since, as the average droplet size decreases, the specific area increases, which leads to an increase of the fraction of adsorbed proteins. Above 100 and up to ≈210 MPa, d_{32} increased and reached a plateau (Fig. 4), which can be attributed to the 'overprocessing' phenomenon. Simultaneously, the fraction of adsorbed proteins decreased strongly and then increased (Fig. 7). Viscosity followed the same behaviour as d_{32} (Fig. 4). Above 200–210 MPa the behaviour of the structural and textural properties was complicated and, is probably explained, by the effect of the high pressure on the protein conformation. Indeed, studies on isostatic high-pressure treatment of proteins have shown that pressure has a huge effect on food protein functionality (Messens *et al.*, 1997). High-pressure effects on proteins are primarily related to the rupture of noncovalent interactions within protein molecules and to the subsequent re-formation of intra- and intermolecular bonds within or between protein molecules (Smith *et al.*, 2000). As extensively described by Messens *et al.* (1997), the whey proteins, particularly the β-lactoglobulin, are far more sensitive to isostatic pressure than other proteins such as BSA. In our case the treatment at high pressure was very short, estimated at 10^{-4} s from the flow rate and the size of the gap (≈1 µm), but was associated with a significant rise in temperature (Fig. 3). The complicated effects of pressure on emulsions properties could be explained by a change of conformation of the emulsifying whey proteins during the emulsification process. Only a small part of the whey protein is likely to be absorbed at the water/oil interface in the coarse emulsion, because the kinetics of absorption requires a much longer time than that for emulsification. Thus, a large part of the whey protein was in the aqueous phase during the homogenization and the absorption of the whey protein at the interface occurred after homogenization. In order to understand the possible change of the whey protein, we tested aqueous whey protein solutions (1.5%) before and after a single run in the homogenizer at 300 MPa (Fig. 2). Comparing the µDSC graph with the µDSC graph obtained before treatment in the high-pressure homogenizer (Fig. 2), it can be seen that the endothermic peaks disappeared, indicating that the proteins had probably denatured. This phenomenon is because of the combined

effects of the high shear rate inside the gap (velocity at 300 MPa estimated at 500 m s^{-1}) and the rise of temperature observed. At such a high pressure, it was impossible to slow down the rise of temperature inside the valve, the temperature at the exit being directly proportional to the pressure of homogenization. Electrophoresis measurements of extracted proteins after treatment in the high-pressure homogenizer did not show any significant change in the molecular weights (Fig. 1b): the proteins were not broken down into smaller entities during the homogenization, the time of treatment (estimated at 10^{-4} s) probably being too short.

Over 200–210 MPa, the proteins were denatured and had probably partially lost their emulsifying activity (Fig. 4). The effect of the high-pressure homogenization could be protein aggregation; however, the electrophoresis experiments in the presence of SDS prevents observation of protein aggregation.

Conclusions

The effects of high-pressure homogenization on oil in water emulsions are complicated. From 20 to 100 MPa, the Sauter diameter decreased, confirming the results of Davies (1985) and Robin *et al.* (1992). Over 100 MPa, d_{32}, viscosity and the fraction of adsorbed protein displayed up to four zones of behaviour: from 100 to 210 MPa, the Sauter diameter and viscosity increased up to a maximum. This behaviour could be because of the 'overprocessing' phenomenon. Over 210 MPa, μDSC graphs on whey proteins before and after a single run at 300 MPa in the homogenizer confirmed changes in protein conformation, probably because of the combined effects of high-pressure treatment and the rise in temperature observed. This change in the conformation of proteins probably modifies the emulsifying properties of the whey proteins. There is a strong correlation between the formulation of emulsion and the range of pressure used in homogenization. For sunflower oil in water emulsion (20% oil) stabilized with whey proteins, the optimum pressure of homogenization according to the light scattering measurements is ≈100 MPa. At this pressure the d_{32} and the size dispersion coefficient reach a minimum.

Acknowledgments

The authors wish to thank Pierre Cantoni for his technical assistance.

References

Arrese, E.L., Sorgentini, D.A., Wagner, J.R. & Anon, M.C. (1991). Electrophoretic, solubility, and functional properties of commercial soy protein isolate. *Journal of Agricultural Food Chemistry*, 39, 1029–1032.

Davies, J.T. (1985). Drop sizes of emulsions related to turbulent energy dissipation rates. *Chemical Engineering Science*, 40, 839–842.

Desrumaux, A. & Della Valle, D. (1999). Rhéologie d'émulsions huile dans eau: influence du procédé. *Les Cahiers de Rhéologie*, 16, 358–363.

Dumay, E., Lambert, C., Funtenberger, S. & Cheftel, J.C. (1996). Effects of high pressures on the physicochemical characteristics of dairy creams and model oil in water emulsions. *Lebensmittelwissenchaft und Technologie*, 29, 606–625.

McClement, D.J. (1999). *Food Emulsions: Principles, Practice and Techniques*. Pp. 161–183, Boca Raton, FL: CRC Press.

McKenzie, H.A. (1971). β-Lactoglobulins. In: *Milk Proteins 2*. Pp. 257–330. New York: Academic Press.

Messens, W., Van Camp, J. & Huyghebaert, A. (1997). The use of high pressure to modify the functionality of food proteins. *Trends in Food Science and Technology*, 8, 107–112.

Mulder, H. & Walstra, P. (1974). *The Milk Fat Globule, Emulsion Science as Applied to Milk Products and Comparable Foods*. Pp. 163–192, UK: CABI.

Paulsson, M., Hegg, P.O. & Castberg, H.B. (1985). Thermal stability of whey proteins studied by differential scanning calorimetry. *Thermochemica Acta*, 95, 435–440.

Phipps, L.W. (1975). The fragmentation of oil drops in emulsions by a high-pressure homogenizer. *Journal of Physics D: Applied Physics*, 8, 448–462.

Robin, O., Blanchot, V., Vuillemard, J.C. & Paquin, P. (1992). Microfluidization of dairy model emulsions. I. Preparation of emulsions and influence of processing on the size distribution of milk fat globules. *Lait*, 72, 511–550.

Smith, P.K., Krohn, R.I., Hermanson, G.T. & Mallia, A.K. (1985). Measurement of protein using bicinchoninic acid. *Analytical Biochemistry*, 150, 76–85.

Smith, D., Galazka, V.B., Wellner, N. & Sumner, I.G. (2000). High pressure unfolding of ovalbumin. *International Journal of Food Science and Technology*, 35, 361–371.

Tornberg, E. (1980). Functional characteristics of protein stabilized emulsions: emulsifying behavior of proteins in a sonifier. *Journal of Food Science.*, 45, 1662–1668.

Walstra, P. & Smulders, P. (1997). Formation of emulsions. In: *Proceedings of the Second World Congress on Emulsion*, Vol 1. Paris: Lavoisier Press.

Lait (1992) 72, 511-531
© Elsevier/INRA

Original article

Microfluidization of dairy model emulsions. I. Preparation of emulsions and influence of processing and formulation on the size distribution of milk fat globules

O Robin, V Blanchot, JC Vuillemard, P Paquin

Université Laval, Sainte-Foy, centre de recherche en sciences et technologies du lait (STELA), département de sciences et technologie des aliments, (Québec), Canada G1K7P4

(Received 1st July 1992; accepted 17 September 1992)

Summary — The influence of certain process variables (pressure and temperature) as well as composition variables (fat, protein and low molecular weight emulsifier concentrations) on the size distribution of milk fat globules was studied in a dairy model emulsion (oil-in-water) produced by microfluidization, a mechanical emulsification technique. The use of a central composite experimental design allowed us to obtain 2 nonlinear multiple regression equations relating the volume-weighted average diameter of the fat globules ($\bar{d}_v$) as well as the relative size distribution width *(cv)* to the emulsification pressure (7.8–76.3 MPa) and temperature (35–100 °C), and to sodium caseinate (0.5–3.9 wt%), butter oil (5.2–14.7 wt%) and monoglyceride (0.08–0.88 wt%) concentrations. These 2 functions account respectively for 93.7 and 81.7% of the variation in the average diameter and in the size distribution width of the microfluidized fat globules and were used to explain certain interactions between the different variables affecting the size of the microfluidized fat globules. They were also used to demonstrate the existence of the optimal conditions that correspond to the extremes of the average particle diameter and of the distribution width of the fat globules. Finally, these 2 functions allowed us to predict fat globule size parameters as a function of process and formulation conditions.

emulsification / microfluidization / oil-in-water emulsion / fat globule

Résumé — Microfluidisation d'émulsions laitières modèles. I. Préparation des émulsions et influence des facteurs de procédé et de formulation sur la distribution de la taille des globules de gras. *L'influence de certaines variables opératoires (pression et température) et des variables de composition (teneurs en huile de beurre, en protéine et en émulsifiant de faible poids mo-*

Symbols used and SI units: [*BO*] = butter oil concentration (wt%); *cv* = coefficient of variation or relative standard deviation of the volume-weighted size distribution (%); $\bar{d}_v$ = volume-weighted average fat globule diameter (m); D = diffusion coefficient ($m^2.s^{-1}$); *F* = number of factorial points of the design and Fisher ratio; *k* = number of independent variables or conductivity of a solution ($S.m^{-1} = m^{-3}.kg^{-1}.s^3.A^2$); [*MGS*] = monoglyceride concentration (wt%); [*Prof*] = protein concentration (wt%); *P* = emulsification pressure ($Pa = m^{-1}.kg.s^{-2}$); *Q* = flow rate ($m^3.s^{-1}$); *S* = interfacial area (m^2); *T* = emulsification temperature (K); α = distance separating a star point from a factorial point in terms of coded variables (dimensionless); ε = power density ($W.m^{-3} = m^{-1}.kg.s^{-3}$); Φ = volume fraction of the disperse phase (dimensionless); γ = interfacial tension ($N.m^{-1} = kg.s^{-2}$); ρ = mass density ($kg.m^{-3}$).

léculaire) sur la distribution de la taille des globules de gras d'une émulsion laitière modèle (huile dans l'eau) a été étudiée pour une technologie d'émulsification mécanique donnée : la microfluidisation. L'utilisation d'un dispositif expérimental central composite a permis l'obtention de 2 équations de régression multiple non linéaires reliant le diamètre moyen des globules de gras ($\bar{d}_v$) ainsi que l'étendue relative de la dispersion des tailles (cv) à la pression (7,8–76,3 MPa) et à la température d'émulsification (35–100 °C), aux teneurs en caséinate de sodium (0,5–3,9% de la masse totale), en huile de beurre (5,2–14,7%) et en monoglycéride (0,08–0,88%). Ces 2 fonctions expliquent respectivement 93,7% et 81,7% des variations du diamètre moyen des globules de gras microfluidisés et de l'étendue relative de la distribution des tailles dans les valeurs considérées des paramètres. Ces fonctions ont en outre permis d'expliquer certaines interactions entre les différentes variables précitées sur la distribution de la taille des globules de gras microfluidisés. Elles ont également permis de mettre en évidence l'existence de conditions optimales correspondant à des extremums du diamètre particulaire moyen et de l'étendue de la distribution de la taille des globules de gras. Finalement, ces 2 fonctions nous ont permis de prédire la distribution de la taille des globules de gras en fonction des conditions de procédés et de formulation.

émulsification / microfluidisation / émulsions huile dans l'eau / globules de gras

INTRODUCTION

For a number of industries, the homogenization, and more generally the mechanical emulsification of liquids, dietary as well as others, has become over the past many years an important technological process. The use of this type of process in the food, pharmaceutical and cosmetic industries in general and in certain dairy operations in particular is essential for the production of emulsions with certain desirable rheological properties (creams and ointments), textures (ice cream, mayonnaise) and degrees of stability (milk, salad dressing) (Dickinson and Stainsby, 1988). The principle of homogenization and mechanical emulsification processes which, according to Gaulin, must allow "de fixer la composition des liquides" remains simple: in the case of milk, the homogenization process results in a considerable decrease in the size of the fat globules found in the initial suspension, and has the effect of increasing the creaming stability of the emulsion (Tadros and Vincent, 1983). Aside from conventional homogenizers, relatively few mechanical emulsification processes have been and are used in an industrial setting (Walstra, 1983). During the 1980s, however, other mechanical emulsification processes appeared. One of them, called microfluidization (Cook and Lagace, 1985; Washington, 1987), was initially used principally in the cosmetic and pharmaceutical industries (Chandonnet *et al*, 1985). More recently, microfluidization was suggested as an alternative method for the production of milk fat microcapsules (Vuillemard, 1991), alcoholized creams (Paquin and Giasson, 1989) and for milk homogenization (Pouliot *et al*, 1991). If the result of the process is similar to that of homogenization (reduction in the size of the fat globules), the means used to achieve such a result are different. As is the case for conventional homogenization processes, the liquid is forced under high pressure into a chamber. However, in the case of the microfluidization process, the liquid is then divided into 2 microstreams that are projected against one another at high speed and at an angle of 180° (Cook and Lagace, 1985).

Other than a considerable change in the dispersion state of the fat, the emulsification of dietary liquids also results in a considerable rearrangement of the oil–water interface

(Walstra and Oortwijn, 1982) where mainly 2 classes of molecules can be adsorbed: amphiphilic macromolecules (mainly proteins) and low molecular weight emulsifiers (lecithins, monoglycerides, Tweens, Spans, etc) (Dickinson *et al*, 1990). Proteins and low molecular weight emulsifiers affect the production and stabilization of emulsions. Proteins play 2 major roles: on the one hand they lower surface tension between the interfaces that are formed during the emulsification process, and on the other hand, they form a macromolecular layer surrounding the dispersed particles which structurally stabilizes the emulsion by reducing the rate of recoalescence (Fisher and Parker, 1988). Low molecular weight emulsifiers affect the production and stabilization of emulsions in several ways: during emulsification, by reducing interfacial tension more rapidly than would the proteins alone, they allow the production of smaller-sized dispersed particles (Darling and Birkett, 1987). Furthermore, while proteins generally stabilize oil-in-water emulsions, low molecular weight emulsifiers tend to destabilize them (Dickinson *et al*, 1990) by removing protein from the surface of the dispersed particles. This ability of low molecular weight emulsifiers to dislodge macromolecules is due to their greater energy of adsorption compared to individual segments of macromolecules. Finally, if the distribution of these 2 classes of molecules between the surfaces of the dispersed particles and the bulk phase is directly affected by the competitive adsorption between the macromolecules and the emulsifiers at the oil–water interface, it is also a result of the nature of macromolecule–emulsifier interactions at the interface and in the bulk phase (Dickinson, 1986).

Opinions are divided as to the usefulness of using experimental model systems (systems containing a single protein source and/or low molecular weight emulsifier) rather than real food systems (Darling and Birkett, 1987; Dickinson *et al*, 1990). Even if the model systems allow relatively precise information to be obtained, they can rarely be extrapolated to real food systems. An alternative would be to use systems that can be called "quasi-foods", that is systems that contain a known mixture of proteins and low molecular weight surfactants and whose concentrations are controlled.

The aim of the study presented here was to examine the influence of certain process (pressure and temperature) and composition (butter oil, protein and surfactant concentrations) variables on the size distribution of fat globules in a model dairy emulsion (oil-in-water) using a given mechanical emulsification technology, *ie* microfluidization.

MATERIALS AND METHODS

Experimental design

Description

A central composite rotatable design made up of $k = 5$ factors with 3 levels and 1 repetition was developed. This type of design, the most widely used for fitting experimental results to a second-order model (Piggot, 1986; Box and Drapper, 1987), is called rotatable because the variance of the estimated response $\hat{y}$ at point x is uniquely a function of the distance separating this point from the centre point and not of the direction. These designs are composed of 2^k factorial points (usually coded ± 1) with 2^k star points coded [(± α, 0, 0, ..., 0), (0, ± α, 0, ..., 0), ..., (0, 0, 0, ..., ± α)] and n_0 centre points coded (0, 0, ..., 0). The value of α, on which the rotability of the design depends, is such that $\alpha = (F)^{1/4}$ where F is the number of factorial points of the design: in the present case $F = 2^k$. The complex principles for the development of these designs have been presented by various authors including Montgomery (1976), Gacula and Singh (1984), and Box and Drapper (1987).

The design used was therefore composed of 2^5 factorial points, with 10 star points (with α =

2.38) and 10 centre points which results in a total of 52 experimental units or emulsions.

The 5 factors that were varied in the preparation of the emulsions are the following: 2 process factors–emulsification pressure (7.8, 20.7, 41.4, 62.1 and 76.3 MPa) and temperature (35, 55, 70, 85 and 100 °C), and 3 formulation factors–protein concentration (0.5, 0.9, 1.5, 2.5 and 3.9 wt%), butter oil concentration (5.2, 8, 10, 12 and 14.8 wt%) and monoglyceride concentration (0.08, 0.2, 0.4, 0.6 and 0.88 wt%).

Statistical analysis

An analysis of variance was first conducted on the values of the volume-weighted average diameters of the emulsified fat globules ($\bar{d}_v$) and on the relative width *(cv)* of the particle size distribution. This analysis allowed the split of the total variation of the measured parameters ($\bar{d}_v$ and *cv*) according to the principal effects of the treatments, the interactions and the error. The sum of the squares of the differences of the principal effects was split in unitary degree of freedom using an orthogonal comparison method (Box and Drapper, 1987). This calculation allowed an individual estimation of effects without mutual interference. Two tests were then carried out: a Fisher test allowed a differentiation between the treatments and the interactions which had a significant effect on a given parameter, and an adjustment test (Neter *et al*, 1985) confirmed that the second-order model allowed an adequate description (to ± 1%) of the variances in the experimental results.

The effects of the principal treatments and/or interactions which were not significant at the level 95% have been included in the error term. This pooling, which has been justified by Little (1981), increases the degree of significance of the variance due to an increase in the number of degrees of freedom. Although a lower probability threshold could be used in the selection of the effects to be considered in the determination of the regression equation, a probability threshold of at least 95% was used in order to simplify the expression and use of the regression equations.

Finally, following this second analysis of variance, each of the 2 measured parameters ($\bar{d}_v$ and cv) was analyzed as a function of the principal effects and interactions of process and composition variables. The nullity of the regression coefficients was tested using Student's test (Neter *et al*, 1985).

This method for interpreting results is supported and recommended by Little (1981) and Box and Drapper (1987). According to these authors, all the treatment levels in the experimental range are significantly different in their effects after a significant tendency has been established. The best estimates of the effects of the treatments are those values calculated using the regression equation.

Statistical procedure and graphic

The analysis of variance and regression calculations were carried out using the General Linear Model procedure (Proc GLM and Proc REG) of the SAS (1990).

The 3-dimensional picture of the equations was carried out using Mathematica (Wolfram, 1991).

Emulsion preparation

Ingredients

Sodium caseinates (89.3% protein) were obtained from ICN Nutritional Biochemicals, Canada Ltd (Dorval, Que, Canada). Butter oil (99.4% anhydrous) was purchased from a local dairy cooperative (Agropur, Granby, Quebec, Canada) and was stored at 4 °C. Distilled monoglycerides (EXCEL, T-95) with a hydrophile-lipophile balance (HLB) of 4.5 (Shinoda and Kunieda, 1983) were purchased from Atkemix (Bratford, Ontario, Canada). Sodium azide was purchased from Fisher Scientific (Quebec, Que, Canada).

Emulsion production

Fifty-two emulsions (600 g) containing 0.5, 0.9, 1.5, 2.5 or 3.9 wt% (based on protein content) sodium caseinates, 5.2, 8, 10, 12 or 14.8 wt% butter oil, and 0.08, 0.2, 0.4, 0.6 or 0.88 wt% monoglyceride were prepared in the following manner: various sodium caseinate solutions, hydrated and solubilized in deionized water (k = 1.1 $\mu S.cm^{-1}$) for 90 min, and butter oil, preheated to 50 °C, were mixed using a magnetic stirrer. The solutions were then brought to the appropriate emul-

Table I. Process variables (protein, butter oil and monoglyceride concentrations, emulsification pressure and temperature) and responses of the central composite rotatable design in terms of volume-weighted average diameter and relative width of the emulsified fat globules distribution.
Variables de procédés (concentrations en protéine, huile de beurre et monoglycéride, pression et température d'émulsification) et réponses en termes du diamètre pondéré en volume et du coefficient de variation de la distribution de la taille des globules de gras émulsifiés.

Trials	[Prot] (wt%)	[BO] (wt%)	[MGS] (wt%)	P (MPa)	T (°C)	$(\bar{d}_v)$ (nm)	cv (%)
Factorial points							
1	0.5	8	0.2	20.7	55	584	51
2	0.5	8	0.2	20.7	85	594	49
3	0.5	8	0.2	62.1	55	480	56
4	0.5	8	0.2	62.1	85	466	55
5	0.5	8	0.6	20.7	55	427	39
6	0.5	8	0.6	20.7	85	382	38
7	0.5	8	0.6	62.1	55	317	48
8	0.5	8	0.6	62.1	85	326	38
9	0.5	12	0.2	20.7	55	806	69
10	0.5	12	0.2	20.7	85	793	69
11	0.5	12	0.2	62.1	55	808	52
12	0.5	12	0.2	62.1	85	777	53
13	0.5	12	0.6	20.7	55	460	67
14	0.5	12	0.6	20.7	85	491	64
15	0.5	12	0.6	62.1	55	407	47
16	0.5	12	0.6	62.1	85	419	43
17	2.5	8	0.2	20.7	55	509	41
18	2.5	8	0.2	20.7	85	482	47
19	2.5	8	0.2	62.1	55	439	42
20	2.5	8	0.2	62.1	85	358	50
21	2.5	8	0.6	20.7	55	423	41
22	2.5	8	0.6	20.7	85	407	47
23	2.5	8	0.6	62.1	55	361	46
24	2.5	8	0.6	62.1	85	300	51
25	2.5	12	0.2	20.7	55	574	56
26	2.5	12	0.2	20.7	85	593	59
27	2.5	12	0.2	62.1	55	538	52
28	2.5	12	0.2	62.1	85	539	40
29	2.5	12	0.6	20.7	55	609	45
30	2.5	12	0.6	20.7	85	653	46
31	2.5	12	0.6	62.1	55	563	28
32	2.5	12	0.6	62.1	85	509	32
Centre points							
33	1.5	10	0.4	41.4	70	420	46
34	1.5	10	0.4	41.4	70	427	45
35	1.5	10	0.4	41.4	70	451	45
36	1.5	10	0.4	41.4	70	448	45
37	1.5	10	0.4	41.4	70	415	46
38	1.5	10	0.4	41.4	70	441	46
39	1.5	10	0.4	41.4	70	465	43
40	1.5	10	0.4	41.4	70	433	45
41	1.5	10	0.4	41.4	70	471	41
42	1.5	10	0.4	41.4	70	444	46
Star points							
43	0.9	10	0.4	41.1	70	442	50
44	3.9	10	0.4	41.4	70	403	29
45	1.5	5.2	0.4	41.4	70	291	31
46	1.5	14.8	0.4	41.4	70	633	52
47	1.5	8	0.08	41.4	70	549	53
48	1.5	8	0.88	41.4	70	324	30
49	1.5	8	0.4	7.8	70	942	39
50	1.5	8	0.4	76.3[1]	70	461	66
51	1.5	8	0.4	41.1	35[2]	655	55
52	1.5	8	0.4	41.4	100[3]	513	58

For the design rotability to be perfect ($\alpha = 2.378$), the values of some independent parameters should be: [1] emulsion 50, $P = 90.6$ MPa (in fact, the maximum pressure given by the air feed system was 76.5 MPa); [2] Emulsion 51, $T = 34.3$ °C; [3] Emulsion 52, $T = 105.7$ °C.

sification temperature (35, 55, 70, 85 or 100 °C) and the emulsifiers were added. The dispersions, maintained at the emulsification temperature (± 1.5 °C), were then mixed for 2 min using a stirrer (Braun CDN Ltd, Model MR7, Mississauga, Ont, Canada). The oil-in-water dispersions were then immediately emulsified using a Microfluidizer (M-110™, Microfluidic Corporation, Boston, MA, USA) at its maximum power setting.

The microfluidization procedure was performed in 2 stages: the first processing was at 7.8, 20.7, 41.4, 62.1 or 76.3 MPa and the second at 4.8 MPa in order to eliminate aggregates formed during the first processing procedure (Ogden, 1973; Walstra, 1975). The composition of the emulsions is given in table I.

Sodium azide, an antibacterial agent, was added to each emulsion (0.2% vol/wt), and 2 pH

measurements (pH-meter, Corning 140, electrode 476530, Canlab, Montreal, Que, Canada) were carried out.

Size distribution of the emulsified fat globules

Sampling

A sample of each emulsion was taken and stored at 4 °C for 24 h in a 20 ml bottle completely filled. Before analysis, the samples were heated (T = 20 °C) and manually stirred. This procedure, proposed by Walstra (1975), was used in order to prevent a change in the size distribution of the fat globules due to churning.

Dissociation of protein structures

The samples were mixed with a buffer (urea, EDTA and β-mercaptoethanol, pH 7) designed by Dalgleish *et al* (1987) to dissociate protein structures. Despite the presence of sodium caseinates in the emulsions, the composition of the dissociating buffer was not modified. Measurements were carried out immediately after vigorous manual stirring.

Photon correlation spectrophotometry

The size distributions of the fat globules were determined by photon correlation spectrometry (PCS) using the method proposed by Robin and Paquin (1991). The measurements were taken using the Nicomp multibit (7 bit) 64-channel photon correlation system (Pacific Scientific, Hiac/Royce Instruments Division, Model 370, Menlo Park, CA, USA); the correlation functions were measured on the light that was diffused at an angle of 90° by the particles in suspension. The correlation functions were analyzed by the cumulants method (Koppel, 1972). The first cumulant yielded an average diffusion coefficient *(D)*, and the second yielded a mean squared deviation of the average diffusion coefficient (σ^2). The volume-weighted average particle diameters ($\bar{d}_v$) were calculated using the Stokes-Einstein law, and polydispersity was expressed by the relative standard deviation or coefficient of variation *(cv)* of the volume-weighted distribution calculated as the distribution width divided by the average diameter. The accuracy (≅ 1%), the reproducibility (≅ 1%) as well as the length of the analysis (2.5 x 10^6 photo-impulses or ≈ 20 min) were determined on latex sphere solutions (Robin and Paquin, 1991).

Three measurements of the size distribution of the fat globules were carried out on each sample. The values of the average diameters and relative widths of the size distribution of the fat globules are shown in table I.

Average size distributions

A logarithmic transformation was applied to the emulsified fat globule volume-weighted average diameter ($\bar{d}_v$) and to the homogenization pressure. Indeed, using the theory of isotropic turbulence developed by Kolmogorov (Walstra, 1969, 1983) showed that the maximum size of a fat globule undergoing the homogenization process is a function of the energy density ε (energy dissipated per unit of volume and time) or of the pressure P ($\varepsilon \propto P^{3/2}\ \rho^{-1/2}$), of the interfacial tension γ, and of the mass density ρ according to:

$$d_{max} \propto (\varepsilon^{-2}\ \gamma^3\ \rho^{-1})^{\frac{1}{5}} \propto P^{-\frac{3}{5}} \quad [1]$$

or

$$\log_{10}(d_{max})\ \alpha\ -\frac{3}{5}\ \log_{10}(P) \quad [2]$$

Goulden and Phipps (1964), Walstra (1975) and others have experimentally confirmed these results.

RESULTS

Accuracy and reproducibility of the PCS technique

The 10 centre points serve as an indication of the reproducibility of the PCS technique for determining the parameters of the size distribution of the fat globules. These centre points correspond to values obtained from the same emulsion. Using these results, the reproducibility of the evaluation of the $\bar{d}_v$ and *cv* parameters was approximately 4.2, and

3.2% respectively. However, even though the reproducibility of the results seem satisfying, that is, comparable with those obtained by other methods, their accuracy must be interpreted with some caution. Even though the validity of the PCS technique, in terms of precision and reproducibility, has been demonstrated by scattering from known mixtures of relatively monodispersed polystyrene latex beads (Bargeron, 1974; Brown and Pusey, 1975), results become less reliable when distributions are larger and polydispersed (Weiner and Tschamuter, 1987). Moreover, if the second cumulant is generally dominated by polydispersity rather than by statistical noise in the autocorrelation function, in large distributions the analysis of the cumulant can lead to an underestimation of the variance (Chu and Dinapoli, 1983). Higher order terms should be taken into account, but this remains a difficult problem (Nicoli, personal communication).

Influence of process variables on the average diameter of fat globules and on the distribution width of the diameters

An analysis of variance was carried out on the values given in table I using orthogonal comparisons between the principal treatments and between the interactions (Box and Drapper, 1987). An *F* test was carried out to differentiate the treatments and the interactions which had a significant effect on the volume-weighted average diameter of the fat globules ($\bar{d}_v$) and on the size distribution of the relative width *(cv)*. An adjustment test of the experimental results for a second-order model was also carried out.

Average diameter of the emulsified fat globules

Table II shows the analysis of variance of the $\log_{10}$ ($\bar{d}_v$) as a function of process

Table II. Analysis of variance of the logarithm of the volume-weighted average fat globule diameter versus process and composition variables.
Analyse de variance du logarithme du diamètre moyen pondéré en volume des globules de gras, en fonction des variables de procédé et de composition.

	df[1]	*SS*[2]	*F*[3]	r^2[4]
Model	20	0.624	36.0[a]	0.959
Linear effects				
[*Prof*]	1	0.008	9.6[c]	
[*BO*]	1	0.217	251.4[a]	
[*MGS*]	1	0.147	170.4[a]	
$\log_{10}$ *(P)*	1	0.103	119.1[a]	
T	1	0.006	6.6[d]	
Quadratic effects				
[*Prof*]^2	1	$< 10^{-3}$	< 0.1	
[*BO*]^2	1	0.002	1.9	
[*MGS*]^2	1	$< 10^{-3}$	< 0.1	
$\log_{10}{}^2$ (P)	1	0.038	43.5[a]	
T^2	1	0.025	28.9[a]	
[*Prof*] x [BO]	1	$< 10^{-3}$	0.5	
[*Prof*] x [MGS]	1	0.064	73.8[a]	
[*Prof*] x $\log_{10}$ (P)	1	$< 10^{-3}$	0.4	
[*Prof*] x *T*	1	0.001	1.3	
[*BO*] x [*MGS*]	1	$< 10^{-3}$	< 0.1	
[*BO*] x $\log_{10}$ *(P)*	1	0.006	7.0	
[*BO*] x *T*	1	0.002	2.6	
[*MGS*] x $\log_{10}$*(P)*	1	0.001	1.4	
[*MGS*] x *T*	1	$< 10^{-3}$	< 0.1	
T x $\log_{10}$ *(P)*	1	0.002	2.0	
Error	31	0.027		
Lack of fit	22	0.002	3.4[c]	
Pure error	9	0.003		
Total	51	0.651		
Model	8	0.610	80.8[a]	0.937
Error	43	0.041		
Total	51	0.651		

[1] df = degree of freedom; [2] SS = sum of squares; [3] F = Fisher ratio; [4] r^2 = coefficient of determination. Significance levels [a] $p \leq 0.0001$; [b] $p \leq 0.001$; [c] $p \leq 0.01$; [d] $p \leq 0.05$.

variables. According to the adjustment test, for $p \leq 0.01$ ($F < 4.77$), the second-order model allowed an adequate description of the variance of $\log_{10}$ $(\bar{d}_v)$. Furthermore, the linear effects of all the principal factors were significant (from 95% to 99.999%). Butter oil ([*BO*]) and monoglyceride ([*MGS*]) concentrations had a major effect on the variance of the fat globule diameter: they explained 33.4% and 22.6%, respectively, of the total variance. The emulsification pressure *(P)* and temperature *(T)* represented 21.7% and 4.8% respectively, of the variance (the sum of the linear and quadratic effects: $\log_{10}$ *(P)* + $\log_{10}^2$ *(P)* or $T + T^2$) of $\log_{10}$ $(\bar{d}_v)$. The effect of the protein concentration was significant ($p \leq 0.001$) but represented only 1.3% of the variance of the $\log_{10}$ $(\bar{d}_v)$. The last significant effect given by the analysis of variance was the [*Prot*] x [MGS] interaction which represented 9.8% of the variance of the $\log_{10}$ $(\bar{d}_v)$. Other effects were not significant ($p > 0.05$). The error term represented ≈ 4% of the variance of $\log_{10}$ $(\bar{d}_v)$.

A regression equation calculated from the significant effects ($p \leq 0.05$ or more) of the analysis of variance of $\log_{10}$ $(\bar{d}_v)$ is shown in table III. This second-order model was highly significant ($p \leq 0.0001$) and explains 93.7% of the total variance of $\log_{10}$ $(\bar{d}_v)$. All of the regression coefficients were highly significant ($p \leq 0.0001$). It is, however, worth noting that the existence of a minimum average diameter as a function of pressure (regression equation) was not significant, and resulted from an artefact produced by one of the extreme point (star point No 48). A separate regression analysis revealed that the increase in size beyond $P \cong 50$ MPa (the emulsification pressure from the regression model for which the derivative equals 0) was not significant.

Figure 1 is the response surface obtained from a second-order model relating the values of $\bar{d}_v$ as a function of the butter oil concentration ([*BO*], wt%) and of the emulsification pressure (P, MPa) for a fixed temperature (50 °C) and for fixed protein (1.5 wt%) and monoglyceride (0.4 wt%) concentrations. As has been reported elsewhere, the average diameter of the fat globules decreases and reaches a plateau as emulsification pressure increases

Table III. Analysis of regression and second-order model of the logarithm of the volume-weighted average fat globule diameter versus significant variables and interactions.
Analyse de régression et modèle de second ordre du logarithme du diamètre moyen pondéré en volume des globules de gras émulsifiés, en fonction des variables et des interactions significatives.

	Estimate [1]	*STD* [2]	*t* [3]
Parameter:			
Intercept	14.293	1.6	9.1[a]
[*Prot*]	–0.102	$1.2\ 10^{-2}$	–8.5[a]
[*BO*]	0.035	$2\ 10^{-3}$	15.2[a]
[*MGS*]	–0.633	$5\ 10^{-2}$	–13.4[a]
$\log_{10}$ *(P)*	–4.755	0.7	–6.9[a]
T	–0.016	$3\ 10^{-3}$	–5.5[a]
$\log_{10}^2$ *(P)*	0.506	0.1	6.6[a]
T^2	$1.1\ 10^{-4}$	$2\ 10^{-5}$	5.2[a]
[*Prot*] x [*MGS*]	0.223	$2.7\ 10^{-2}$	8.2[a]

$$\log_{10}(\bar{d}_v) = 14.293 - 0.102\,[Prot] + 0.035\,[BO] - 0.633\,[MGS] - 4.755\log_{10}(P) - 0.016\,T + 0.506\log_{10}^2(P) + 10^{-4}\,T^2 + 0.223\,[Prot] \times MGS$$

Validity intervals:
$7\,800 \leq P \leq 76\,310$ kPa $0.5 \leq [Prot] \leq 3.9$ wt%
$35 \leq T \leq 100$ °C $5.2 \leq [BO] \leq 14.8$ wt%
$0.08 \leq [MGS] \leq 0.88$ wt%

[1] Estimate = parameter estimated under the regression model (table II). [2] *STD* = standard error of the estimate. [3] *t* = value of Student's *t*-test. Significance level: a: $p \leq 0.0001$.

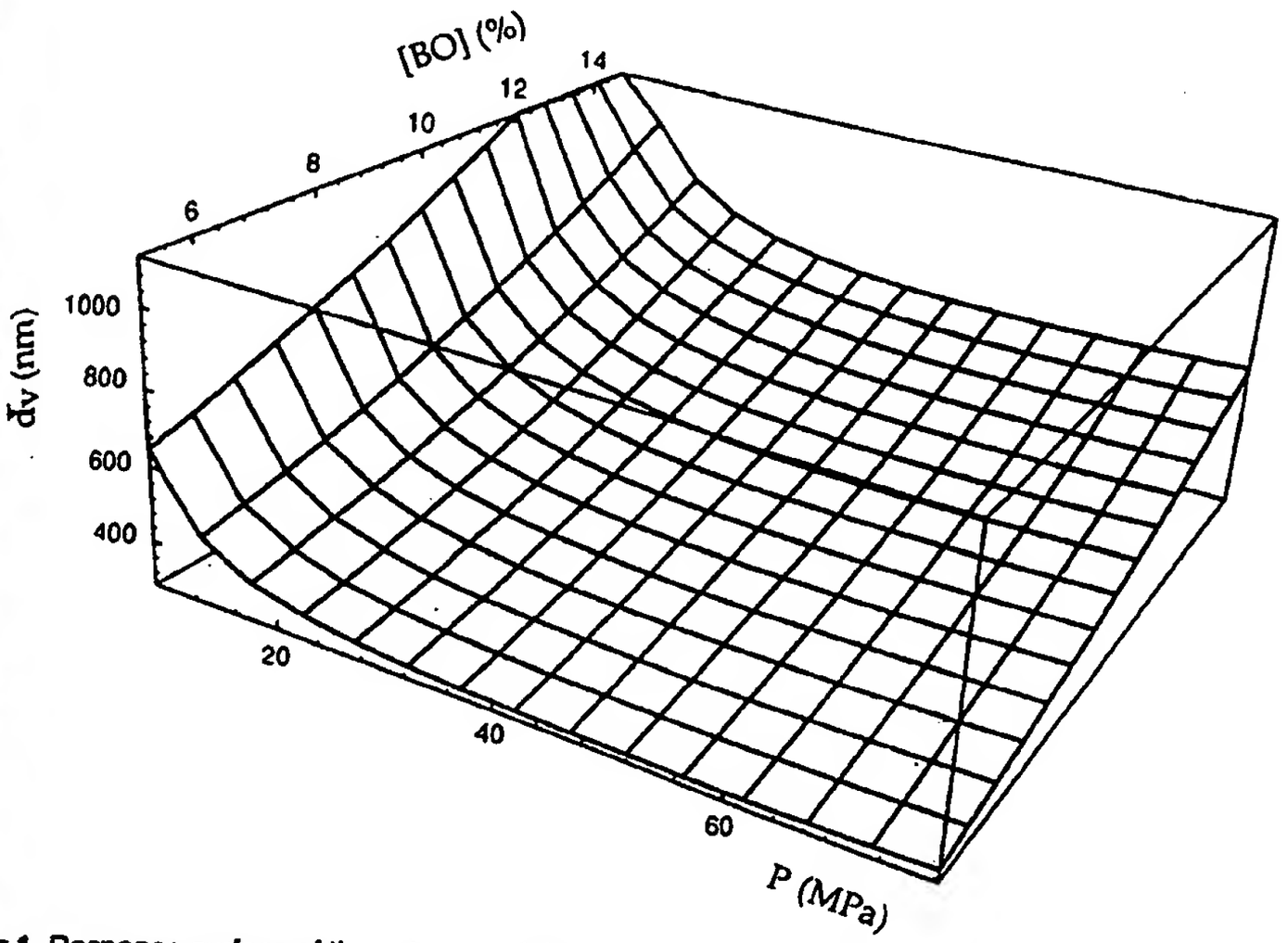

Fig 1. Response surface of the volume-weighted average fat globule diameter as a function of emulsification pressure, *P* (MPa), and butter oil concentration, [*BO*] (wt%), for a fixed temperature (*T* = 50 °C), a fixed protein concentration ([*Prot*] = 1.5 wt%), and a fixed monoglyceride concentration ([*MGS*] = 0.4 wt%).

Surface de réponse du diamètre moyen pondéré en volume des globules de gras en fonction de la pression d'émulsification, P (MPa), et de la concentration en huile de beurre, [BO] (%), pour une température donnée T = 50 °C), et des concentrations fixées en protéines ([Prot] = 1.5% et en monoglycérides ([MGS] = 0.4%).

but increases as the fat content increases (Walstra, 1975; Phipps, 1985).

Figure 2 shows the complex influences of emulsifier type and concentration on fat globule size, for emulsions produced under conditions of constant pressure (50.0 MPa), temperature (50 °C), and butter oil concentration (10 wt%). Our results are in agreement with previous reports in that, if the presence of a single surfactant results in a dramatic lowering of the size of the fat globules, the near absence of surfactants ($[Prot]_{min}$ = 0.5 wt%, and $[MGS]_{min}$ = 0.08 wt%) results in a maximum value for $\bar{d}_v$ (678 nm).

Relative width of the size distribution of the emulsified fat globules

A preliminary statistical analysis has revealed that the variations of *cv* as a function of various independent variables could not be adequately described by a second-order model (r^2 = 0.71 after pooling; the adjustment test was not significant) in the original validity interval. A reduction of the

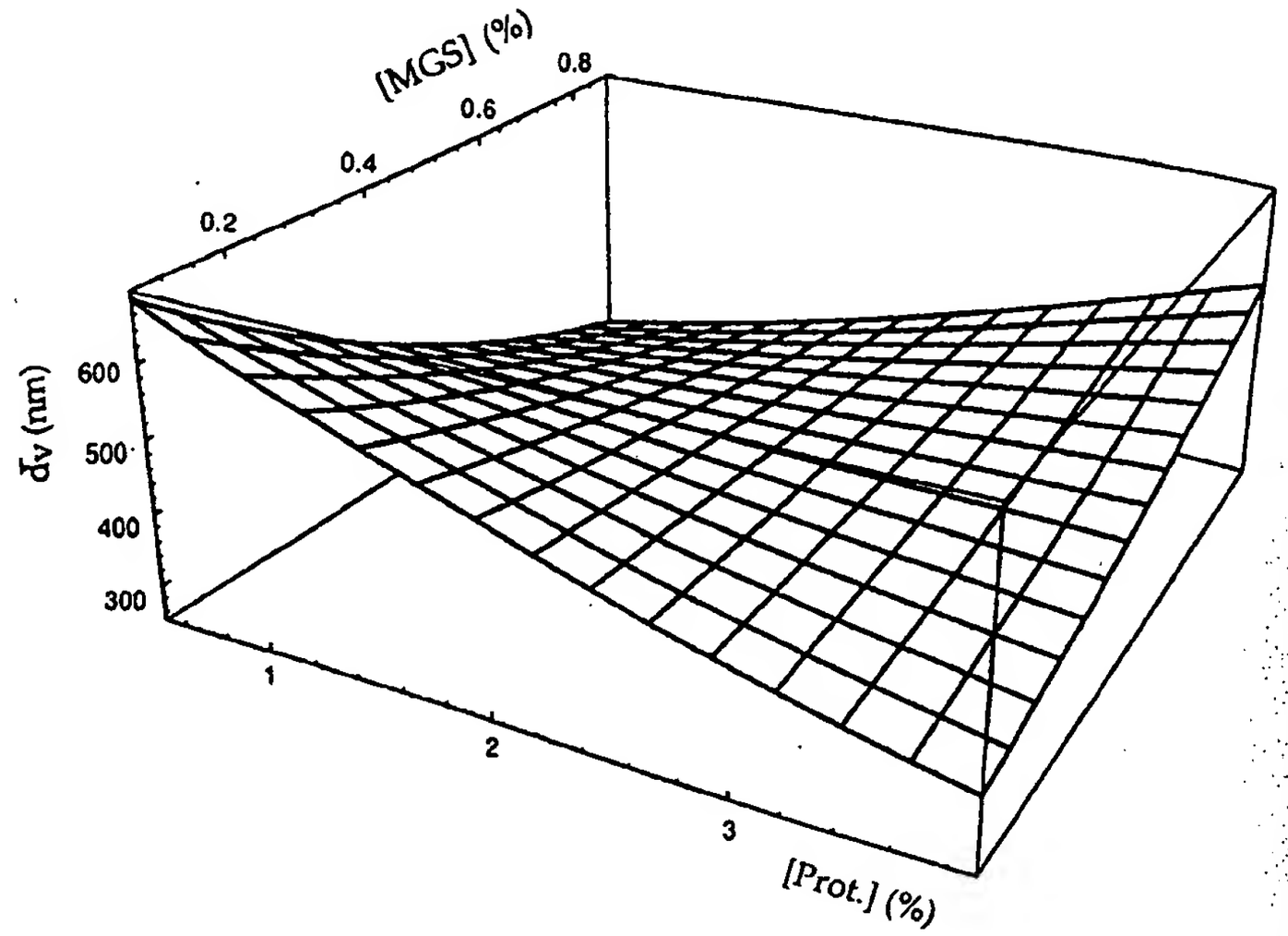

Fig 2. Response surface of the volume-weighted average fat globule diameter as a function of protein, [*Prot*] (wt%), and monoglyceride, [*MGS*] (wt%), concentrations for a fixed temperature (T = 50 °C), a fixed pressure (P = 50 MPa), and butter oil concentration [*BO*] = 10 wt%).
Surface de réponse du diamètre moyen pondéré en volume des globules de gras en fonction des concentrations en protéines, [Prot] (%), et monoglycérides, [MGS] (%), pour une température (T = 50 °C), une pression (P = 50 MPa), et une concentration en huile de beurre ([BO] = 10%) fixées.

interval corresponding to the elimination of an extreme point (No 49) has consequently been effected.

Table IV shows the analysis of variance of *cv* as a function of the process variables. According to the adjustment test, for $p \leq 0.01$ ($F < 4.77$), a second-order model could adequately describe the variances of *cv* in this new validity interval. As mentioned previously, the linear effects of the principal factors, except the temperature one, were significant (from 95% to 99.999%). The protein and monoglyceride concentrations had an important effect on the variance of *cv*: they explained respectively 16.0% and 13.4% of the total variance. The emulsification pressure and temperature represented respectively 16.8% and 2.7% (the sum of the linear and quadratic effects: $P + P^2$ and T^2) of the variance of *cv*. The effect of the butter oil concentration ($p \leq 0.0001$) represented 7.7% of the variance of *cv*. The other highly significant interactions ([*Prot*] x [*BO*] and [*BO*] x *P*) represented 28.5% of the total variance. The error represented approximately 10.2% of the variance of *cv*.

A regression equation, calculated using the highly significant effects ($p \leq 0.000\,1$) from the analysis of variance of *cv*, is shown in

Table IV. Analysis of variance of the standard deviation of the volume-weighted size distribution of fat globules versus process and composition variables.
Analyse de variance de la déviation standard de la distribution des tailles pondérées en volume des globules de gras en fonction des variables de procédé et de composition.

	df [1]	SS [2]	F [3]	r^2 [4]
Model	20	4 196.5	13.1[a]	0.897
Linear effects				
[*Prot*]	1	749.1	46.9[a]	
[*BO*]	1	361.2	22.6[a]	
[*MGS*]	1	626.7	39.2[a]	
P	1	156.9	9.8[a]	
T	1	4.6	0.3	
Quadratic effects				
[*Prot*]^2	1	17.9	1.1	
[*BO*]^2	1	39.4	2.5	
[*MGS*]^2	1	20.8	1.3	
P^2	1	630.9	39.5[a]	
T^2	1	123.9	7.8[a]	
[*Prot*] x [*BO*]	1	359.4	22.5[a]	
[*Prot*] x [*MGS*]	1	23.5	1.5	
[*Prot*] x *P*	1	0.2	< 0.1	
[*Prot*] x *T*	1	75.0	4.7	
[*BO*] x [*MGS*]	1	19.7	1.2	
[*BO*] x *P*	1	974.8	61.0[a]	
[*BO*] x *T*	1	2.1	< 0.1	
[*MGS*] x *P*	1	0.5	< 0.1	
[*MGS*] x *T*	1	7.2	0.4	
T x *P*	1	3.0	0.2	
Error	30	479.3		
Lack of fit	21	3 592.7	4.1[c]	
Pure error	9	358.5		
Total	50	4 675.8		
Model	9	3 823.0	20.4[a]	0.818
Error	41	852.9		
Total	50	4 675.9		

See table II for statistical abbreviations.

table V. The second-order model, which was highly significant ($p. \leq 0.0001$), was able to explain 81.8% of the total variance

Table V. Analysis of regression and second-order model of the variation coefficient of the volume-weighted size distribution of fat globules versus significant variables and interactions.
Analyse de régression et modèle de second ordre du coefficient de variation de la distribution des tailles pondérées en volume des globules de gras, en fonction des variables et des interactions significatives.

	Estimate [1]	STD [2]	t [3]
Parameter:			
Intercept	25.127	18.2	1.4
[Prot]	12.532	4.1	3.1
[*BO*]	9.477	1.1	8.9[a]
[*MGS*]	−19.278	3.6	−5.4[a]
P	$+2.8\ 10^{-4}$	$3\ 10^{-4}$	0.9
T	−1.133	0.4	−2.6
P^2	10^{-7}	10^{-8}	4.1[a]
T^2	0.0083	0.03	2.7
[*Prot*] x [*BO*]	−1.676	0.4	−4.2[a]
[*BO*] x *P*	$-1.3\ 10^{-4}$	$2\ 10^{-5}$	−6.8[a]

$$cv = 25.127 + 12.532\,[Prot] + 9.477\,[BO] - 19.278\,[MGS] - 2.8\ 10^{-4}\,P - 1.133\,T + 10^{-7}\,P^2 + 0.008\,T^2 - 1.676\,[Prot] \times [BO] - 1.3\ 10^{-4}\,[BO] \times P$$

Validity intervals
20 400 ≤ P ≤ 76 300 kPa 0.5 ≤ [*Prot*] ≤ 3.9 wt%
35 ≤ *T* ≤ 100 °C 5.2 ≤ [*BO*] ≤ 14.8 wt%
0.08 ≤ [*MGS*] ≤ 0.88 wt%

See table III for statistical abbreviations.

cv. The value of the regression coefficients of the P term was not significantly different from 0 ($p > 0.05$).

Figure 3, obtained from a second-order model, corresponds to the response surface of the standard deviation of the volume-weighted size distribution of fat globules as a function of emulsification pressure, *P* (MPa), and butter oil concentration [*BO*] (wt%), for a fixed temperature

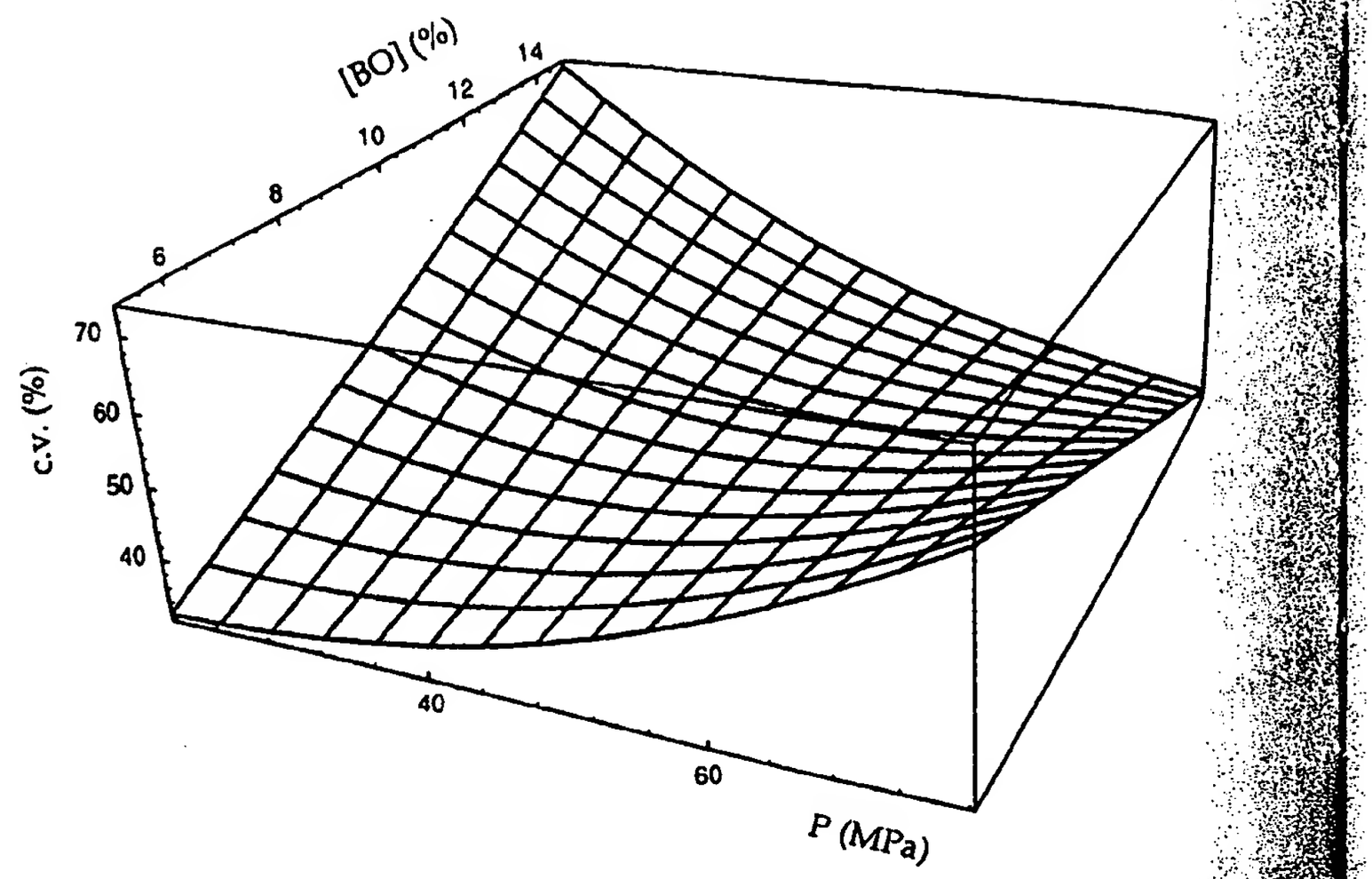

Fig 3. Response surface of the coefficient of variation standard of the volume-weighted size distribution of fat globules as a function of emulsification pressure, *P* (MPa), and butter oil concentration, [*BO*] (wt%), for a fixed temperature (*T* = 50 °C), a fixed protein concentration ([*Prot*] = 1.5 wt%), and a fixed monoglyceride concentration ([*MGS*] = 0.4 wt%).
Surface de réponse du coefficient de variation de la distribution des tailles pondérées en volume des globules de gras en fonction de la pression d'émulsification, P *(MPa), et de la concentration en huile de beurre, [BO] (%), pour une température donnée (T = 50 °C), et des concentrations fixées en protéines ([Prot] = 1.5%) et en monoglycérides ([MGS] = 0.4%).*

(*T* = 50 °C), a fixed protein concentration ([*Prot*] = 1.5 wt%), and a fixed monoglyceride concentration ([*MGS*] = 0.4 wt%). An increase in the emulsification pressure and/or butter oil concentration resulted in an increase in the value of *cv*. This figure also shows the minimal values for *cv* that are a function of both *P* and [*BO*] (table IV).

Figure 4 shows the response surface obtained from a second-order model of the volume-weighted size distribution of fat globules as a function of protein and monoglyceride concentration, for a fixed temperature (50 °C), pressure (50 MPa), and butter oil concentration (10 wt%). This figure indicates the cooperative effect of surfactant content on the reduction in *cv* of this volume-weighted distribution.

pH of the emulsions

The average pH of the 52 emulsions was 7.06 with a standard deviation of ± 0.04. All emulsions therefore had similar acid/base properties.

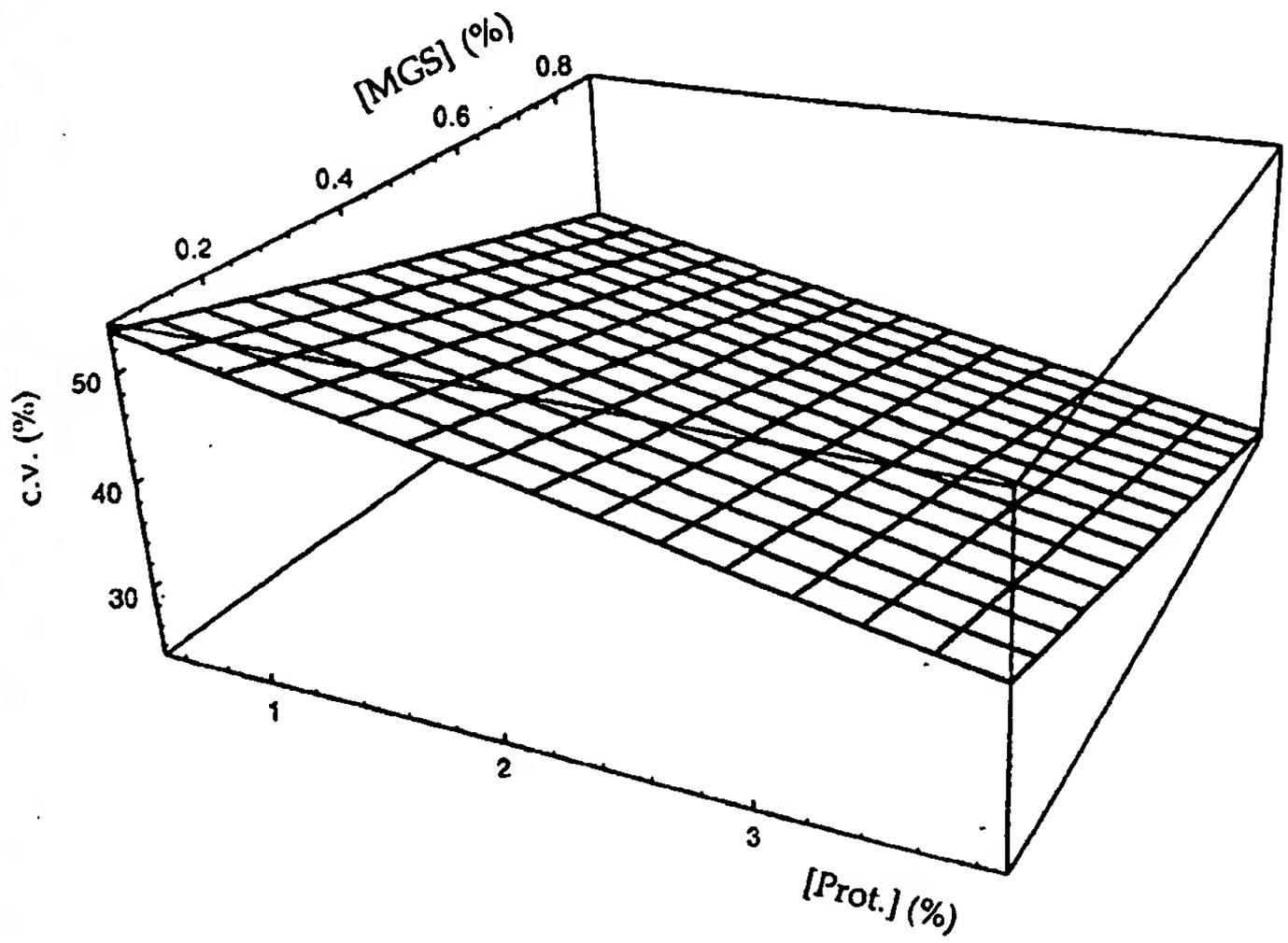

Fig 4. Response surface of the coefficient of variation of the volume-weighted size distribution of fat globules as a function of protein, [*Prot*] (wt%), and monglyceride, [*MGS*] (wt%), concentrations for a fixed temperature (T = 50 °C), a fixed pressure (P = 50 MPa), and butter oil concentration ([*BO*] = 10 wt%).

Surface de réponse du coefficient de variation de la distribution des tailles pondérées en volume des globules de gras en fonction des concentration en protéines, [Prot] (%), et monoglycérides, [MGS] (%), pour une température (T = 50 °C), une pression (P = 50 MPa), et une concentration en huile de beurre ([BO] = 10%) fixées.

DISCUSSION

Emulsification is a dynamic process where the disruption and recombination or coalescence of the fat globules take place simultaneously, each with its own rate constant or time scale (Walstra, 1983; Tornberg *et al*, 1990). Consequently, not only the final droplet size distribution but also other emulsion properties such as rheological behavior will be determined by the conditions leading to an equilibrium between breakdown and coalescence. The probability of newly formed droplets coalescing depends on the time available for the interfaces to be covered by the surfactants. The time available depends on emulsifying conditions (*eg* emulsifying machine, power density), which are influenced by the fat content, the ratio of surfactant to fat, and the nature of the surfactants. In order to be active (prevent coalescence), surfactants must not only be transported to the interfaces, they must also be able to adsorb. Adsorption depends on the number of surfactant collisions with fat particles,

and on the probability of the surfactants adsorbing after colliding with the interface. Adsorption is likely influenced by molecular properties such as hydrophobicity, flexibility and charge density (Kato, 1991; Lorient *et al*, 1991). However, the adsorption process occurs on a time scale of less than a millisecond during the homogenization process (Walstra, 1983), so it is very unlikely that an adsorption equilibrium is obtained.

For a given process, the emulsification efficiency is the result of an optimal combination of process variables and of the composition of the liquid to be emulsified. Six major variables are generally considered: emulsification pressure *(P)* and temperature *(T)*, liquid flow rate *(Q)*, the fraction *(Φ)* of the disperse phase and the surfactant concentration(s) (Walstra, 1983; Phipps, 1985). In the present study, the effect of flow rate on the size distribution of the fat globules was not considered. It has, however, been shown for oil-in-water emulsions (Phipps, 1975, 1982, 1983; Walstra, 1975) and for conventional homogenizers (Manton-Gaulin and/or Rannie), that there is little or no influence of the flow rate of the liquid to be emulsified when $\Phi \leq 30\%$.

Influence of process variables on the size distribution of fat globules

Effect of emulsification pressure

It was empirically shown (Goulden and Phipps, 1964; among others) and then vindicated by Walstra (1969, 1975) that classic homogenization processes (the systems of Manton-Gaulin or Rannie), at moderate emulsification pressures (0.25 MPa $\leq P \leq$ 40.5 MPa), using milk, cream with a fat concentration of $\Phi \leq 12\%$ or any other dilute emulsion, could be quantified by a relation such as $d \propto P^m$ where the exponent m has a value of –3/5 ([1]). The exponent m in the descending slope of the curve $d_v = f(P^m)$ (fig 1) is of the order –0.53 ± 0.04. These results, therefore, seem to corroborate the theories linked to the breakdown of fat globules during turbulent flow conditions. However, there is no general agreement on the functioning of conventional homogenizers at high pressure. According to Walstra (1969, 1983) and Davies (1985) the breakdown of the fat globules can be described by the turbulence theory put forward by Kolmogorov. According to Phipps (1975, 1985), the breakdown of the globules at the entrance to the homogenization valve can be described by the Taylor analysis of shearing forces. The design of the microfluidization chamber (microchannels, mixing zone, etc) differs fundamentally from an homogenization chamber (basically a valve and a seat). Even if the forces that lead to the breakdown of the fat globules are the same, their respective influence on the breakdown is apparently not the same.

Although the convex nature of the curve $\bar{d}_v = f(P)_{[BO]}$ (fig 1) is the result of an experimental artefact and of its statistical consequence (the minimum is very shallow), some authors (Becher, 1967; Phipps, 1975; Tornberg, 1980) have reported that an increase in homogenization intensity *(E)*, and/or fat concentration above optimal yields ($P \geq 40$ MPa or $E \geq 60$ W and/or $\Phi \geq 12\%$) could result in an increase in droplet size. This increase, called overprocessing by Tornberg (1980), should indicate that coalescence is the dominant factor governing the final droplet size of the emulsion. However, the validity of the methods that have been used for producing emulsions and determining average size is questionable. In the present study, it is reasonable to think that an increase in collision frequency with increasing pressure would at most lead to no further decrease in globule size as the minimum is very shallow. An in-

crease in emulsification intensity above optimal conditions, which causes a relatively small change in average droplet size, results in unnecessary energy consumption. The optimal condition corresponded to $P \cong 50$ MPa. The reduction in fat globule size have various consequences. Emulsions which contain small droplets have a tendency to be more stable with respect to creaming (Stokes' law), and to coalesce more than those containing large droplets (MacRitchie, 1976). According to the MacRitchie approach, which correlates film stability to an energy barrier, the compressional free energy barrier can be, under some conditions, proportional to $1/d^2$. However, in practice the effects are not as great as predicted by these equations (Walstra and Oortwijn, 1975; Dickinson and Stainsby, 1982).

If the average particle size can provide some information about the behavior of emulsions, most attention should, however, be paid to the top end of the size distribution as most types of instability are usually first manifested by the behavior of the largest droplets. Although the distribution width of fat globules is an extremely important parameter when characterizing an emulsion, it has not been studied in great depth. Walstra (1975) demonstrated that the relative width of fat globules in homogenized milk sharply increases with the homogenization pressure ($0 < P < 5$ MPa), reaches a maximum ($P \cong 5$ MPa) before remaining fairly constant and attaining a limit ($P \cong 30$ MPa). These results were partly confirmed by Tornberg (1980) studying the behavior of various protein stabilized emulsions made by a sonifier. In the present study, valid for 20.4 MPa $\leq P \leq$ 76.3 MPa, the results revealed a behavior that differed as a function of butter oil concentration ([*BO*], wt%). At quite high [*BO*], in conformity with previously mentioned results, the relative width of the fat globule distribution diminished as a function of emulsification pressure. However, at lower concentrations, the behavior was reversed. Although these trends should be interpreted with some caution (lack of accuracy in the determination of the standard deviation, low r^2 value), it appears that trends near central points are similar to those reported elsewhere. At the endpoints of the experimental design, trends are much more difficult to establish, particularly when the decrease in *cv* as a function of [*BO*] at high *P* should arise from the standard deviation(s) being less affected than $\bar{d}_v$ by the emulsification intensity.

Effect of emulsification temperature

Since Gaulin, it has been recognized that the efficiency of the emulsification process is very low in the presence of solid fat (Kessler, 1981). Consequently, the production of oil-in-water emulsions is normally carried out at temperatures above the final melting temperature of the fat ($T_f \cong 40$ °C, Jenness and Walstra, 1984). Several authors, studying the homogenization of milk, have shown that an increase of 10 °C in temperature between 40–70 °C decreases the average diameter of the fat globules by 6–8% (Walstra, 1975) to 10–15% (Sweetsur and Muir, 1983). This effect weakens or disappears above 80 °C. As expected, an increase in temperature between 35–82 °C resulted in a decrease in the average diameter of ≈ 8%/10 °C. Although equation [1] does not predict that the viscosity of either phase can have an effect on the droplet size resulting from the emulsification process in turbulent flow, a decrease of viscosity will understandably affect the rate of passage through the emulsifier and the ease of disruption of the globules. Walstra (1974, 1983) suggested that an increase in the viscosity of the dispersed phase (η_D) should correspond to a deformation time of a droplet larger than the character-

istic time of an eddy. As the smallest eddies are presumably the most effective (they have the highest kinetic energy), an increase in η_D should lead to a larger spread in flow conditions and consequently in droplet size distribution *(cv)*, as was indeed the case. Moreover, an increase in temperature changes all the composition variables that determine adsorption; fat changes to oil and the macromolecular penetration into the oil becomes possible, hydrophobic interactions at the interface probably become more intense (at least up to 60–65 °C), and the molecular structure of water weakens, which affects its quality as a solvent for surfactants and for hydrophobic interactions. Above 82 °C, the average particle diameter increased slightly. Although this result has not been explained, it should be noted that the influence of the temperature on the average diameter of the fat globules is relatively low: temperature only explains 4.8% (table II) of the total variance of $\log_{10}$ (d_v) and between 82 and 100 °C it represents < 1% which is much lower than the experimental error (≈ 6.3%). Moreover, the statistical increase in d_v is a consequence of the measurements obtained from an emulsion that was not repeated (No = 48) and corresponds to an extreme point (star point) in the experimental design. *cv* was influenced in a similar manner by the temperature (table V).

Effect of composition variables on the size distribution of fat globules

Effect of butter oil concentration

The concentration of fat affects the homogenization efficiency of dairy products when it is > 10% (Walstra, 1975; Phipps, 1985). The microfluidization of the model emulsion demonstrated that an increase in the butter oil concentration ($5.2 \leq [BO] \leq 14$ wt%) resulted in a very significant increase in the average diameter of the fat globules (d_v) (table II, fig 1) and in the size distribution (*cv* at low pressure) (table III, fig 3). An increase in the fat concentration resulted in a relative decrease in the concentration of surfactant available to cover the new interfacial surface that was formed during the emulsification process. The fat content and the ratio of surfactants to fat affected the extent of coalescence of the newly formed globules by governing the probability that the latter collide before they recover by a surfactant layer. Also, with higher oil concentrations, distances between fat globules decrease and the probability of bridging could increase. This results in a general tendency to increase "particle" diameter.

Effect of surfactant concentration

The addition of surfactants, which results in a decrease in interfacial tension (γ), reduces the interfacial free energy (ΔG) of the system,

$$\Delta G = \gamma \Delta S \qquad [3]$$

where ΔS is the change in the interfacial area

and thereby the Laplace pressure which is beneficial in reducing both the energy requirement to form emulsions and the droplet size that can be obtained. However, this only holds if the ratio (surfactant/interfacial surface) is large enough to cover the new interfacial surface formed during the emulsification process and leading to minimize the coalescence or polymeric bridging (Halling, 1981; Tadros and Vincent, 1983). For minimal protein and monoglyceride concentrations ($[Prot]$ = 0.5 wt%, $[MGS]$ = 0.08 wt%, with P = 50 MPa, T = 50 °C, $[BO]$ = 10 wt%), the average diameter of the fat globules was at a maximum ($\bar{d}_v$ = 678 nm).

Although certain general rules can be deduced from simple thermodynamic principles, the degree and, more importantly, the consequences of the adsorption of protein to the interface can vary considerably with the type of protein and with emulsification conditions. Thus, while Oortwijn and Walstra (1979) reported that whey protein concentration (0.01–2.0%) had relatively little effect on the size of fat globules in homogenized emulsions, Pearce and Kinsella (1978) demonstrated, using homogenized emulsions stabilized with various proteins, that increasing the protein concentration (0.5–5%) could decrease the average diameter of the fat globules by a factor of 2.5. Thus, the nature of the surfactant (hydrophile-lipophile balance, molecular weight, molecular flexibility) as well as its relative concentration (with respect to other surfactants) directly influence the size of the fat globules. Figure 2 illustrates the complex influences of the chemical structure and of protein and monoglyceride concentration on the average diameter of emulsified fat globules; the other variables were kept constant (P = 50 MPa, T = 50 °C, [*BO*] = 10 wt%). During the emulsification process, smaller droplets (d_v = 259 nm) are produced in the presence of low concentrations of proteins and high concentrations of monoglycerides ([*Prot*] = 0.5 wt% and [*MGS*] = 0.88 wt%, respectively) because monoglycerides are better able to lower interfacial tension than proteins alone. With high protein concentrations and low monoglyceride concentrations, d_v = 350 nm. Dickinson *et al* (1989) reported similar trends when studying the effect of octaoxyethylene dodecyl ether ($C_{12}E_8$) with 0.1 wt% caseinate on the droplet diameter of O/W emulsion (20 wt% *n*-tetradecane, pH 7, 25 °C). However, care is needed when analysing these results as the surfactants used were different and hydrocarbons have a higher interfacial tension with water than do mixtures of triglycerides with water (Fisher *et al*, 1985).

Moreover, the increase in the concentration of surfactant (for a given [*BO*], P and T) results in a decrease in the average particle diameter (Dickinson *et al*, 1989) if the monoglycerides to protein ratio is lower or equal to 0.15, *eg* [*Prot*] = 2.85 wt% and [*MGS*] = 0.46 wt% (fig 2). Although these concentrations are independent of the [*BO*], which is rather surprising, it is suggested that an increase in the size of the fat globules above these concentrations can be attributed to,

– a competition between fat and monoglycerides to bind proteins due to the high number of monoglyceride molecules per residue of caseinate and to the formation of hydrophobic bonds between a polar amino acids and the hydrocarbon groups of the monoglycerides (Dickinson and Woskett, 1989). These weak complexes, if they form, should be rather surface-inactive, as the hydrophobic areas of protein and nonionic surfactant bind together, and

– to protein displacement from the interface by monoglycerides. In another study using casein and *MGS*, Paquin *et al* (1987) found that surface pressure isotherms in the high-pressure region are essentially the same as for the monoglycerides alone, suggesting protein displacement from the interface. It is likely, as suggested by Doxastakis and Sherman (1986), that mono- and diglycerides present in commercial glycerol monostearate form complexes with caseinate at the oil–water interface. It would appear that this (mixed) emulsifier does not behave simply as a nonionic, noninteracting surfactant.

Surfactants (proteins and low molecular weight surfactants) seem to have a cooperative effect on the reduction of *cv* (fig 4). As was mentioned in the discussion on the determination of *cv*, these results must be interpreted with caution.

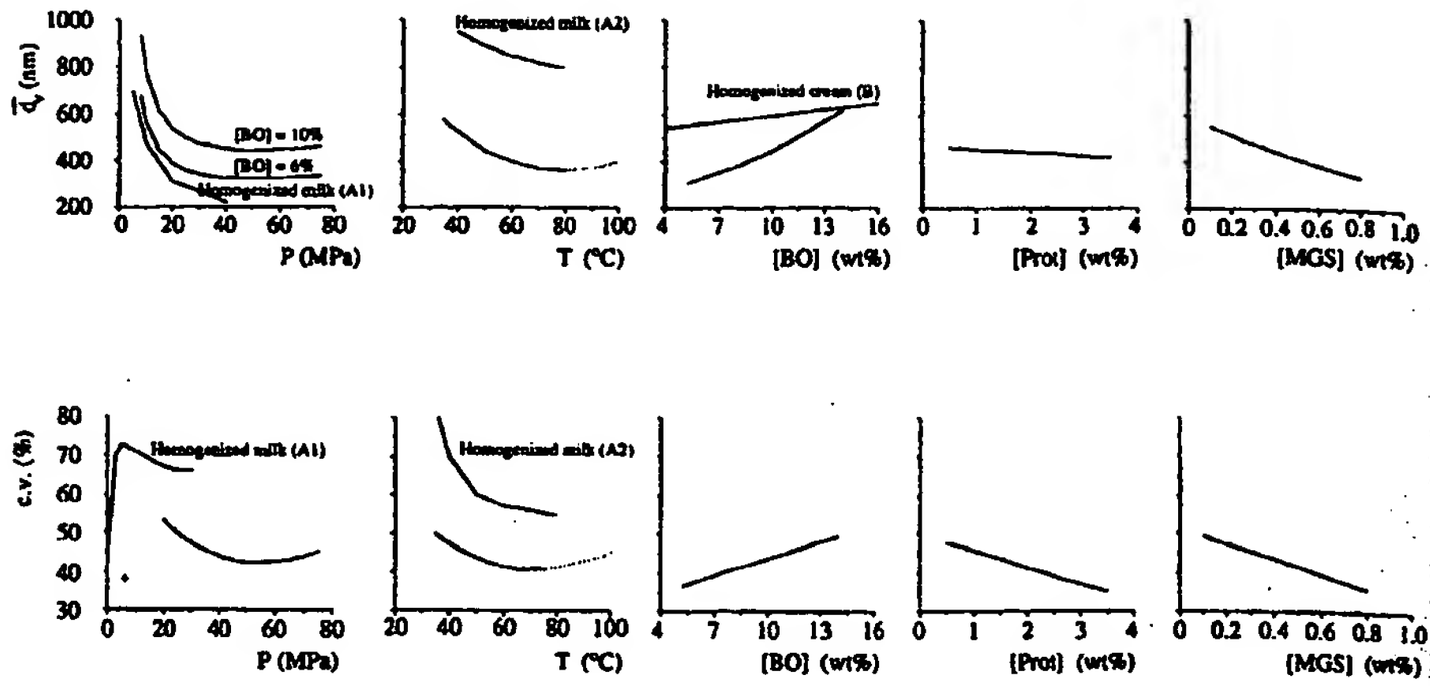

Fig 5. Effect of process and composition variables on fat globule size distribution parameters. For each graph, values of 4 variables were either fixed or specified. Values of fixed variables were: $P = 50$ MPa, $T = 50$ °C, $[BO] = 10$ wt%, $[Prot] = 1.5$ wt%, $[MGS] = 0.4$ wt%.
Effets des variables de procédés et de composition sur les paramètres de la distribution des tailles des globules de gras. Pour chaque figure, les valeurs des 4 variables étaient soit fixées soit spécifiées. Lorsque les variables étaient fixées, leur valeur était : P = 50 MPa, T = 50 °C, [BO] = 10%, [Prot] = 1.5%, [MGS] = 0.4%.
(A): Walstra. 1975; A_1, p 282; A_2, p 289. (B): Phipps, 1985, p 12.

CONCLUSIONS

The process and composition variables which were studied affect, in varying proportions, the efficiency of the emulsification process called microfluidization. Some of these influences are summarized in figure 5. The variables that had the greatest influence on the size distribution of the fat globules are the butter oil concentration, the concentration of low molecular weight surfactants (monoglycerides), the emulsification pressure, the protein concentration (sodium caseinates) and the emulsification temperature. However, if the average sizes are fairly reliable, the results on relative distribution width must be taken with caution.

The utilization of an experimental design, applied to a dairy-type emulsion, demonstrated the complexity of the influences and interactions (depending on the area of study, pressure, temperature or concentrations) of process and composition variables on the size distribution of the fat globules. If the usefulness of mechanistic and thermodynamic principles is not in doubt, it is still impossible to completely predict all aspects of the behavior of an emulsion.

Finally, although this work was carried out on a model system and although it was demonstrated that for other conditions (the existence of interaction terms) the effects would be different, the results should pro

vide a guide for optimizing the emulsification process.

ACKNOWLEDGMENTS

We are indebted to the first reviewer for his helpful comments.

REFERENCES

Bargeron CB (1974) Analysis of intensity correlation spectra of mixtures of polystyrene latex spheres: a comparison of direct least squares fitting with the method of cumulants. *J Chem Phys* 60, 2516-2519

Becher P (1967) Effect of preparation parameters on the initial size distribution functions in oil-in-water emulsions. *J Colloid Interface Sci* 24, 91-96

Box GE, Drapper NR (1987) *Empirical Model Building and Response Surfaces*. John Wiley and Sons, NY

Brown JC, Pusey PN (1975) Photon correlation study on the initial size distribution function in oil-in-water emulsions. *J Chem Phys* 62, 1136-1144

Chandonnet S, Korstvedt H, Siciliano AA (1985) Preparation of microemulsions by microfluidization. *Soap Cosmet Chem Spec* (Feb) 37-38

Cook EJ, Lagace AP (1985) Apparatus for forming emulsions. *US Pat* 4 533 254

Chu B, Dinapoli A (1983) Extraction of distributions of decay times in photon correlation of polydisperse macromolecular solutions. *In: Measurement of Suspended Particles by Quasi-Elastic Light Scattering* (Dahneke BE, ed) John Wiley and Sons, NY, 81-105

Dalgleish DG, Pouliot Y, Paquin P (1987) Studies on heat stability of milk. II. Association and dissociation of particles and the effect of added urea. *J Dairy Res* 54, 39-49

Darling DF, Birkett RJ (1987) Food colloids in practice. *In: Food Emulsions and Foams* (Dickinson E, ed) R Soc Chem, London, 1-29

Davies JT (1985) Drop sizes of emulsions related to turbulent energy dissipation rates. *Chem Eng Sci* 40, 839-842

Dickinson E (1986) Mixed proteinaceous emulsifiers: review of competitive protein adsorption and the relationship to food colloid stabilization. *Food Hydrocol* 1, 3-23

Dickinson E, Stainsby G (1982) *Food Colloids*. Elsevier Appl Sci Publ, London

Dickinson E, Stainsby G (1988) Emulsion stability. *In: Advances in Food Emulsions and Foams* (Dickinson E, Stainsby G, eds) Elsevier Appl Sci Publ, London, 1-44

Dickinson E, Woskett CM (1989) Competitive adsorption between proteins and small-molecule surfactants in food emulsions. *In: Food Colloids* (Bee RD, Richmond P, Mingins J, eds) R Soc Chem, London, 74-96

Dickinson E, Mauffret A, Rolfe SE, Woskett CM (1989) Adsorption at interfaces in dairy systems. *J Soc Dairy Technol* 42, 18-22

Dickinson E, Euston SR, Woskett CM (1990) Competitive adsorption of food macromolecules and surfactants at the oil-water interface. *Prog Colloid Polym Sci* 82, 65-75

Doxatakis G, Sherman P (1986) The interaction of sodium caseinate with monoglyceride and diglyceride at the oil-water interface and its effect on interfacial rheological properties. *Colloid Polym Sci* 264, 254-259

Fisher LR, Parker NS (1988) Effect of surfactants on the interactions between emulsion droplets. *In: Advances in Food Emulsions and Foams* (Dickinson E, Stainsby G, eds) Elsevier Appl Sci Publ, London, 45-90

Fisher LR, Mitchell EE, Parker NS (1985) Interfacial tensions of commercial vegetable oils with water. *J Food Sci* 50, 1201-1202

Gacula MC, Singh J (1984) *Statistical Methods in Food and Consumer Research. Food Science and Technology*. Academic Press, NY, 214-272

Goulden JDS, Phipps LW (1964) Factors affecting the fat globule size during the homogenization of milk and cream. *J Dairy Sci* 31, 195-200

Halling PJ (1981) Protein-stabilized foams and emulsions. *CRC Crit Rev Food Sci Nutr* 13, 155-203

Jenness R, Walstra P (1984) *Dairy Chemistry and Physics*. John Wiley and Sons, NY, 88-89

Kato A (1991) Significance of macromolecular interaction and stability in functional properties of food proteins. *In: Interaction of Food Proteins* (Parris N, Barford R, eds) ACS Symp Ser 454, Am Chem Soc, Washington, DC, 13-24

Kessler HG (1981) *Food Engineering and Dairy Technology*. Verlag A Kessler, Freising, 119-138

Koppel DE (1972) Analysis of macromolecular polydispersity in intensity correlation spectroscopy: the method of cumulants. *J Chem Phys* 57, 4814-4820

Little TM (1981) Interpretation and presentation of results. *Hortic Sci* 16, 19-31

Lorient D, Closs B, Courthaudon JL (1991) Connaissances nouvelles sur les propriétés fonctionnelles des protéines du lait et de ses dérivés. *Lait* 71, 141-171

MacRitchie F (1976) Monolayer compression barrier in emulsion and foam stability. *J Colloid Interface Sci* 56, 53-56

Montgomery DC (1976) *Design and Analysis of Experiments*. John Wiley and Sons, NY, 341-368

Neter J, Wasserman W, Kutner M (1985) *Applied Linear Statistical Models: Regression, Analysis of Variance and Experimental Designs*. Irwin, Homewood, 2nd edn

Ogden LV (1973) The homogenization-induced clustering of fat globules in cream and model systems. Ph Dissertation, Univ Minnesota, St Paul, MN

Oorwijn H, Walstra P (1979) The membranes of recombined fat globules. 2. Composition. *Neth Milk Dairy J* 33, 134-154

Paquin P, Britten M, Laliberté MF, Boulet M (1987) Interfacial properties of milk casein proteins. *In: Proteins at Interfaces: Physicochemical and Biochemical Studies* (Brash JL, Horbett TA, eds) ACS Symp Ser 343, Washington DC, 677-686

Paquin P, Glasson J (1989) La microfluidisation comme procédé d'homogénéisation d'une boisson à base de matière grasse laitière. *Lait* 69, 491-498

Pearce KN, Kinsella JE (1978) Emulsifying properties of proteins: evaluation of a turbidimetric technique. *J Agric Food Chem* 26, 716-723

Phipps LW (1975) The fragmentation of oil drops in emulsions by high-pressure homogenizer. *J Phys D: Appl Phys* 8, 448-462

Phipps LW (1982) Homogenizing valve design and its influence on milk fat globule dispersion. I. Low rate of flow (100 l.h–1 Re ≤ 3000). *J Dairy Res* 49, 309-315

Phipps LW (1983) Effects of fat concentration on the homogenization of cream. *J Dairy Res* 50, 91-96

Phipps LW (1985) *The High Pressure Dairy Homogenizer. Tech Bull 6*. Nat Inst Res Dairying, Reading, UK

Piggott JR (1986) *Statistical Procedures in Food Research*. Elsevier Appl Sci Publ, London, 101-123

Pouliot Y, Paquin P, Robin O, Glasson J (1991) Étude comparative de l'effet de la microfluidisation et de l'homogénéisation sur la distribution de la taille des globules de gras du lait de vache. *Int Dairy J* 1, 39-49

Robin O, Paquin P (1991) Evaluation of the particle size of fat globules in a milk model emulsion by photon correlation spectroscopy. *J Dairy Sci* 74, 2440-2447

SAS® (1990) SAS User's Guide: statistics Version 6.06. SAS Inst Inc, Cary, NC

Shinoda K, Kunieda H (1983) Phase properties of emulsions: PIT and HLB. *In Encyclopedia of Emulsion Technology. 1. Basic Theory* (Becher P, ed) Marcel Dekker, NY, 337-367

Sweetsur MA, Muir DD (1983) Effect of homogenization on the heat stability of milk. *J Dairy Res* 50, 291-300

Tadros TF, Vincent B (1983) Emulsion stability. *In: Encyclopedia of Emulsion Technology. 1. Basic Theory* (Becher P, ed) Marcel Dekker, NY, 129-285

Tornberg E (1980) Functional characteristics of protein stabilized emulsions: emulsifying behavior of proteins in a sonifier. *J Food Sci* 45, 1662-1668

Tornberg E, Olson A, Persson K (1990) Structural and interfacial properties of food proteins in relation to their function in emulsions. *In: Food Emulsions* (Larsson K, Friberg SE, eds) Marcel Dekker, NY, 247-326

Vuillemard JC (1991) Recent advances in the large scale production of lipid vesicles for use

in food products: microfluidization. *J Microencapsul* 8, 547-562

Walstra P (1969) Preliminary note on the mechanism of homogenization. *Neth Milk Dairy J* 23, 290-292

Walstra P (1974) Influence of rheological properties of both phases on droplet size of O/W emulsions obtained by homogenization and similar processes. *Dechema Monogr* 77, 87-94

Walstra P (1975) Effect of homogenization on the fat globule size distribution in milk. *Neth Milk Dairy J* 29, 279-294

Walstra P (1983) Emulsion formation. *In: Encyclopedia of Emulsion Technology. 1. Basic Theory* (Becher P, ed) Marcel Dekker, NY, 57-127

Walstra P, Oortwijn H (1982) The membranes of recombined fat globules. 3. Mode of formation. *Neth Milk Dairy J* 36, 103-113

Washington C (1987) Emulsion production by microfluidizer. *Lab Equip Dig* 85, 69-71

Weiner BB, Tschamuter WW (1987) Uses and abuses of photon correlation spectroscopy in particle sizing. *In: Particle Size Distribution: Assessment and Characterization* (Provder T, ed) ACS Symp Ser 332, Am Chem Soc, Washington DC, 48-64

Wolfram S (1991) *Mathematica: A System for Doing Mathematics by Computer.* Addison-Wesley Publ Co Inc, Champaign, IL, 2nd edn

Docket No. 20523 US (C038435/0120240)

IN THE UNITED STATES PATENT AND TRADEMARK OFFICE

In re Patent Application of:	)	
Chyi-Cheng CHEN and Bruno LEUENBERGER	)	
Serial No.: 09/726,880	)	Examiner: L.S. Channavajjala
Filed: November 30, 2000	)	Art Unit: 1615
For: **A VITAMIN POWDER COMPOSITION AND METHOD OF MAKING**	)	

New York, New York
December 2, 2009

FIFTH SUPPLEMENTAL INFORMATION DISCLOSURE STATEMENT

Mail Stop RCE
Commissioner for Patents
P.O. Box 1450
Alexandria, VA 22313-1450

Sir:

Applicants wish to make of record the following documents (a Form PTO/SB/08b listing the documents is enclosed).

OTHER PUBLICATIONS

C9. Robin, et al. "Microfluidization of dairy model emulsions. I. Preparation of emulsions and influence of processing and formulation on the size distribution of milk fat globules," *Lait* (1992) 72, 511-531

C10. Pozharski *et al.*, "Relationship Between Turbidity of Lipid Vesicle Suspensions and Particle Size," Analytical Biochemistry (2001) 291, 158-162

C11. The Merck Index, Fourteenth Ed. (2006) 1853, 1854, and 9494

C12. Desrumaux et al. "Formation of Sunflower Oil Emulsions Stabilized by Whey Proteins with High-Pressure Homogenization (up to 350 MPa); Effect of Pressure on Emulsion Characteristics," *Intl J. Food Science and Tech.* (2002) 37, 263-269

The Examiner's independent consideration of these documents and their relevance before issuance of the first official action subsequent to the filing of the concurrent request for continued examination is respectfully requested. The Examiner is also requested to initial and return a copy of the accompanying form PTO/SB/08 to evidence such consideration.

This submission does not represent an admission that the listed documents are material or constitute "prior art." If the Examiner applies the documents as references against any claim in the application and applicants determine that the cited documents do not constitute "prior art" under United States law, applicants reserve the right to present to the Office the relevant facts and law regarding the appropriate status of the documents.

All documents cited in these reports are identified herein and copies of all documents, other than the U.S. patent documents, are provided. See MPEP § 609(III)(A)(2)(A) (8th Ed., Rev. 2, May 2004, p. 600-128).

This Fifth Supplemental Information Disclosure Statement is being filed in accordance with the provisions of 37 CFR § 1.97(b)(4), before the mailing of a first Office Action after the filing of a request for continued examination under § 1.114.

Accordingly, it is believed that no fee is due. If any fee is due, please charge the same to Deposit Account No. 02-4467. A duplicate copy of this sheet is enclosed.

C12. Desrumaux et al. "Formation of Sunflower Oil Emulsions Stabilized by Whey Proteins with High-Pressure Homogenization (up to 350 MPa); Effect of Pressure on Emulsion Characteristics," *Intl J. Food Science and Tech.* (2002) 37, 263-269

The Examiner's independent consideration of these documents and their relevance before issuance of the first official action subsequent to the filing of the concurrent request for continued examination is respectfully requested. The Examiner is also requested to initial and return a copy of the accompanying form PTO/SB/08 to evidence such consideration.

This submission does not represent an admission that the listed documents are material or constitute "prior art." If the Examiner applies the documents as references against any claim in the application and applicants determine that the cited documents do not constitute "prior art" under United States law, applicants reserve the right to present to the Office the relevant facts and law regarding the appropriate status of the documents.

All documents cited in these reports are identified herein and copies of all documents, other than the U.S. patent documents, are provided. See MPEP § 609(III)(A)(2)(A) (8th Ed., Rev. 2, May 2004, p. 600-128).

This Fifth Supplemental Information Disclosure Statement is being filed in accordance with the provisions of 37 CFR § 1.97(b)(4), before the mailing of a first Office Action after the filing of a request for continued examination under § 1.114.

Accordingly, it is believed that no fee is due. If any fee is due, please charge the same to Deposit Account No. 02-4467. A duplicate copy of this sheet is enclosed.

If the Examiner has any questions regarding this paper, please contact the undersigned attorney.

I hereby certify that this correspondence is being deposited with the United States Postal Service with sufficient postage as first class mail in an envelope addressed to: Mail Stop RCE, Commissioner for Patents, P.O. Box 1450, Alexandria, VA 22313-1450, on December 2, 2009

Eileen M. Ebel, Reg.No. 37,316

Respectfully submitted,

By: _____

Eileen M. Ebel
Registration No. 37,316
BRYAN CAVE LLP
1290 Avenue of the Americas
New York, NY 10104
Phone: (212) 541-2000
Fax: (212) 541-4630

PTO/SB/08b (08-08)
Approved for use through 09/30/2008. OMB 0651-0031
U.S. Patent and Trademark Office; U.S. DEPARTMENT OF COMMERCE

Substitute for form 1449/PTO

INFORMATION DISCLOSURE STATEMENT BY APPLICANT

(Use as many sheets as necessary)

Sheet 1 of 1

Complete if Known	
Application Number	09/726,880
Filing Date	November 30, 2000
First Named Inventor	Chyi-Cheng CHEN
Art Unit	1615
Examiner Name	L.S. Channavajjala
Attorney Docket Number	20523US (C038435/0120240)

NON PATENT LITERATURE DOCUMENTS

Examiner Initials*	Cite No.[1]	Include name of the author (in CAPITAL LETTERS), title of the article (when appropriate), title of the item (book, magazine, journal, serial, symposium, catalog, etc.), date, page(s), volume-issue number(s), publisher, city and/or country where published.	T[2]
	C9	Robin, et al. "Microfluidization of dairy model emulsions. I. Preparation of emulsions and influence of processing," Lait (1992) 72, 511-531	
	C10	Pozharski et al., "Relationship Between Turbidity of Lipid Vesicle Suspensions and Particle Size," Analytical Biochemistry (2001) 291, 158-162	
	C11	The Merck Index, Fourteenth Ed. . (2006) 1853, 1854, and 9494	
	C12	Desrumaux et al. "Formation of Sunflower Oil Emulsions Stabilized by Whey Proteins..." Intl J. Food Science and Tech. (2002) 37, 263-269	

Examiner Signature		Date Considered	

*EXAMINER: Initial if reference considered, whether or not citation is in conformance with MPEP 609. Draw line through citation if not in conformance and not considered. Include copy of this form with next communication to applicant.

[1] Applicant's unique citation designation number (optional). [2] Applicant is to place a check mark here if English language Translation is attached.

C9

Lait (1992) 72, 511-531
© Elsevier/INRA

Original article

Microfluidization of dairy model emulsions. I. Preparation of emulsions and influence of processing and formulation on the size distribution of milk fat globules

O Robin, V Blanchot, JC Vuillemard, P Paquin

Université Laval, Sainte-Foy, centre de recherche en sciences et technologies du lait (STELA), département de sciences et technologie des aliments, (Québec), Canada G1K7P4

(Received 1st July 1992; accepted 17 September 1992)

Summary — The influence of certain process variables (pressure and temperature) as well as composition variables (fat, protein and low molecular weight emulsifier concentrations) on the size distribution of milk fat globules was studied in a dairy model emulsion (oil-in-water) produced by microfluidization, a mechanical emulsification technique. The use of a central composite experimental design allowed us to obtain 2 nonlinear multiple regression equations relating the volume-weighted average diameter of the fat globules ($\bar{d}_v$) as well as the relative size distribution width *(cv)* to the emulsification pressure (7.8–76.3 MPa) and temperature (35–100 °C), and to sodium caseinate (0.5–3.9 wt%), butter oil (5.2–14.7 wt%) and monoglyceride (0.08–0.88 wt%) concentrations. These 2 functions account respectively for 93.7 and 81.7% of the variation in the average diameter and in the size distribution width of the microfluidized fat globules and were used to explain certain interactions between the different variables affecting the size of the microfluidized fat globules. They were also used to demonstrate the existence of the optimal conditions that correspond to the extremes of the average particle diameter and of the distribution width of the fat globules. Finally, these 2 functions allowed us to predict fat globule size parameters as a function of process and formulation conditions.

emulsification / microfluidization / oil-in-water emulsion / fat globule

Résumé — Microfluidisation d'émulsions laitières modèles. I. Préparation des émulsions et influence des facteurs de procédé et de formulation sur la distribution de la taille des globules de gras. *L'influence de certaines variables opératoires (pression et température) et des variables de composition (teneurs en huile de beurre, en protéine et en émulsifiant de faible poids mo-*

Symbols used and SI units: [*BO*] = butter oil concentration (wt%); *cv* = coefficient of variation or relative standard deviation of the volume-weighted size distribution (%); $\bar{d}_v$ = volume-weighted average fat globule diameter (m); D = diffusion coefficient ($m^2.s^{-1}$); *F* = number of factorial points of the design and Fisher ratio; *k* = number of independent variables or conductivity of a solution ($S.m^{-1} = m^{-3}.kg^{-1}.s^3.A^2$); [*MGS*] = monoglyceride concentration (wt%); [*Prot*] = protein concentration (wt%); *P* = emulsification pressure ($Pa = m^{-1}.kg.s^{-2}$); *Q* = flow rate ($m^3.s^{-1}$); *S* = interfacial area (m^2); *T* = emulsification temperature (K); α = distance separating a star point from a factorial point in terms of coded variables (dimensionless); ε = power density ($W.m^{-3} = m^{-1}.kg.s^{-3}$); Φ = volume fraction of the disperse phase (dimensionless); γ = interfacial tension ($N.m^{-1} = kg.s^{-2}$); ρ = mass density ($kg.m^{-3}$).

léculaire) sur la distribution de la taille des globules de gras d'une émulsion laitière modèle (huile dans l'eau) a été étudiée pour une technologie d'émulsification mécanique donnée : la microfluidisation. L'utilisation d'un dispositif expérimental central composite a permis l'obtention de 2 équations de régression multiple non linéaires reliant le diamètre moyen des globules de gras ($\bar{d}_v$) ainsi que l'étendue relative de la dispersion des tailles (cv) à la pression (7,8–76,3 MPa) et à la température d'émulsification (35–100 °C), aux teneurs en caséinate de sodium (0,5–3,9% de la masse totale), en huile de beurre (5,2–14,7%) et en monoglycéride (0,08–0,88%). Ces 2 fonctions expliquent respectivement 93,7% et 81,7% des variations du diamètre moyen des globules de gras microfluidisés et de l'étendue relative de la distribution des tailles dans les valeurs considérées des paramètres. Ces fonctions ont en outre permis d'expliquer certaines interactions entre les différentes variables précitées sur la distribution de la taille des globules de gras microfluidisés. Elles ont également permis de mettre en évidence l'existence de conditions optimales correspondant à des extremums du diamètre particulaire moyen et de l'étendue de la distribution de la taille des globules de gras. Finalement, ces 2 fonctions nous ont permis de prédire la distribution de la taille des globules de gras en fonction des conditions de procédés et de formulation.

émulsification / microfluidisation / émulsions huile dans l'eau / globules de gras

INTRODUCTION

For a number of industries, the homogenization, and more generally the mechanical emulsification of liquids, dietary as well as others, has become over the past many years an important technological process. The use of this type of process in the food, pharmaceutical and cosmetic industries in general and in certain dairy operations in particular is essential for the production of emulsions with certain desirable rheological properties (creams and ointments), textures (ice cream, mayonnaise) and degrees of stability (milk, salad dressing) (Dickinson and Stainsby, 1988). The principle of homogenization and mechanical emulsification processes which, according to Gaulin, must allow "de fixer la composition des liquides" remains simple: in the case of milk, the homogenization process results in a considerable decrease in the size of the fat globules found in the initial suspension, and has the effect of increasing the creaming stability of the emulsion (Tadros and Vincent, 1983). Aside from conventional homogenizers, relatively few mechanical emulsification processes have been and are used in an industrial setting (Walstra, 1983). During the 1980s, however, other mechanical emulsification processes appeared. One of them, called microfluidization (Cook and Lagace, 1985; Washington, 1987), was initially used principally in the cosmetic and pharmaceutical industries (Chandonnet *et al*, 1985). More recently, microfluidization was suggested as an alternative method for the production of milk fat microcapsules (Vuillemard, 1991), alcoholized creams (Paquin and Giasson, 1989) and for milk homogenization (Pouliot *et al*, 1991). If the result of the process is similar to that of homogenization (reduction in the size of the fat globules), the means used to achieve such a result are different. As is the case for conventional homogenization processes, the liquid is forced under high pressure into a chamber. However, in the case of the microfluidization process, the liquid is then divided into 2 microstreams that are projected against one another at high speed and at an angle of 180° (Cook and Lagace, 1985).

Other than a considerable change in the dispersion state of the fat, the emulsification of dietary liquids also results in a considerable rearrangement of the oil–water interface

(Walstra and Oortwijn, 1982) where mainly 2 classes of molecules can be adsorbed: amphiphilic macromolecules (mainly proteins) and low molecular weight emulsifiers (lecithins, monoglycerides, Tweens, Spans, etc) (Dickinson *et al*, 1990). Proteins and low molecular weight emulsifiers affect the production and stabilization of emulsions. Proteins play 2 major roles: on the one hand they lower surface tension between the interfaces that are formed during the emulsification process, and on the other hand, they form a macromolecular layer surrounding the dispersed particles which structurally stabilizes the emulsion by reducing the rate of recoalescence (Fisher and Parker, 1988). Low molecular weight emulsifiers affect the production and stabilization of emulsions in several ways: during emulsification, by reducing interfacial tension more rapidly than would the proteins alone, they allow the production of smaller-sized dispersed particles (Darling and Birkett, 1987). Furthermore, while proteins generally stabilize oil-in-water emulsions, low molecular weight emulsifiers tend to destabilize them (Dickinson *et al*, 1990) by removing protein from the surface of the dispersed particles. This ability of low molecular weight emulsifiers to dislodge macromolecules is due to their greater energy of adsorption compared to individual segments of macromolecules. Finally, if the distribution of these 2 classes of molecules between the surfaces of the dispersed particles and the bulk phase is directly affected by the competitive adsorption between the macromolecules and the emulsifiers at the oil–water interface, it is also a result of the nature of macromolecule–emulsifier interactions at the interface and in the bulk phase (Dickinson, 1986).

Opinions are divided as to the usefulness of using experimental model systems (systems containing a single protein source and/or low molecular weight emulsifier) rather than real food systems (Darling and Birkett, 1987; Dickinson *et al*, 1990). Even if the model systems allow relatively precise information to be obtained, they can rarely be extrapolated to real food systems. An alternative would be to use systems that can be called "quasi-foods", that is systems that contain a known mixture of proteins and low molecular weight surfactants and whose concentrations are controlled.

The aim of the study presented here was to examine the influence of certain process (pressure and temperature) and composition (butter oil, protein and surfactant concentrations) variables on the size distribution of fat globules in a model dairy emulsion (oil-in-water) using a given mechanical emulsification technology, *ie* microfluidization.

MATERIALS AND METHODS

Experimental design

Description

A central composite rotatable design made up of $k = 5$ factors with 3 levels and 1 repetition was developed. This type of design, the most widely used for fitting experimental results to a second-order model (Piggot, 1986; Box and Drapper, 1987), is called rotatable because the variance of the estimated response $\hat{y}$ at point x is uniquely a function of the distance separating this point from the centre point and not of the direction. These designs are composed of 2^k factorial points (usually coded ± 1) with 2^k star points coded [(± α, 0, 0, ..., 0), (0, ± α, 0, ..., 0), ..., (0, 0, 0, ..., ± α)] and n_0 centre points coded (0, 0, ..., 0). The value of α, on which the rotability of the design depends, is such that $\alpha = (F)^{1/4}$ where F is the number of factorial points of the design: in the present case $F = 2^k$. The complex principles for the development of these designs have been presented by various authors including Montgomery (1976), Gacula and Singh (1984), and Box and Drapper (1987).

The design used was therefore composed of 2^5 factorial points, with 10 star points (with α =

2.38) and 10 centre points which results in a total of 52 experimental units or emulsions.

The 5 factors that were varied in the preparation of the emulsions are the following: 2 process factors–emulsification pressure (7.8, 20.7, 41.4, 62.1 and 76.3 MPa) and temperature (35, 55, 70, 85 and 100 °C), and 3 formulation factors–protein concentration (0.5, 0.9, 1.5, 2.5 and 3.9 wt%), butter oil concentration (5.2, 8, 10, 12 and 14.8 wt%) and monoglyceride concentration (0.08, 0.2, 0.4, 0.6 and 0.88 wt%).

Statistical analysis

An analysis of variance was first conducted on the values of the volume-weighted average diameters of the emulsified fat globules ($\bar{d}_v$) and on the relative width *(cv)* of the particle size distribution. This analysis allowed the split of the total variation of the measured parameters ($\bar{d}_v$ and *cv*) according to the principal effects of the treatments, the interactions and the error. The sum of the squares of the differences of the principal effects was split in unitary degree of freedom using an orthogonal comparison method (Box and Drapper, 1987). This calculation allowed an individual estimation of effects without mutual interference. Two tests were then carried out: a Fisher test allowed a differentiation between the treatments and the interactions which had a significant effect on a given parameter, and an adjustment test (Neter *et al*, 1985) confirmed that the second-order model allowed an adequate description (to ± 1%) of the variances in the experimental results.

The effects of the principal treatments and/or interactions which were not significant at the level 95% have been included in the error term. This pooling, which has been justified by Little (1981), increases the degree of significance of the variance due to an increase in the number of degrees of freedom. Although a lower probability threshold could be used in the selection of the effects to be considered in the determination of the regression equation, a probability threshold of at least 95% was used in order to simplify the expression and use of the regression equations.

Finally, following this second analysis of variance, each of the 2 measured parameters ($\bar{d}$, and cv) was analyzed as a function of the principal effects and interactions of process and composition variables. The nullity of the regression coefficients was tested using Student's test (Neter *et al*, 1985).

This method for interpreting results is supported and recommended by Little (1981) and Box and Drapper (1987). According to these authors, all the treatment levels in the experimental range are significantly different in their effects after a significant tendency has been established. The best estimates of the effects of the treatments are those values calculated using the regression equation.

Statistical procedure and graphic

The analysis of variance and regression calculations were carried out using the General Linear Model procedure (Proc GLM and Proc REG) of the SAS (1990).

The 3-dimensional picture of the equations was carried out using Mathematica (Wolfram, 1991).

Emulsion preparation

Ingredients

Sodium caseinates (89.3% protein) were obtained from ICN Nutritional Biochemicals, Canada Ltd (Dorval, Que, Canada). Butter oil (99.4% anhydrous) was purchased from a local dairy cooperative (Agropur, Granby, Quebec, Canada) and was stored at 4 °C. Distilled monoglycerides (EXCEL, T-95) with a hydrophile-lipophile balance (HLB) of 4.5 (Shinoda and Kunieda, 1983) were purchased from Atkemix (Bratford, Ontario, Canada). Sodium azide was purchased from Fisher Scientific (Quebec, Que, Canada).

Emulsion production

Fifty-two emulsions (600 g) containing 0.5, 0.9, 1.5, 2.5 or 3.9 wt% (based on protein content) sodium caseinates, 5.2, 8, 10, 12 or 14.8 wt% butter oil, and 0.08, 0.2, 0.4, 0.6 or 0.88 wt% monoglyceride were prepared in the following manner: various sodium caseinate solutions, hydrated and solubilized in deionized water (k = 1.1 µS.cm^{-1}) for 90 min, and butter oil, preheated to 50 °C, were mixed using a magnetic stirrer. The solutions were then brought to the appropriate emul-

Table I. Process variables (protein, butter oil and monoglyceride concentrations, emulsification pressure and temperature) and responses of the central composite rotatable design in terms of volume-weighted average diameter and relative width of the emulsified fat globules distribution.
Variables de procédés (concentrations en protéine, huile de beurre et monoglycéride, pression et température d'émulsification) et réponses en termes du diamètre pondéré en volume et du coefficient de variation de la distribution de la taille des globules de gras émulsifiés.

Trials	[Prot] (wt%)	[BO] (wt%)	[MGS] (wt%)	P (MPa)	T (°C)	$(\bar{d}_v)$ (nm)	cv (%)
Factorial points							
1	0.5	8	0.2	20.7	55	584	51
2	0.5	8	0.2	20.7	85	594	49
3	0.5	8	0.2	62.1	55	480	56
4	0.5	8	0.2	62.1	85	466	55
5	0.5	8	0.6	20.7	55	427	39
6	0.5	8	0.6	20.7	85	382	38
7	0.5	8	0.6	62.1	55	317	48
8	0.5	8	0.6	62.1	85	326	38
9	0.5	12	0.2	20.7	55	806	69
10	0.5	12	0.2	20.7	85	793	69
11	0.5	12	0.2	62.1	55	808	52
12	0.5	12	0.2	62.1	85	777	53
13	0.5	12	0.6	20.7	55	460	67
14	0.5	12	0.6	20.7	85	491	64
15	0.5	12	0.6	62.1	55	407	47
16	0.5	12	0.6	62.1	85	419	43
17	2.5	8	0.2	20.7	55	509	41
18	2.5	8	0.2	20.7	85	482	47
19	2.5	8	0.2	62.1	55	439	42
20	2.5	8	0.2	62.1	85	358	50
21	2.5	8	0.6	20.7	55	423	41
22	2.5	8	0.6	20.7	85	407	47
23	2.5	8	0.6	62.1	55	361	46
24	2.5	8	0.6	62.1	85	300	51
25	2.5	12	0.2	20.7	55	574	56
26	2.5	12	0.2	20.7	85	593	59
27	2.5	12	0.2	62.1	55	538	52
28	2.5	12	0.2	62.1	85	539	40
29	2.5	12	0.6	20.7	55	609	45
30	2.5	12	0.6	20.7	85	653	46
31	2.5	12	0.6	62.1	55	563	28
32	2.5	12	0.6	62.1	85	509	32
Centre points							
33	1.5	10	0.4	41.4	70	420	46
34	1.5	10	0.4	41.4	70	427	45
35	1.5	10	0.4	41.4	70	451	45
36	1.5	10	0.4	41.4	70	448	45
37	1.5	10	0.4	41.4	70	415	46
38	1.5	10	0.4	41.4	70	441	46
39	1.5	10	0.4	41.4	70	465	43
40	1.5	10	0.4	41.4	70	433	45
41	1.5	10	0.4	41.4	70	471	41
42	1.5	10	0.4	41.4	70	444	46
Star points							
43	0.9	10	0.4	41.1	70	442	50
44	3.9	10	0.4	41.4	70	403	29
45	1.5	5.2	0.4	41.4	70	291	31
46	1.5	14.8	0.4	41.4	70	633	52
47	1.5	8	0.08	41.4	70	549	53
48	1.5	8	0.88	41.4	70	324	30
49	1.5	8	0.4	7.8	70	942	39
50	1.5	8	0.4	76.3[1]	70	461	66
51	1.5	8	0.4	41.1	35[2]	655	55
52	1.5	8	0.4	41.4	100[3]	513	58

For the design rotability to be perfect ($\alpha = 2.378$), the values of some independent parameters should be: [1] emulsion 50, $P = 90.6$ MPa (in fact, the maximum pressure given by the air feed system was 76.5 MPa); [2] Emulsion 51, $T = 34.3$ °C; [3] Emulsion 52, $T = 105.7$ °C.

sification temperature (35, 55, 70, 85 or 100 °C) and the emulsifiers were added. The dispersions, maintained at the emulsification temperature (± 1.5 °C), were then mixed for 2 min using a stirrer (Braun CDN Ltd, Model MR7, Mississauga, Ont, Canada). The oil-in-water dispersions were then immediately emulsified using a Microfluidizer (M-110™, Microfluidic Corporation, Boston, MA, USA) at its maximum power setting.

The microfluidization procedure was performed in 2 stages: the first processing was at 7.8, 20.7, 41.4, 62.1 or 76.3 MPa and the second at 4.8 MPa in order to eliminate aggregates formed during the first processing procedure (Ogden, 1973; Walstra, 1975). The composition of the emulsions is given in table I.

Sodium azide, an antibacterial agent, was added to each emulsion (0.2% vol/wt), and 2 pH

measurements (pH-meter, Corning 140, electrode 476530, Canlab, Montreal, Que, Canada) were carried out.

Size distribution of the emulsified fat globules

Sampling

A sample of each emulsion was taken and stored at 4 °C for 24 h in a 20 ml bottle completely filled. Before analysis, the samples were heated (T = 20 °C) and manually stirred. This procedure, proposed by Walstra (1975), was used in order to prevent a change in the size distribution of the fat globules due to churning.

Dissociation of protein structures

The samples were mixed with a buffer (urea, EDTA and β-mercaptoethanol, pH 7) designed by Dalgleish *et al* (1987) to dissociate protein structures. Despite the presence of sodium caseinates in the emulsions, the composition of the dissociating buffer was not modified. Measurements were carried out immediately after vigorous manual stirring.

Photon correlation spectrophotometry

The size distributions of the fat globules were determined by photon correlation spectrometry (PCS) using the method proposed by Robin and Paquin (1991). The measurements were taken using the Nicomp multibit (7 bit) 64-channel photon correlation system (Pacific Scientific, Hiac/Royce Instruments Division, Model 370, Menlo Park, CA, USA); the correlation functions were measured on the light that was diffused at an angle of 90° by the particles in suspension. The correlation functions were analyzed by the cumulants method (Koppel, 1972). The first cumulant yielded an average diffusion coefficient (D), and the second yielded a mean squared deviation of the average diffusion coefficient (σ^2). The volume-weighted average particle diameters ($\bar{d}_v$) were calculated using the Stokes-Einstein law, and polydispersity was expressed by the relative standard deviation or coefficient of variation (cv) of the volume-weighted distribution calculated as the distribution width divided by the average diameter. The accuracy (≅ 1%), the reproducibility (≅ 1%) as well as the length of the analysis (2.5 x 10^6 photo-impulses or ≈ 20 min) were determined on latex sphere solutions (Robin and Paquin, 1991).

Three measurements of the size distribution of the fat globules were carried out on each sample. The values of the average diameters and relative widths of the size distribution of the fat globules are shown in table I.

Average size distributions

A logarithmic transformation was applied to the emulsified fat globule volume-weighted average diameter ($\bar{d}_v$) and to the homogenization pressure. Indeed, using the theory of isotropic turbulence developed by Kolmogorov (Walstra, 1969, 1983) showed that the maximum size of a fat globule undergoing the homogenization process is a function of the energy density ε (energy dissipated per unit of volume and time) or of the pressure P ($\varepsilon \propto P^{3/2}\ \rho^{-1/2}$), of the interfacial tension γ, and of the mass density ρ according to:

$$d_{max} \propto (\varepsilon^{-2}\ \gamma^3\ \rho^{-1})^{\frac{1}{5}} \propto P^{-\frac{3}{5}} \quad [1]$$

or

$$\log_{10}(d_{max})\ \alpha\ -\frac{3}{5}\ \log_{10}(P) \quad [2]$$

Goulden and Phipps (1964), Walstra (1975) and others have experimentally confirmed these results.

RESULTS

Accuracy and reproducibility of the PCS technique

The 10 centre points serve as an indication of the reproducibility of the PCS technique for determining the parameters of the size distribution of the fat globules. These centre points correspond to values obtained from the same emulsion. Using these results, the reproducibility of the evaluation of the $\bar{d}_v$ and cv parameters was approximately 4.2, and

3.2% respectively. However, even though the reproducibility of the results seem satisfying, that is, comparable with those obtained by other methods, their accuracy must be interpreted with some caution. Even though the validity of the PCS technique, in terms of precision and reproducibility, has been demonstrated by scattering from known mixtures of relatively monodispersed polystyrene latex beads (Bargeron, 1974; Brown and Pusey, 1975), results become less reliable when distributions are larger and polydispersed (Weiner and Tschamuter, 1987). Moreover, if the second cumulant is generally dominated by polydispersity rather than by statistical noise in the autocorrelation function, in large distributions the analysis of the cumulant can lead to an underestimation of the variance (Chu and Dinapoli, 1983). Higher order terms should be taken into account, but this remains a difficult problem (Nicoli, personal communication).

Influence of process variables on the average diameter of fat globules and on the distribution width of the diameters

An analysis of variance was carried out on the values given in table I using orthogonal comparisons between the principal treatments and between the interactions (Box and Drapper, 1987). An *F* test was carried out to differentiate the treatments and the interactions which had a significant effect on the volume-weighted average diameter of the fat globules (d_v) and on the size distribution of the relative width *(cv)*. An adjustment test of the experimental results for a second-order model was also carried out.

Average diameter of the emulsified fat globules

Table II shows the analysis of variance of the $\log_{10}$ (d_v) as a function of process

Table II. Analysis of variance of the logarithm of the volume-weighted average fat globule diameter versus process and composition variables.
Analyse de variance du logarithme du diamètre moyen pondéré en volume des globules de gras, en fonction des variables de procédé et de composition.

	df[1]	SS[2]	F[3]	r²[4]
Model	20	0.624	36.0[a]	0.959
Linear effects				
[*Prof*]	1	0.008	9.6[c]	
[*BO*]	1	0.217	251.4[a]	
[*MGS*]	1	0.147	170.4[a]	
$\log_{10}$ *(P)*	1	0.103	119.1[a]	
T	1	0.006	6.6[d]	
Quadratic effects				
[*Prof*]²	1	$< 10^{-3}$	< 0.1	
[*BO*]²	1	0.002	1.9	
[*MGS*]²	1	$< 10^{-3}$	< 0.1	
$\log_{10}{}^2$ (P)	1	0.038	43.5[a]	
T^2	1	0.025	28.9[a]	
[*Prof*] x [BO]	1	$< 10^{-3}$	0.5	
[*Prof*] x [MGS]	1	0.064	73.8[a]	
[*Prof*] x $\log_{10}$ (P)	1	$< 10^{-3}$	0.4	
[*Prof*] x *T*	1	0.001	1.3	
[*BO*] x [*MGS*]	1	$< 10^{-3}$	< 0.1	
[*BO*] x $\log_{10}$ *(P)*	1	0.006	7.0	
[*BO*] x *T*	1	0.002	2.6	
[*MGS*] x $\log_{10}$*(P)*	1	0.001	1.4	
[*MGS*] x *T*	1	$< 10^{-3}$	< 0.1	
T x $\log_{10}$ *(P)*	1	0.002	2.0	
Error	31	0.027		
Lack of fit	22	0.002	3.4[c]	
Pure error	9	0.003		
Total	51	0.651		
Model	8	0.610	80.8[a]	0.937
Error	43	0.041		
Total	51	0.651		

[1] df = degree of freedom; [2] SS = sum of squares; [3] F = Fisher ratio; [4] r^2 = coefficient of determination. Significance levels [a] $p \leq 0.0001$; [b] $p \leq 0.001$; [c] $p \leq 0.01$; [d] $p \leq 0.05$.

variables. According to the adjustment test, for $p \leq 0.01$ ($F < 4.77$), the second-order model allowed an adequate description of the variance of $\log_{10}$ $(\bar{d}_v)$. Furthermore, the linear effects of all the principal factors were significant (from 95% to 99.999%). Butter oil ([*BO*]) and monoglyceride ([*MGS*]) concentrations had a major effect on the variance of the fat globule diameter: they explained 33.4% and 22.6%, respectively, of the total variance. The emulsification pressure *(P)* and temperature *(T)* represented 21.7% and 4.8% respectively, of the variance (the sum of the linear and quadratic effects: $\log_{10}$ *(P)* + $\log_{10}^2$ *(P)* or $T + T^2$) of $\log_{10}$ $(\bar{d}_v)$. The effect of the protein concentration was significant ($p \leq 0.001$) but represented only 1.3% of the variance of the $\log_{10}$ $(\bar{d}_v)$. The last significant effect given by the analysis of variance was the [*Prot*] x [MGS] interaction which represented 9.8% of the variance of the $\log_{10}$ $(\bar{d}_v)$. Other effects were not significant ($p > 0.05$). The error term represented ≈ 4% of the variance of $\log_{10}$ $(\bar{d}_v)$.

A regression equation calculated from the significant effects ($p \leq 0.05$ or more) of the analysis of variance of $\log_{10}$ $(\bar{d}_v)$ is shown in table III. This second-order model was highly significant ($p \leq 0.0001$) and explains 93.7% of the total variance of $\log_{10}$ $(\bar{d}_v)$. All of the regression coefficients were highly significant ($p \leq 0.0001$). It is, however, worth noting that the existence of a minimum average diameter as a function of pressure (regression equation) was not significant, and resulted from an artefact produced by one of the extreme point (star point No 48). A separate regression analysis revealed that the increase in size beyond $P \cong 50$ MPa (the emulsification pressure from the regression model for which the derivative equals 0) was not significant.

Figure 1 is the response surface obtained from a second-order model relating

Table III. Analysis of regression and second-order model of the logarithm of the volume-weighted average fat globule diameter versus significant variables and interactions.
Analyse de régression et modèle de second ordre du logarithme du diamètre moyen pondéré en volume des globules de gras émulsifiés, en fonction des variables et des interactions significatives.

	Estimate [1]	*STD* [2]	t [3]
Parameter:			
Intercept	14.293	1.6	9.1[a]
[*Prot*]	–0.102	$1.2\ 10^{-2}$	–8.5[a]
[*BO*]	0.035	$2\ 10^{-3}$	15.2[a]
[*MGS*]	–0.633	$5\ 10^{-2}$	–13.4[a]
$\log_{10}$ *(P)*	–4.755	0.7	–6.9[a]
T	–0.016	$3\ 10^{-3}$	–5.5[a]
$\log_{10}^2$ *(P)*	0.506	0.1	6.6[a]
T^2	$1.1\ 10^{-4}$	$2\ 10^{-5}$	5.2[a]
[*Prot*] x [*MGS*]	0.223	$2.7\ 10^{-2}$	8.2[a]

$$\log_{10}(\bar{d}_v) = 14.293 - 0.102\,[Prot] + 0.035\,[BO] - 0.633\,[MGS] - 4.755\,\log_{10}(P) - 0.016\,T + 0.506\,\log_{10}^2(P) + 10^{-4}\,T^2 + 0.223\,[Prot] \times MGS$$

Validity intervals:
7 800 ≤ P ≤ 76 310 kPa 0.5 ≤ [*Prot*] ≤ 3.9 wt%
35 ≤ *T* ≤ 100 °C 5.2 ≤ [*BO*] ≤ 14.8 wt%
0.08 ≤ [*MGS*] ≤ 0.88 wt%

[1] Estimate = parameter estimated under the regression model (table II). [2] *STD* = standard error of the estimate. [3] *t* = value of Student's *t*-test. Significance level: a: $p \leq 0.0001$.

the values of $\bar{d}_v$ as a function of the butter oil concentration ([*BO*], wt%) and of the emulsification pressure (P, MPa) for a fixed temperature (50 °C) and for fixed protein (1.5 wt%) and monoglyceride (0.[illegible] wt%) concentrations. As has been reported elsewhere, the average diameter of the fat globules decreases and reaches a plateau as emulsification pressure increases

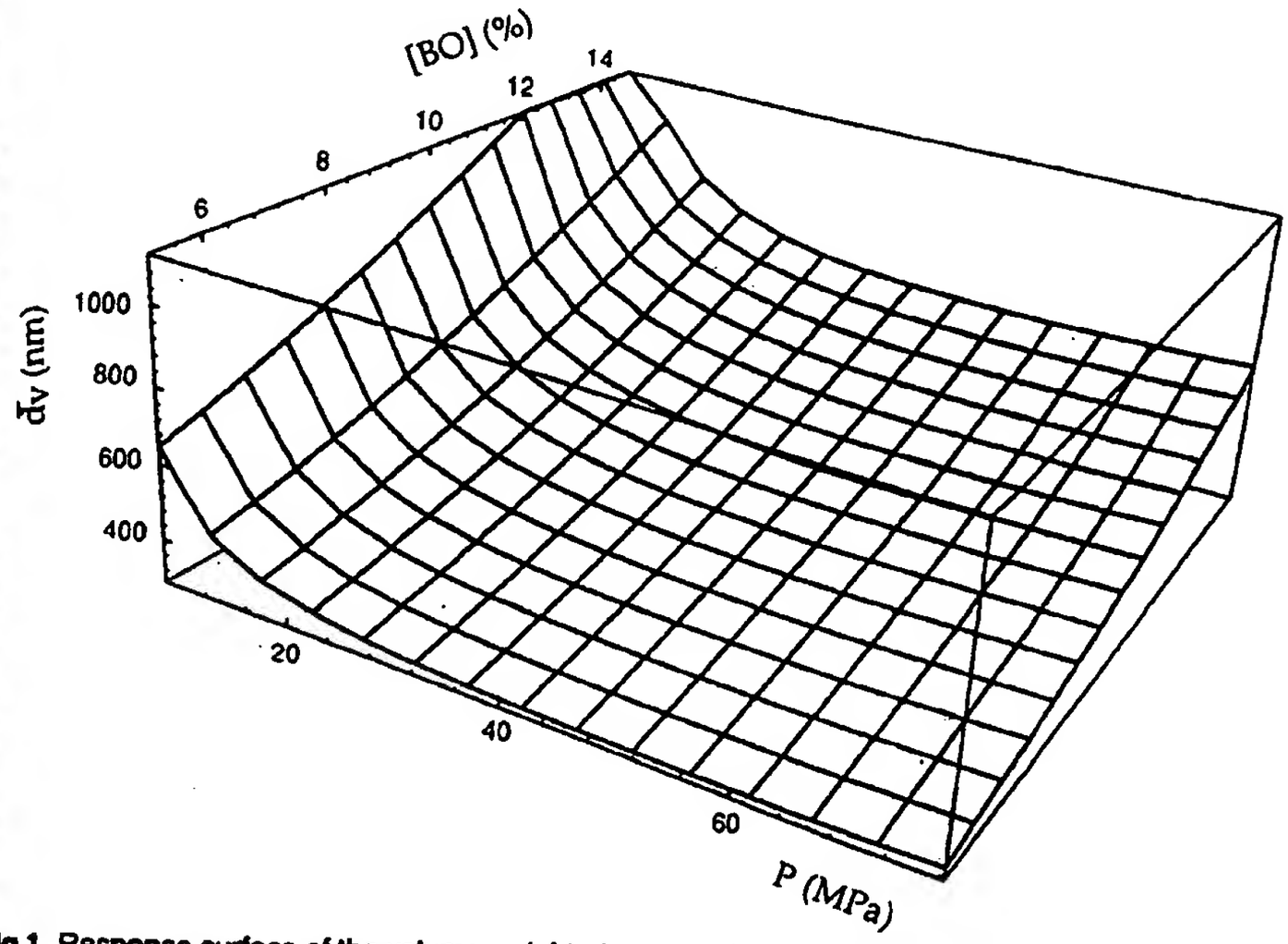

Fig 1. Response surface of the volume-weighted average fat globule diameter as a function of emulsification pressure, *P* (MPa), and butter oil concentration, [*BO*] (wt%), for a fixed temperature (*T* = 50 °C), a fixed protein concentration ([*Prot*] = 1.5 wt%), and a fixed monoglyceride concentration ([*MGS*] = 0.4 wt%).

Surface de réponse du diamètre moyen pondéré en volume des globules de gras en fonction de la pression d'émulsification, P *(MPa), et de la concentration en huile de beurre, [BO] (%), pour une température donnée* T *= 50 °C), et des concentrations fixées en protéines (*[Prot] *= 1.5% et en monoglycérides (*[MGS] *= 0.4%).*

but increases as the fat content increases (Walstra, 1975; Phipps, 1985).

Figure 2 shows the complex influences of emulsifier type and concentration on fat globule size, for emulsions produced under conditions of constant pressure (50.0 MPa), temperature (50 °C), and butter oil concentration (10 wt%). Our results are in agreement with previous reports in that, if the presence of a single surfactant results in a dramatic lowering of the size of the fat globules, the near absence of surfactants ($[Prot]_{min}$ = 0.5 wt%, and $[MGS]_{min}$ = 0.08 wt%) results in a maximum value for $\bar{d}_v$ (678 nm).

Relative width of the size distribution of the emulsified fat globules

A preliminary statistical analysis has revealed that the variations of *cv* as a function of various independent variables could not be adequately described by a second-order model (r^2 = 0.71 after pooling; the adjustment test was not significant) in the original validity interval. A reduction of the

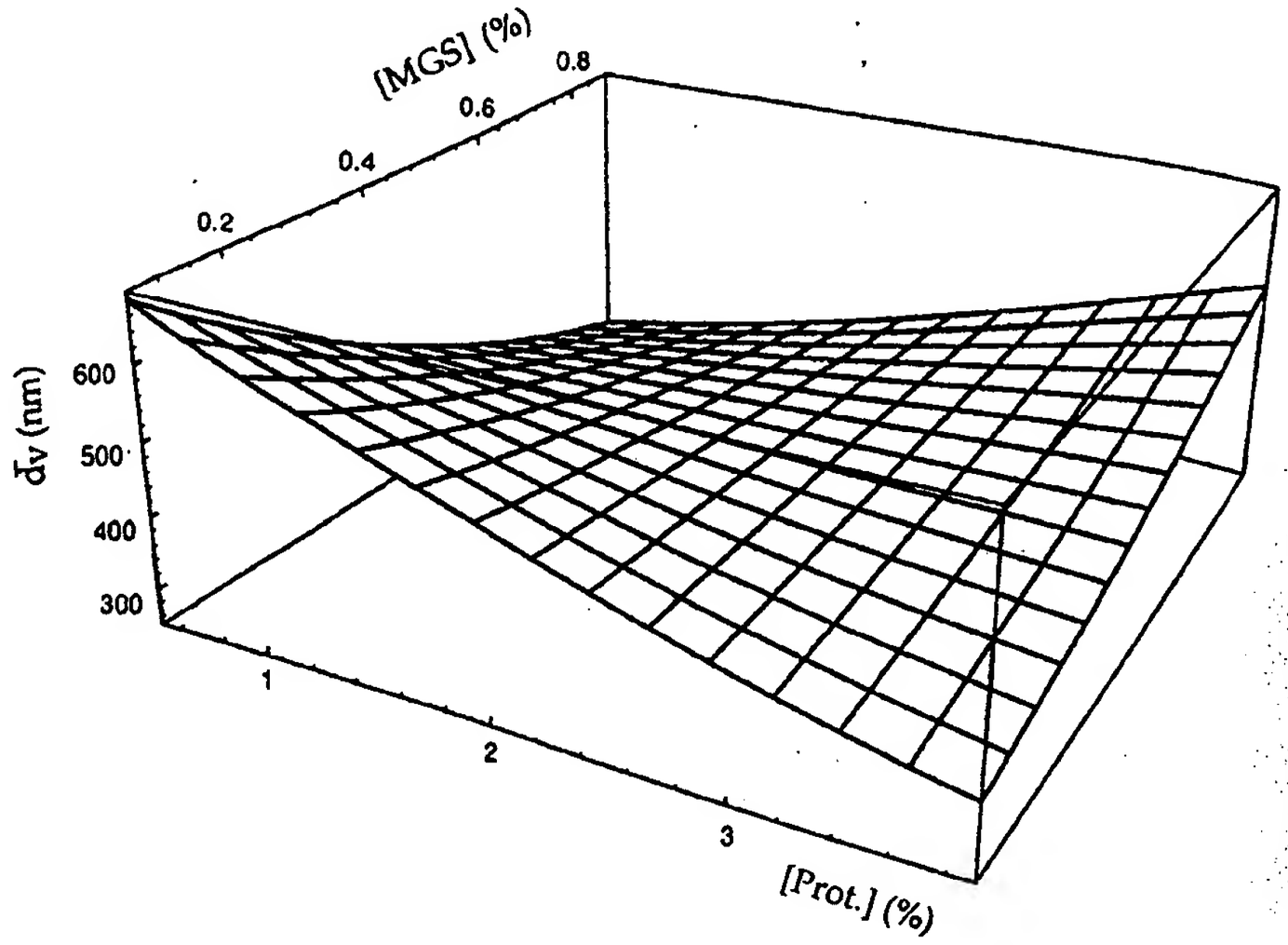

Fig 2. Response surface of the volume-weighted average fat globule diameter as a function of protein, [*Prot*] (wt%), and monoglyceride, [*MGS*] (wt%), concentrations for a fixed temperature (T = 50 °C), a fixed pressure (P = 50 MPa), and butter oil concentration [*BO*] = 10 wt%).
Surface de réponse du diamètre moyen pondéré en volume des globules de gras en fonction des concentrations en protéines, [Prot] (%), et monoglycérides, [MGS] (%), pour une température (T = 50 °C), une pression (P = 50 MPa), et une concentration en huile de beurre ([BO] = 10%) fixées.

interval corresponding to the elimination of an extreme point (No 49) has consequently been effected.

Table IV shows the analysis of variance of *cv* as a function of the process variables. According to the adjustment test, for $p \leq 0.01$ ($F < 4.77$), a second-order model could adequately describe the variances of *cv* in this new validity interval. As mentioned previously, the linear effects of the principal factors, except the temperature one, were significant (from 95% to 99.999%). The protein and monoglyceride concentrations had an important effect on the variance of *cv*: they explained respectively 16.0% and 13.4% of the total variance. The emulsification pressure and temperature represented respectively 16.8% and 2.7% (the sum of the linear and quadratic effects: $P + P^2$ and T^2) of the variance of *cv*. The effect of the butter oil concentration ($p \leq 0.0001$) represented 7.7% of the variance of *cv*. The other highly significant interactions ([*Prot*] x [*BO*] and [*BO*] x *P*) represented 28.5% of the total variance. The error represented approximately 10.2% of the variance of *cv*.

A regression equation, calculated using highly significant effects ($p \leq 0.000\,1$) from the analysis of variance of *cv*, is shown in

Table IV. Analysis of variance of the standard deviation of the volume-weighted size distribution of fat globules versus process and composition variables.
Analyse de variance de la déviation standard de la distribution des tailles pondérées en volume des globules de gras en fonction des variables de procédé et de composition.

	df [1]	SS [2]	F [3]	r² [4]
Model	20	4 196.5	13.1[a]	0.897
Linear effects				
[*Prot*]	1	749.1	46.9[a]	
[*BO*]	1	361.2	22.6[a]	
[*MGS*]	1	626.7	39.2[a]	
P	1	156.9	9.8[a]	
T	1	4.6	0.3	
Quadratic effects				
[*Prot*]²	1	17.9	1.1	
[*BO*]²	1	39.4	2.5	
[*MGS*]²	1	20.8	1.3	
*P*²	1	630.9	39.5[a]	
*T*²	1	123.9	7.8[a]	
[*Prot*] x [*BO*]	1	359.4	22.5[a]	
[*Prot*] x [*MGS*]	1	23.5	1.5	
[*Prot*] x *P*	1	0.2	< 0.1	
[*Prot*] x *T*	1	75.0	4.7	
[*BO*] x [*MGS*]	1	19.7	1.2	
[*BO*] x *P*	1	974.8	61.0[a]	
[*BO*] x *T*	1	2.1	< 0.1	
[*MGS*] x *P*	1	0.5	< 0.1	
[*MGS*] x *T*	1	7.2	0.4	
T x *P*	1	3.0	0.2	
Error	30	479.3		
Lack of fit	21	3 592.7	4.1[c]	
Pure error	9	358.5		
Total	50	4 675.8		
Model	9	3 823.0	20.4[a]	0.818
Error	41	852.9		
Total	50	4 675.9		

See table II for statistical abbreviations.

table V. The second-order model, which was highly significant ($p \leq 0.0001$), was able to explain 81.8% of the total variance

Table V. Analysis of regression and second-order model of the variation coefficient of the volume-weighted size distribution of fat globules versus significant variables and interactions.
Analyse de régression et modèle de second ordre du coefficient de variation de la distribution des tailles pondérées en volume des globules de gras, en fonction des variables et des interactions significatives.

	Estimate [1]	STD [2]	t [3]
Parameter:			
Intercept	25.127	18.2	1.4
[Prot]	12.532	4.1	3.1
[*BO*]	9.477	1.1	8.9[a]
[*MGS*]	−19.278	3.6	−5.4[a]
P	$+2.8\ 10^{-4}$	$3\ 10^{-4}$	0.9
T	−1.133	0.4	−2.6
P^2	10^{-7}	10^{-8}	4.1[a]
T^2	0.0083	0.03	2.7
[*Prot*] x [*BO*]	−1.676	0.4	−4.2[a]
[*BO*] x *P*	$-1.3\ 10^{-4}$	$2\ 10^{-5}$	−6.8[a]

$$cv = 25.127 + 12.532\,[Prot] + 9.477\,[BO] - 19.278\,[MGS] - 2.8\ 10^{-4}\,P - 1.133\,T + 10^{-7}\,P^2 + 0.008\,T^2 - 1.676\,[Prot] \times [BO] - 1.3\ 10^{-4}\,[BO] \times P$$

Validity intervals
20 400 ≤ P ≤ 76 300 kPa 0.5 ≤ [*Prot*] ≤ 3.9 wt%
35 ≤ *T* ≤ 100 °C 5.2 ≤ [*BO*] ≤ 14.8 wt%
0.08 ≤ [*MGS*] ≤ 0.88 wt%

See table III for statistical abbreviations.

cv. The value of the regression coefficients of the P term was not significantly different from 0 ($p > 0.05$).

Figure 3, obtained from a second-order model, corresponds to the response surface of the standard deviation of the volume-weighted size distribution of fat globules as a function of emulsification pressure, *P* (MPa), and butter oil concentration [*BO*] (wt%), for a fixed temperature

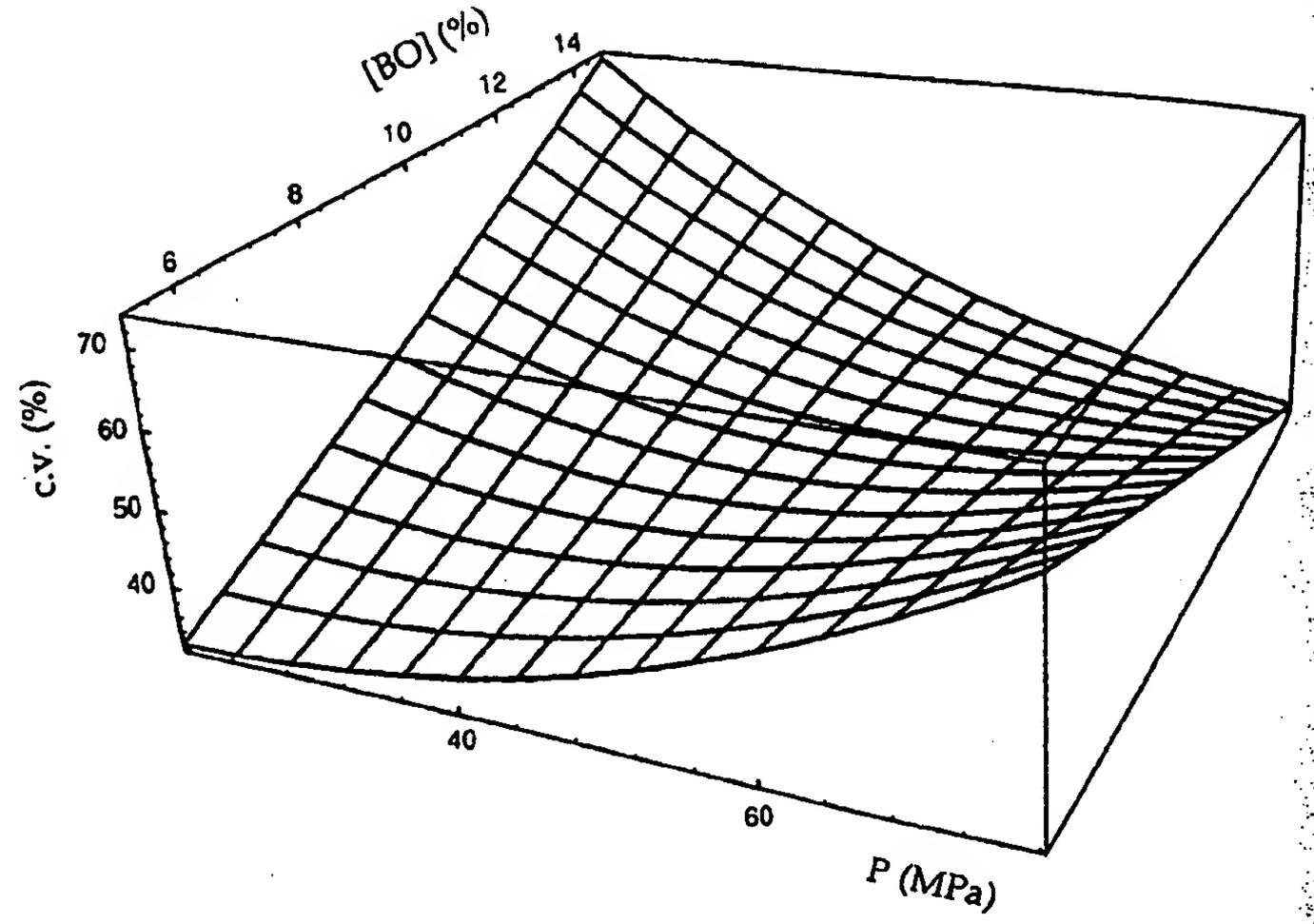

Fig 3. Response surface of the coefficient of variation standard of the volume-weighted size distribution of fat globules as a function of emulsification pressure, *P* (MPa), and butter oil concentration, [*BO*] (wt%), for a fixed temperature (*T* = 50 °C), a fixed protein concentration ([*Prot*] = 1.5 wt%), and a fixed monoglyceride concentration ([*MGS*] = 0.4 wt%).
Surface de réponse du coefficient de variation de la distribution des tailles pondérées en volume des globules de gras en fonction de la pression d'émulsification, P (MPa), et de la concentration en huile de beurre, [BO] (%), pour une température donnée (T = 50 °C), et des concentrations fixées en protéines ([Prot] = 1.5%) et en monoglycérides ([MGS] = 0.4%).

(*T* = 50 °C), a fixed protein concentration ([*Prot*] = 1.5 wt%), and a fixed monoglyceride concentration ([*MGS*] = 0.4 wt%). An increase in the emulsification pressure and/or butter oil concentration resulted in an increase in the value of *cv*. This figure also shows the minimal values for *cv* that are a function of both *P* and [*BO*] (table IV).

Figure 4 shows the response surface obtained from a second-order model of the volume-weighted size distribution of fat globules as a function of protein and monoglyceride concentration, for a fixed temperature (50 °C), pressure (50 MPa), and butter oil concentration (10 wt%). This figure indicates the cooperative effect of surfactant content on the reduction in *cv* of this volume-weighted distribution.

pH of the emulsions

The average pH of the 52 emulsions was 7.06 with a standard deviation of ± 0.04. All emulsions therefore had similar acid/base properties.

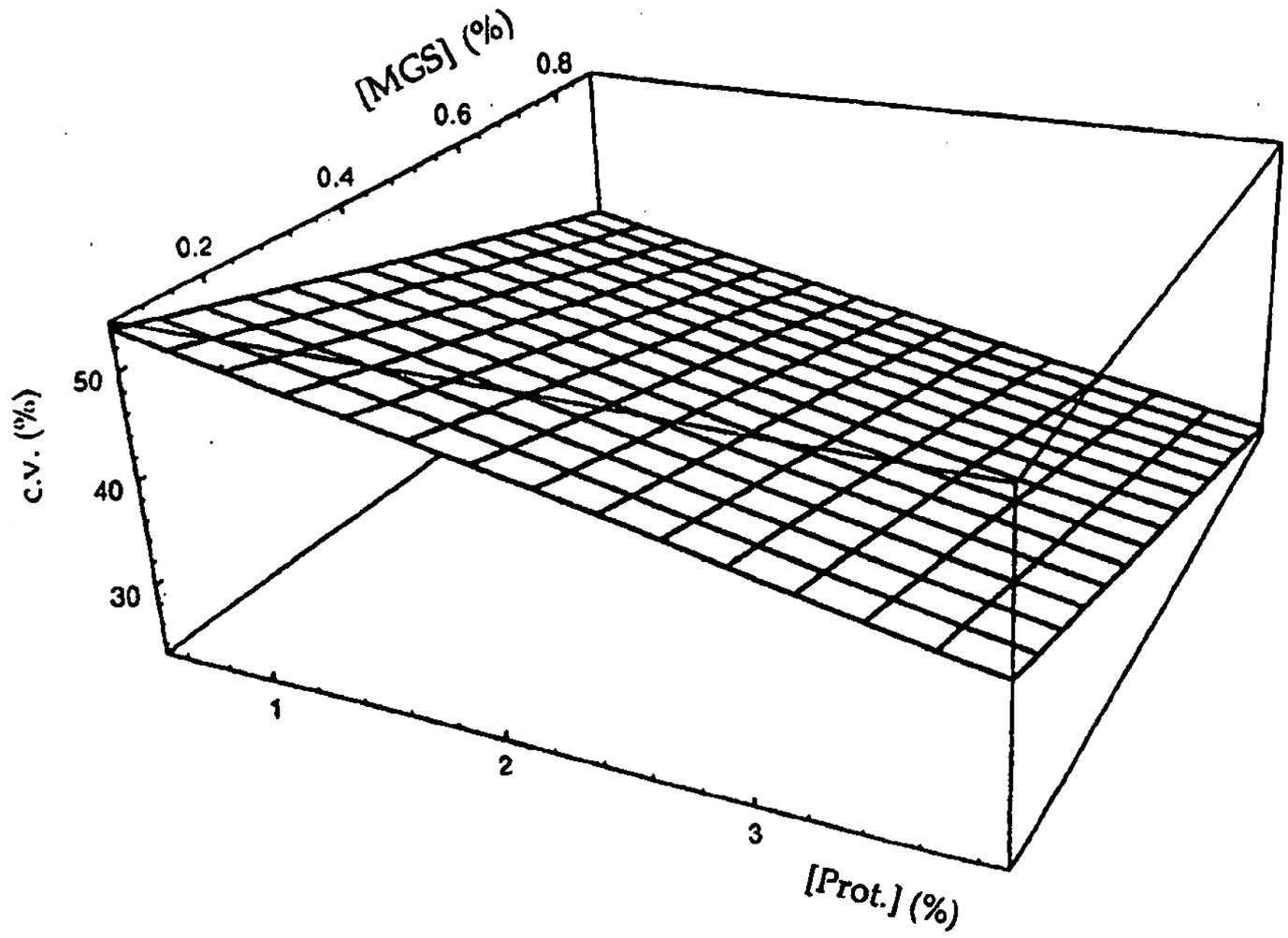

Fig 4. Response surface of the coefficient of variation of the volume-weighted size distribution of fat globules as a function of protein, [*Prot*] (wt%), and monglyceride, [*MGS*] (wt%), concentrations for a fixed temperature (T = 50 °C), a fixed pressure (P = 50 MPa), and butter oil concentration ([*BO*] = 10 wt%).

Surface de réponse du coefficient de variation de la distribution des tailles pondérées en volume des globules de gras en fonction des concentration en protéines, [Prot] (%), et monoglycérides, [MGS] (%), pour une température (T = 50 °C), une pression (P = 50 MPa), et une concentration en huile de beurre ([BO] = 10%) fixées.

DISCUSSION

Emulsification is a dynamic process where the disruption and recombination or coalescence of the fat globules take place simultaneously, each with its own rate constant or time scale (Walstra, 1983; Tomberg *et al*, 1990). Consequently, not only the final droplet size distribution but also other emulsion properties such as rheological behavior will be determined by the conditions leading to an equilibrium between breakdown and coalescence. The probability of newly formed droplets coalescing depends on the time available for the interfaces to be covered by the surfactants. The time available depends on emulsifying conditions (*eg* emulsifying machine, power density), which are influenced by the fat content, the ratio of surfactant to fat, and the nature of the surfactants. In order to be active (prevent coalescence), surfactants must not only be transported to the interfaces, they must also be able to adsorb. Adsorption depends on the number of surfactant collisions with fat particles,

and on the probability of the surfactants adsorbing after colliding with the interface. Adsorption is likely influenced by molecular properties such as hydrophobicity, flexibility and charge density (Kato, 1991; Lorient *et al*, 1991). However, the adsorption process occurs on a time scale of less than a millisecond during the homogenization process (Walstra, 1983), so it is very unlikely that an adsorption equilibrium is obtained.

For a given process, the emulsification efficiency is the result of an optimal combination of process variables and of the composition of the liquid to be emulsified. Six major variables are generally considered: emulsification pressure *(P)* and temperature *(T)*, liquid flow rate *(Q)*, the fraction *(Φ)* of the disperse phase and the surfactant concentration(s) (Walstra, 1983; Phipps, 1985). In the present study, the effect of flow rate on the size distribution of the fat globules was not considered. It has, however, been shown for oil-in-water emulsions (Phipps, 1975, 1982, 1983; Walstra, 1975) and for conventional homogenizers (Manton-Gaulin and/or Rannie), that there is little or no influence of the flow rate of the liquid to be emulsified when $\Phi \leq 30\%$.

Influence of process variables on the size distribution of fat globules

Effect of emulsification pressure

It was empirically shown (Goulden and Phipps, 1964; among others) and then vindicated by Walstra (1969, 1975) that classic homogenization processes (the systems of Manton-Gaulin or Rannie), at moderate emulsification pressures (0.25 MPa $\leq P \leq$ 40.5 MPa), using milk, cream with a fat concentration of $\Phi \leq 12\%$ or any other dilute emulsion, could be quantified by a relation such as $d \propto P^m$ where the exponent m has a value of –3/5 ([1]). The exponent m in the descending slope of the curve $\bar{d}_v = f(P^m)$ (fig 1) is of the order –0.53 ± 0.04. These results, therefore, seem to corroborate the theories linked to the breakdown of fat globules during turbulent flow conditions. However, there is no general agreement on the functioning of conventional homogenizers at high pressure. According to Walstra (1969, 1983) and Davies (1985) the breakdown of the fat globules can be described by the turbulence theory put forward by Kolmogorov. According to Phipps (1975, 1985), the breakdown of the globules at the entrance to the homogenization valve can be described by the Taylor analysis of shearing forces. The design of the microfluidization chamber (microchannels, mixing zone, etc) differs fundamentally from an homogenization chamber (basically a valve and a seat). Even if the forces that lead to the breakdown of the fat globules are the same, their respective influence on the breakdown is apparently not the same.

Although the convex nature of the curve $\bar{d}_v = f(P)_{[BO]}$ (fig 1) is the result of an experimental artefact and of its statistical consequence (the minimum is very shallow), some authors (Becher, 1967; Phipps, 1975; Tornberg, 1980) have reported that an increase in homogenization intensity *(E)*, and/or fat concentration above optimal yields ($P \geq 40$ MPa or $E \geq 60$ W and/or $\Phi \geq 12\%$) could result in an increase in droplet size. This increase, called overprocessing by Tornberg (1980), should indicate that coalescence is the dominant factor governing the final droplet size of the emulsion. However, the validity of the methods that have been used for producing emulsions and determining average size is questionable. In the present study, it is reasonable to think that an increase in collision frequency with increasing pressure would at most lead to no further decrease in globule size as the minimum is very shallow. An in-

crease in emulsification intensity above optimal conditions, which causes a relatively small change in average droplet size, results in unnecessary energy consumption. The optimal condition corresponded to $P \cong 50$ MPa. The reduction in fat globule size have various consequences. Emulsions which contain small droplets have a tendency to be more stable with respect to creaming (Stokes' law), and to coalesce more than those containing large droplets (MacRitchie, 1976). According to the MacRitchie approach, which correlates film stability to an energy barrier, the compressional free energy barrier can be, under some conditions, proportional to $1/d^6$. However, in practice the effects are not as great as predicted by these equations (Walstra and Oortwijn, 1975; Dickinson and Stainsby, 1982).

If the average particle size can provide some information about the behavior of emulsions, most attention should, however, be paid to the top end of the size distribution as most types of instability are usually first manifested by the behavior of the largest droplets. Although the distribution width of fat globules is an extremely important parameter when characterizing an emulsion, it has not been studied in great depth. Walstra (1975) demonstrated that the relative width of fat globules in homogenized milk sharply increases with the homogenization pressure ($0 < P < 5$ MPa), reaches a maximum ($P \cong 5$ MPa) before remaining fairly constant and attaining a limit ($P \cong 30$ MPa). These results were partly confirmed by Tornberg (1980) studying the behavior of various protein stabilized emulsions made by a sonifier. In the present study, valid for 20.4 MPa $\leq P \leq$ 76.3 MPa, the results revealed a behavior that differed as a function of butter oil concentration ([*BO*], wt%). At quite high [*BO*], in conformity with previously mentioned results, the relative width of the fat globule distribution diminished as a function of emulsification pressure. However, at lower concentrations, the behavior was reversed. Although these trends should be interpreted with some caution (lack of accuracy in the determination of the standard deviation, low r^2 value), it appears that trends near central points are similar to those reported elsewhere. At the endpoints of the experimental design, trends are much more difficult to establish, particularly when the decrease in *cv* as a function of [*BO*] at high *P* should arise from the standard deviation(s) being less affected than $\bar{d}_v$ by the emulsification intensity.

Effect of emulsification temperature

Since Gaulin, it has been recognized that the efficiency of the emulsification process is very low in the presence of solid fat (Kessler, 1981). Consequently, the production of oil-in-water emulsions is normally carried out at temperatures above the final melting temperature of the fat ($T_f \cong 40$ °C, Jenness and Walstra, 1984). Several authors, studying the homogenization of milk, have shown that an increase of 10 °C in temperature between 40–70 °C decreases the average diameter of the fat globules by 6–8% (Walstra, 1975) to 10–15% (Sweetsur and Muir, 1983). This effect weakens or disappears above 80 °C. As expected, an increase in temperature between 35–82 °C resulted in a decrease in the average diameter of ≈ 8%/10 °C. Although equation [1] does not predict that the viscosity of either phase can have an effect on the droplet size resulting from the emulsification process in turbulent flow, a decrease of viscosity will understandably affect the rate of passage through the emulsifier and the ease of disruption of the globules. Walstra (1974, 1983) suggested that an increase in the viscosity of the dispersed phase (η_D) should correspond to a deformation time of a droplet larger than the character-

istic time of an eddy. As the smallest eddies are presumably the most effective (they have the highest kinetic energy), an increase in η_D should lead to a larger spread in flow conditions and consequently in droplet size distribution *(cv)*, as was indeed the case. Moreover, an increase in temperature changes all the composition variables that determine adsorption; fat changes to oil and the macromolecular penetration into the oil becomes possible, hydrophobic interactions at the interface probably become more intense (at least up to 60–65 °C), and the molecular structure of water weakens, which affects its quality as a solvent for surfactants and for hydrophobic interactions. Above 82 °C, the average particle diameter increased slightly. Although this result has not been explained, it should be noted that the influence of the temperature on the average diameter of the fat globules is relatively low: temperature only explains 4.8% (table II) of the total variance of $\log_{10}$ $(\bar{d}_v)$ and between 82 and 100 °C it represents < 1% which is much lower than the experimental error (≈ 6.3%). Moreover, the statistical increase in $\bar{d}_v$ is a consequence of the measurements obtained from an emulsion that was not repeated (No = 48) and corresponds to an extreme point (star point) in the experimental design. *cv* was influenced in a similar manner by the temperature (table V).

Effect of composition variables on the size distribution of fat globules

Effect of butter oil concentration

The concentration of fat affects the homogenization efficiency of dairy products when it is > 10% (Walstra, 1975; Phipps, 1985). The microfluidization of the model emulsion demonstrated that an increase in the butter oil concentration ($5.2 \leq [BO] \leq 14$ wt%) resulted in a very significant increase in the average diameter of the fat globules $(\bar{d}_v)$ (table II, fig 1) and in the size distribution (*cv* at low pressure) (table III, fig 3). An increase in the fat concentration resulted in a relative decrease in the concentration of surfactant available to cover the new interfacial surface that was formed during the emulsification process. The fat content and the ratio of surfactants to fat affected the extent of coalescence of the newly formed globules by governing the probability that the latter collide before they recover by a surfactant layer. Also, with higher oil concentrations, distances between fat globules decrease and the probability of bridging could increase. This results in a general tendency to increase "particle" diameter.

Effect of surfactant concentration

The addition of surfactants, which results in a decrease in interfacial tension (γ), reduces the interfacial free energy (ΔG) of the system,

$$\Delta G = \gamma \Delta S \qquad [3]$$

where ΔS is the change in the interfacial area

and thereby the Laplace pressure which is beneficial in reducing both the energy requirement to form emulsions and the droplet size that can be obtained. However, this only holds if the ratio (surfactant/interfacial surface) is large enough to cover the new interfacial surface formed during the emulsification process and leading to minimize the coalescence or polymeric bridging (Halling, 1981; Tadros and Vincent, 1983). For minimal protein and monoglyceride concentrations ($[Prot] = 0.5$ wt%, $[MGS] = 0.08$ wt%, with $P = 50$ MPa, $T = 50$ °C, $[BO] = 10$ wt%), the average diameter of the fat globules was at a maximum ($\bar{d}_v = 678$ nm).

Although certain general rules can be deduced from simple thermodynamic principles, the degree and, more importantly, the consequences of the adsorption of protein to the interface can vary considerably with the type of protein and with emulsification conditions. Thus, while Oortwijn and Walstra (1979) reported that whey protein concentration (0.01–2.0%) had relatively little effect on the size of fat globules in homogenized emulsions, Pearce and Kinsella (1978) demonstrated, using homogenized emulsions stabilized with various proteins, that increasing the protein concentration (0.5–5%) could decrease the average diameter of the fat globules by a factor of 2.5. Thus, the nature of the surfactant (hydrophile-lipophile balance, molecular weight, molecular flexibility) as well as its relative concentration (with respect to other surfactants) directly influence the size of the fat globules. Figure 2 illustrates the complex influences of the chemical structure and of protein and monoglyceride concentration on the average diameter of emulsified fat globules; the other variables were kept constant (P = 50 MPa, T = 50 °C, [*BO*] = 10 wt%). During the emulsification process, smaller droplets (d_v = 259 nm) are produced in the presence of low concentrations of proteins and high concentrations of monoglycerides ([*Prot*] = 0.5 wt% and [*MGS*] = 0.88 wt%, respectively) because monoglycerides are better able to lower interfacial tension than proteins alone. With high protein concentrations and low monoglyceride concentrations, d_v = 350 nm. Dickinson *et al* (1989) reported similar trends when studying the effect of octaoxyethylene dodecyl ether ($C_{12}E_8$) with 0.1 wt% caseinate on the droplet diameter of O/W emulsion (20 wt% *n*-tetradecane, pH 7, 25 °C). However, care is needed when analysing these results as the surfactants used were different and hydrocarbons have a higher interfacial tension with water than do mixtures of triglycerides with water (Fisher *et al*, 1985).

Moreover, the increase in the concentration of surfactant (for a given [*BO*], P and T) results in a decrease in the average particle diameter (Dickinson *et al*, 1989) if the monoglycerides to protein ratio is lower or equal to 0.15, *eg* [*Prot*] = 2.85 wt% and [*MGS*] = 0.46 wt% (fig 2). Although these concentrations are independent of the [*BO*], which is rather surprising, it is suggested that an increase in the size of the fat globules above these concentrations can be attributed to,

– a competition between fat and monoglycerides to bind proteins due to the high number of monoglyceride molecules per residue of caseinate and to the formation of hydrophobic bonds between a polar amino acids and the hydrocarbon groups of the monoglycerides (Dickinson and Woskett, 1989). These weak complexes, if they form, should be rather surface-inactive, as the hydrophobic areas of protein and nonionic surfactant bind together, and

– to protein displacement from the interface by monoglycerides. In another study using casein and *MGS*, Paquin *et al* (1987) found that surface pressure isotherms in the high-pressure region are essentially the same as for the monoglycerides alone, suggesting protein displacement from the interface. It is likely, as suggested by Doxastakis and Sherman (1986), that mono- and diglycerides present in commercial glycerol monostearate form complexes with caseinate at the oil–water interface. It would appear that this (mixed) emulsifier does not behave simply as a nonionic, noninteracting surfactant.

Surfactants (proteins and low molecular weight surfactants) seem to have a cooperative effect on the reduction of *cv* (fig 4). As was mentioned in the discussion on the determination of *cv*, these results must be interpreted with caution.

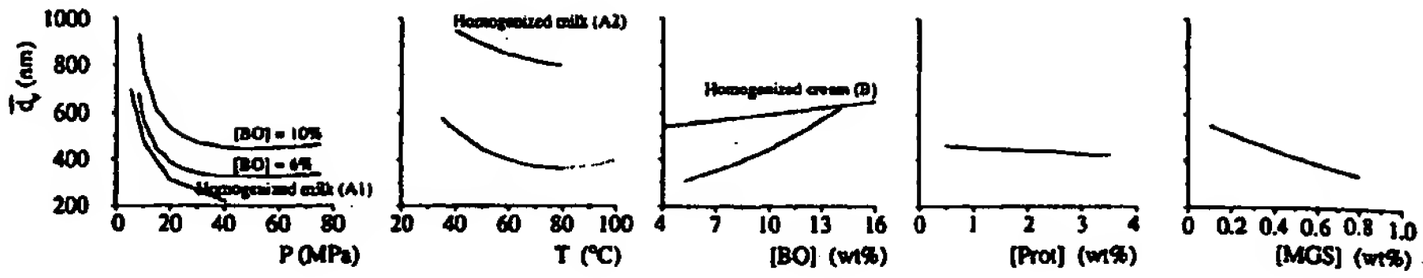

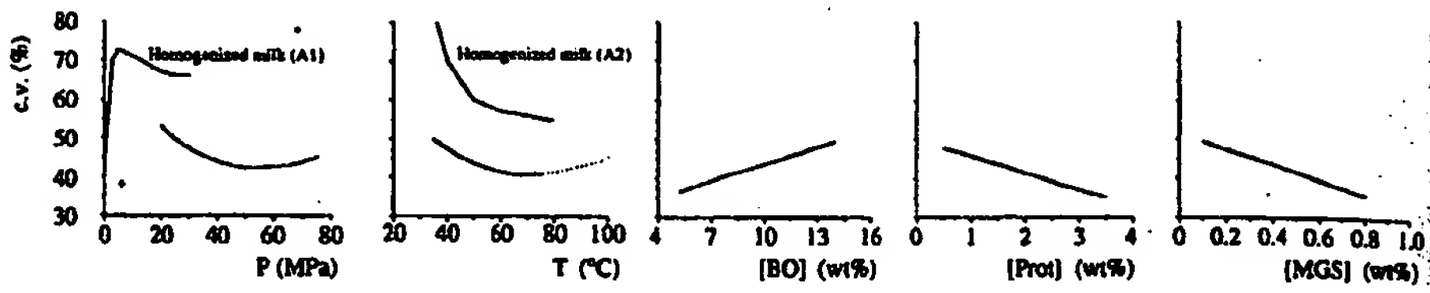

Fig 5. Effect of process and composition variables on fat globule size distribution parameters. For each graph, values of 4 variables were either fixed or specified. Values of fixed variables were: $P = 50$ MPa, $T = 50$ °C, [*BO*] = 10 wt%, [*Prot*] = 1.5 wt%, [*MGS*] = 0.4 wt%.
Effets des variables de procédés et de composition sur les paramètres de la distribution des tailles des globules de gras. Pour chaque figure, les valeurs des 4 variables étaient soit fixées soit spécifiées. Lorsque les variables étaient fixées, leur valeur était : P = *50 MPa,* T = *50 °C,* [BO] = *10%,* [Prot] = *1.5%,* [MGS] = *0.4%.*
(A): Walstra. 1975; A_1, p 282; A_2, p 289. (B): Phipps, 1985, p 12.

CONCLUSIONS

The process and composition variables which were studied affect, in varying proportions, the efficiency of the emulsification process called microfluidization. Some of these influences are summarized in figure 5. The variables that had the greatest influence on the size distribution of the fat globules are the butter oil concentration, the concentration of low molecular weight surfactants (monoglycerides), the emulsification pressure, the protein concentration (sodium caseinates) and the emulsification temperature. However, if the average sizes are fairly reliable, the results on relative distribution width must be taken with caution.

The utilization of an experimental design, applied to a dairy-type emulsion, demonstrated the complexity of the influences and interactions (depending on the area of study, pressure, temperature or concentrations) of process and composition variables on the size distribution of the fat globules. If the usefulness of mechanistic and thermodynamic principles is not in doubt, it is still impossible to completely predict all aspects of the behavior of an emulsion.

Finally, although this work was carried out on a model system and although it was demonstrated that for other conditions (the existence of interaction terms) the effects would be different, the results should pro

vide a guide for optimizing the emulsification process.

ACKNOWLEDGMENTS

We are indebted to the first reviewer for his helpful comments.

REFERENCES

Bargeron CB (1974) Analysis of intensity correlation spectra of mixtures of polystyrene latex spheres: a comparison of direct least squares fitting with the method of cumulants. *J Chem Phys* 60, 2516-2519

Becher P (1967) Effect of preparation parameters on the initial size distribution functions in oil-in-water emulsions. *J Colloid Interface Sci* 24, 91-96

Box GE, Drapper NR (1987) *Empirical Model Building and Response Surfaces*. John Wiley and Sons, NY

Brown JC, Pusey PN (1975) Photon correlation study on the initial size distribution function in oil-in-water emulsions. *J Chem Phys* 62, 1136-1144

Chandonnet S, Korstvedt H, Siciliano AA (1985) Preparation of microemulsions by microfluidization. *Soap Cosmet Chem Spec* (Feb) 37-38

Cook EJ, Lagace AP (1985) Apparatus for forming emulsions. *US Pat* 4 533 254

Chu B, Dinapoli A (1983) Extraction of distributions of decay times in photon correlation of polydisperse macromolecular solutions. *In: Measurement of Suspended Particles by Quasi-Elastic Light Scattering* (Dahneke BE, ed) John Wiley and Sons, NY, 81-105

Dalgleish DG, Pouliot Y, Paquin P (1987) Studies on heat stability of milk. II. Association and dissociation of particles and the effect of added urea. *J Dairy Res* 54, 39-49

Darling DF, Birkett RJ (1987) Food colloids in practice. *In: Food Emulsions and Foams* (Dickinson E, ed) R Soc Chem, London, 1-29

Davies JT (1985) Drop sizes of emulsions related to turbulent energy dissipation rates. *Chem Eng Sci* 40, 839-842

Dickinson E (1986) Mixed proteinaceous emulsifiers: review of competitive protein adsorption and the relationship to food colloid stabilization. *Food Hydrocol* 1, 3-23

Dickinson E, Stainsby G (1982) *Food Colloids*. Elsevier Appl Sci Publ, London

Dickinson E, Stainsby G (1988) Emulsion stability. *In: Advances in Food Emulsions and Foams* (Dickinson E, Stainsby G, eds) Elsevier Appl Sci Publ, London, 1-44

Dickinson E, Woskett CM (1989) Competitive adsorption between proteins and small-molecule surfactants in food emulsions. *In: Food Colloids* (Bee RD, Richmond P, Mingins J, eds) R Soc Chem, London, 74-96

Dickinson E, Mauffret A, Rolfe SE, Woskett CM (1989) Adsorption at interfaces in dairy systems. *J Soc Dairy Technol* 42, 18-22

Dickinson E, Euston SR, Woskett CM (1990) Competitive adsorption of food macromolecules and surfactants at the oil-water interface. *Prog Colloid Polym Sci* 82, 65-75

Doxatakis G, Sherman P (1986) The interaction of sodium caseinate with monoglyceride and diglyceride at the oil-water interface and its effect on interfacial rheological properties. *Colloid Polym Sci* 264, 254-259

Fisher LR, Parker NS (1988) Effect of surfactants on the interactions between emulsion droplets. *In: Advances in Food Emulsions and Foams* (Dickinson E, Stainsby G, eds) Elsevier Appl Sci Publ, London, 45-90

Fisher LR, Mitchell EE, Parker NS (1985) Interfacial tensions of commercial vegetable oils with water. *J Food Sci* 50, 1201-1202

Gacula MC, Singh J (1984) *Statistical Methods in Food and Consumer Research. Food Science and Technology*. Academic Press, NY, 214-272

Goulden JDS, Phipps LW (1964) Factors affecting the fat globule size during the homogenization of milk and cream. *J Dairy Sci* 31, 195-200

Halling PJ (1981) Protein-stabilized foams and emulsions. *CRC Crit Rev Food Sci Nutr* 13, 155-203

Jenness R, Walstra P (1984) *Dairy Chemistry and Physics*. John Wiley and Sons, NY, 88-89

Kato A (1991) Significance of macromolecular interaction and stability in functional properties of food proteins. *In: Interaction of Food Proteins* (Parris N, Barford R, eds) ACS Symp Ser 454, Am Chem Soc, Washington, DC, 13-24

Kessler HG (1981) *Food Engineering and Dairy Technology*. Verlag A Kessler, Freising, 119-138

Koppel DE (1972) Analysis of macromolecular polydispersity in intensity correlation spectroscopy: the method of cumulants. *J Chem Phys* 57, 4814-4820

Little TM (1981) Interpretation and presentation of results. *Hortic Sci* 16, 19-31

Lorient D, Closs B, Courthaudon JL (1991) Connaissances nouvelles sur les propriétés fonctionnelles des protéines du lait et de ses dérivés. *Lait* 71, 141-171

MacRitchie F (1976) Monolayer compression barrier in emulsion and foam stability. *J Colloid Interface Sci* 56, 53-56

Montgomery DC (1976) *Design and Analysis of Experiments*. John Wiley and Sons, NY, 341-368

Neter J, Wasserman W, Kutner M (1985) *Applied Linear Statistical Models: Regression, Analysis of Variance and Experimental Designs*. Irwin, Homewood, 2nd edn

Ogden LV (1973) The homogenization-induced clustering of fat globules in cream and model systems. Ph Dissertation, Univ Minnesota, St Paul, MN

Oorwijn H, Walstra P (1979) The membranes of recombined fat globules. 2. Composition. *Neth Milk Dairy J* 33, 134-154

Paquin P, Britten M, Laliberté MF, Boulet M (1987) Interfacial properties of milk casein proteins. *In: Proteins at Interfaces: Physicochemical and Biochemical Studies* (Brash JL, Horbett TA, eds) ACS Symp Ser 343, Washington DC, 677-686

Paquin P, Glasson J (1989) La microfluidisation comme procédé d'homogénéisation d'une boisson à base de matière grasse laitière. *Lait* 69, 491-498

Pearce KN, Kinsella JE (1978) Emulsifying properties of proteins: evaluation of a turbidimetric technique. *J Agric Food Chem* 26, 716-723

Phipps LW (1975) The fragmentation of oil drops in emulsions by high-pressure homogenizer. *J Phys D: Appl Phys* 8, 448-462

Phipps LW (1982) Homogenizing valve design and its influence on milk fat globule dispersion. I. Low rate of flow (100 l.h–1 Re ≤ 3000). *J Dairy Res* 49, 309-315

Phipps LW (1983) Effects of fat concentration on the homogenization of cream. *J Dairy Res* 50, 91-96

Phipps LW (1985) *The High Pressure Dairy Homogenizer. Tech Bull 6*. Nat Inst Res Dairying, Reading, UK

Piggott JR (1986) *Statistical Procedures in Food Research*. Elsevier Appl Sci Publ, London, 101-123

Pouliot Y, Paquin P, Robin O, Glasson J (1991) Étude comparative de l'effet de la microfluidisation et de l'homogénéisation sur la distribution de la taille des globules de gras du lait de vache. *Int Dairy J* 1, 39-49

Robin O, Paquin P (1991) Evaluation of the particle size of fat globules in a milk model emulsion by photon correlation spectroscopy. *J Dairy Sci* 74, 2440-2447

SAS® (1990) SAS User's Guide: statistics Version 6.06. SAS Inst Inc, Cary, NC

Shinoda K, Kunieda H (1983) Phase properties of emulsions: PIT and HLB. *In Encyclopedia of Emulsion Technology. 1. Basic Theory* (Becher P, ed) Marcel Dekker, NY, 337-367

Sweetsur MA, Muir DD (1983) Effect of homogenization on the heat stability of milk. *J Dairy Res* 50, 291-300

Tadros TF, Vincent B (1983) Emulsion stability. *In: Encyclopedia of Emulsion Technology. 1. Basic Theory* (Becher P, ed) Marcel Dekker, NY, 129-285

Tornberg E (1980) Functional characteristics of protein stabilized emulsions: emulsifying behavior of proteins in a sonifier. *J Food Sci* 45, 1662-1668

Tornberg E, Olson A, Persson K (1990) Structural and interfacial properties of food proteins in relation to their function in emulsions. *In: Food Emulsions* (Larsson K, Friberg SE, eds) Marcel Dekker, NY, 247-326

Vuillemard JC (1991) Recent advances in the large scale production of lipid vesicles for use

in food products: microfluidization. *J Microencapsul* 8, 547-562

Walstra P (1969) Preliminary note on the mechanism of homogenization. *Neth Milk Dairy J* 23, 290-292

Walstra P (1974) Influence of rheological properties of both phases on droplet size of O/W emulsions obtained by homogenization and similar processes. *Dechema Monogr* 77, 87-94

Walstra P (1975) Effect of homogenization on the fat globule size distribution in milk. *Neth Milk Dairy J* 29, 279-294

Walstra P (1983) Emulsion formation. *In: Encyclopedia of Emulsion Technology. 1. Basic Theory* (Becher P, ed) Marcel Dekker, NY, 57-127

Walstra P, Oortwijn H (1982) The membranes of recombined fat globules. 3. Mode of formation. *Neth Milk Dairy J* 36, 103-113

Washington C (1987) Emulsion production by microfluidizer. *Lab Equip Dig* 85, 69-71

Weiner BB, Tscharnuter WW (1987) Uses and abuses of photon correlation spectroscopy in particle sizing. *In: Particle Size Distribution: Assessment and Characterization* (Provder T, ed) ACS Symp Ser 332, Am Chem Soc, Washington DC, 48-64

Wolfram S (1991) *Mathematica: A System for Doing Mathematics by Computer.* Addison-Wesley Publ Co Inc, Champaign, IL, 2nd edn

C10

receptor kinase. Orthovanadate activates insulin receptor kinase by inhibiting the activity of a protein tyrosine phosphatase in the cells. Cephalochromin is a polyphenolic compound that has been observed to activate the IRTK activity (unpublished observation). Compound A is a small molecule that has been shown to enhance IRTK in these cells (21, 22). As shown in Fig. 2C, insulin receptor isolated from cells that have been treated with these agents showed a higher IRTK activity than the untreated cells. Moreover, this activity was similar to what has been observed for these compounds using the radioactive version of IRTK assay (date not shown). Taken together, these data demonstrate the usefulness of this assay for measuring the kinase activity of the insulin receptor that has been treated with diverse kinds of activators.

In summary, we have presented a significant improvement in the method to measure insulin receptor tyrosine kinase activity. This has been accomplished by developing a FRET-based assay, which utilizes a biotinylated substrate peptide from a natural substrate site of the IRTK, a Eu-labeled pT66, an antiphosphotyrosine antibody that specifically recognizes the phosphorylated peptide, and XL665-labeled streptavidin. Utilizing these reagents, we have demonstrated that this detection method yields results similar to what would be expected with the radioactive version of this type of assay. We have also shown that this assay is not only able to detect insulin-stimulated activation of the receptor kinase activity, but is also able to measure increases in the kinase activity of the insulin receptor that has been stimulated with compounds known to enhance insulin receptor kinase activity in cells. In contrast to other formats this assay is performed in a single plate without various washing steps which are often necessary to remove unincorporated ATP from the reaction. Due to this feature of the assay we have been able to process more than twenty-five 96-well plates per day. In short, this assay is a very robust and efficient method of determining the status of insulin receptor kinase isolated from cells *in vitro* without the use of radioactive materials.

Acknowledgments. We thank Debbie Szalkowski for help with the radioactive IRTK assay and Alice Marcy for help during the development of this assay.

REFERENCES

1. White, M. F., and Kahn, C. R. (1994) *J. Biol. Chem.* **269**, 1–4.
2. Parham, P. (1990) *Nature* **345**, 662–664.
3. Turner, R. C., Hattersley, A. T., Shaw, J. T. E., and Levy, J. C. (1995) *Diabetes* **44**, 1–10.
4. Taylor, S. I. (1999) *Cell* **97**, 9–12.
5. Pilch, P. F., and Czech, M. P. (1980) *J. Biol. Chem.* **255**, 1722–1731.
6. Rosen, O. M. (1989) *Diabetes* **38**, 1508–1511.
7. Perlman, R., Bottaro, D. P., White, M. F., and Kahn, C. R. (1989) *J. Biol. Chem.* **264**, 8946–8950.
8. Baron, V., Gautier, N., Komoriya, A., Hainaut, P., Scimeca, J. C., Mervie, M., Lavielle, S., Dolais-Kitabgi, J., and Van Obberghen, E. (1990) *Biochemistry* **29**, 4634–4641.
9. Luo, R. Z., Beniac, D. R., Fernandes, A., Yip, C. C., and Ottensmeyer, F. P. (1999) *Science* **285**, 1077–1080.
10. Kasuga, M., Fujita-Yamaguchi, Y., Blithe, D. L., and Kahn, C. R. (1983) *Proc. Natl. Acad. Sci. USA* **80**, 2137–2141.
11. Yu, K. T., and Czech, M. P. (1984) *J. Biol. Chem.* **259**, 5277–5286.
12. Ellis, L., Morgan, D. O., Clauser, E., Roth, R. A., and Rutter, W. J. (1987) *Mol. Endocrinol.* **1**, 15–24.
13. Wilden, P. A., Kahn, C. R., Siddle, K., and White, M. F. (1992) *J. Biol. Chem.* **267**, 16660–16668.
14. Boge, A., and Roth, R. A. (1995) *Anal. Biochem.* **231**, 323–332.
15. Ozawa, T., Sato, M., Sugawara, M., and Umezawa, Y. (1998) *Anal. Chem.* **70**, 2345–2352.
16. Cummings, R. T., McGovern, H. M., Zheng, S., Park, Y. W., and Hermes, J. D. (1999) *Anal. Biochem.* **269**, 79–93.
17. Shoelson, S. E., Chatterjee, S., Chaudhuri, M., and White, M. F. (1992) *Proc. Natl. Acad. Sci. USA* **89**, 2027–2031.
18. Zhang, B., Salituro, G., Szalkowski, D., Li, Z., Zhang, Y., Royo, I., Vilella, D., Diez, M. T., Pelaez, F., Ruby, C., Kendall, R. L., Mao, X., Griffin, P., Calaycay, J., Zierath, J. R., Heck, J. V., Smith, R. G., and Moller, D. E. (1999) *Science* **284**, 974–977.
19. Kolb, A. J., Kaplita, P. V., Hayes, D. J., Park, Y.-W., Pernell, C., Major, J. S., and Mathis, G. (1998) *Drug Discovery Today* **3**, 333–342.
20. Park, Y.-W., Cummings, R. T., Wu, L., Zheng, S., Cameron, P. M., Woods, A., Zaller, D. M., Marcy, A. I., and Hermes, J. D. (1999) *Anal. Biochem.* **269**, 94–104.
21. Liu, K., Xu, L., Szalkowski, D., Li, Z., Ding, V., Kwei, G., Huskey, S., Moller, D. E., Heck, J. V., Zhang, B. B., and Jones, A. B. (2000) *J. Med. Chem.* **43**, 3487–3494.
22. Qureshi, S. A., Ding, V., Li, Z., Szalkowski, D., Biazzo-Ashnault, D., Xie, D., Saperstein, R., Brady, E., Huskey, S., Shen, X., Liu, K., Xu, L., Salituro, G. M., Heck, J. V., Moller, D. E., Jones, A. B., and Zhang, B. B. (2000) *J. Biol. Chem.* **275**, 36590–36595.
23. Park, Y.-W. (1999) IBC's 8th Annual International Conference, Berkeley, CA, (March 1–3, 1999).

Relationship between Turbidity of Lipid Vesicle Suspensions and Particle Size

Edwin V. Pozharski,[1] Leon McWilliams, and Robert C. MacDonald
Department of Biochemistry, Molecular Biology and Cell Biology, Northwestern University, Evanston, Illinois 60208

Received September 15, 2000; published online March 7, 2001

Various physical methods exist for determining the distribution of sizes of micron and submicron particles in suspension. Light and electron microscopy, viscosimetry, sedimentation techniques, the electrical sens-

[1] To whom correspondence should be addressed at current address: Rosenstiel Basic Medical Sciences Research Center, Brandeis University, 415 South St., Waltham, MA 02254.

Analytical Biochemistry **291**, 158–162 (2001)
doi:10.1006/abio.2001.5012
0003-2697/01 $35.00

ing zone method (Coulter technique), various scattering techniques (static and dynamic light scattering, X-ray and neutron diffraction), chromatography, electrophoresis, and some other more exotic methods have been used for sizing. In liposome applications, the most common in recent years has been the dynamic light scattering technique. The method is relatively fast and easily applied to normal samples without special preparation. Also, it can be extended to assess the shape and size distributions. Electron microscopy, although more complicated, invasive, and time-consuming, helps to obtain detailed and reliable information about lipid particles having an extended size range or nonspherical shape.

A rapid and reliable method of estimating particle size is especially useful when dealing with lipid vesicles and, despite the numerous methods mentioned above, none of them combines both speed and ready availability of the required experimental equipment. In this paper we describe a method for estimating an average size of lipid vesicles with only a spectrophotometer. Theoretical considerations and experimental evidence allow us to propose two possible measurement schemes, both based on calibration with vesicles of known size: (i) fit turbidities measured with more than one vesicle sample of known size to a standard curve; (ii) obtain the turbidity spectrum for a vesicle sample of known size and convert it to the size dependence of turbidity. The vesicle samples of known size can readily be produced by extrusion (1, 2). The details of both approaches are discussed further.

Experimental Approach (Procedure 1)

Figure 1 represents the experimentally obtained relationship between the turbidity of a lipid suspension and the size of the constituent vesicles. Egg L-α-phosphatidylcholine (Avanti) at 1 mg/ml was used, samples of different sizes having been obtained by sonication for different durations of time in a water bath sonicator. The actual diameter of vesicles was measured by dynamic light scattering (Brookhaven Instruments BI-200SM goniometer and BI-9000 digital correlator; correlation curves analyzed by quadratic cumulants (3)). The turbidity was measured as the apparent optical density with a Beckman DU-50 spectrophotometer at 440 nm (upper curve) and 780 nm (lower curve).

The first important observation is the general shape of the curve. The turbidity as a function of vesicle diameter fits two intersecting lines, being linear for small and constant for large sizes. These two lines intersect at some wavelength, λ_i, which is proportional to (although smaller than) the wavelength of the incident light. The plateau value of turbidity depends upon the wavelength of incident light. The turbidity at any wavelength of the sample of any particle size was pro-

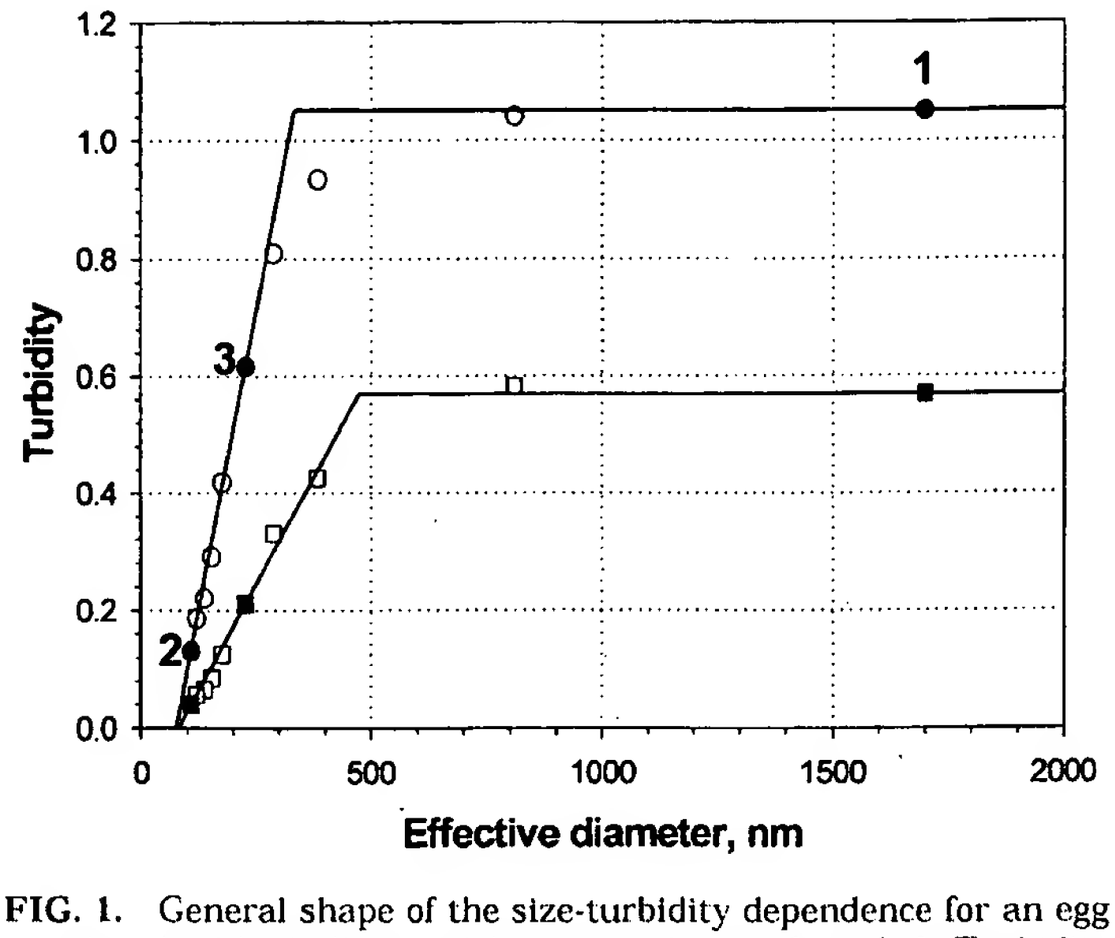

FIG. 1. General shape of the size-turbidity dependence for an egg L-α-phosphatidylcholine vesicle suspension at 1 mg/ml. Turbidity was measured at two wavelengths: λ = 440 nm (circles) and 780 nm (squares). Closed symbols indicate size standards. Lines show the result of fitting by two intersecting lines as described in procedure 1.

portional to the lipid concentration up to 5 mg/ml (data not shown). We conducted similar experiments with egg lecithin and its 7:3 mixture (by weight) with cholesterol and in all cases obtained the same general size-turbidity dependence (data not shown), indicating that such behavior is inherent in the properties of lipid vesicles as light scatterers.

The explanation of the experimental size-turbidity dependence is given below in terms of Rayleigh-Debye scattering theory; however, even without a theoretical model, one can propose the following approach based only on the experimental results:

1. Measure the turbidity of a handshaken lipid suspension (in most cases these vesicles are larger than a wavelength, so it allows estimation of the turbidity maximum)—point 1 in Fig. 1.
2. Measure the turbidity of two standards smaller than the chosen wavelength (for instance, obtained by extrusion)—points 2 and 3 in Fig. 1.
3. Fit the above three values with two intersecting lines.

The linear region of the curve can then be used to assess the size of the unknown vesicles. The maximum turbidity, although useless by itself for size estimates, determines the range of sizes where a calibration is applicable.

Theory-Based Approach (Procedure 2)

The overall turbidity of a lipid vesicle suspension can be related to the scattering characteristics of the individual vesicle (4). If we consider a homogeneous ensem-

ble of thin shells as the model, one can show that turbidity, A, is given by[2]

$$A = 0.054 c S_0 N_a l \alpha_S / M \qquad [1]$$

(see footnote for meaning of the symbols). The scattering efficiency, α_S, is the fraction of light scattered by an individual vesicle of given size, and in order to complete the model it is necessary to apply scattering theory to obtain its analytical expression.

As long as a lipid vesicle is considered to be a thin shell or hollow sphere, the scattering efficiency can be determined within Rayleigh-Debye light scattering theory (5, 6). We generally followed this theory to derive an expression (below) for the scattering efficiency. Therefore, we will not present the complete derivation, which is rather straightforward, but limit our discussion to few important considerations.

Rayleigh-Debye theory is applicable to lipid vesicles. The applicability of Rayleigh-Debye theory is limited to the cases when there is no significant change of phase of the incident light when it penetrates the particle. In order to satisfy that condition, the thickness of the bilayer h (or stacked bilayers in multilamellar structure) should obey the condition,

$$h \ll \lambda_0/(4\pi m_0(m-1)) \sim 1.1\lambda_0, \qquad [2]$$

when $m_0 \sim 1.33$—refractive index of water; $m = m_{lipid}/m_0 \sim 1.4/1.33 = 1.05$ and λ_0 is the wavelength of incident light. Since the bilayer thickness is about 5 nm, even highly multilamellar structures obey the above condition, as long as visible or ultraviolet light is used. It is especially important to emphasize that it is the "longest dimension through the particle" (Ref. 7, p. 415), i.e., the bilayer thickness rather than its overall size (vesicle diameter), that is the decisive parameter for Rayleigh-Debye scattering. In the case of lipid vesicles, this means that it is still applicable when the diameter of the vesicle is comparable to or even larger than the wavelength.

Lipid vesicle: Thin shell or hollow sphere? The hollow sphere model of lipid vesicles is clearly closer to reality than that of a thin shell. However, this model leads to undesirable complications of the final equations. We compared the scattering efficiency α_S, calculated for both models, and found that the correction introduced by the hollow sphere model is less than 0.2% in the case of unilamellar vesicles. Even for multilamellar vesicles with as many as 10 bilayers it is less than ~6%. We thus find Rayleigh-Debye scattering by thin shells to be adequate to describe the turbidity of lipid vesicle suspensions. The theory gives the following relationship between the turbidity A and diameter of vesicle D

$$A = 4.82 \frac{c S_0 N_a l m_0^2 h^2 (m^2-1)^2}{M\lambda_0^2 (m^2+2)^2} \int_{\theta_0}^{\pi} \frac{\sin\theta(1+\cos^2\theta)\sin^2(2\pi m_0 D \sin(\theta/2)/\lambda_0)}{\sin^2(\theta/2)}\, d\theta, \qquad [3]$$

where θ_0 is the acceptance angle of the detector (see footnote 2 for the meaning of other symbols). We introduce this parameter in order to indicate the fact that some part of the light scattered into small angles could impinge upon the detector, thus decreasing the apparent turbidity.

Calculations based on Eq. [3] show that, as size increases, turbidity rises to a plateau value, given a finite but small acceptance angle. The physical reason for this behavior is that larger particles scatter more and more light into the small scattering angle domain as diameter increases. As a consequence, experimental readings will strongly depend upon spectrophotometer geometry. We found, for instance, that the turbidity changes dramatically when the sample-detector distance is changed. The calibration procedure 1 (see above) and the experimental measurement must, therefore, be done under the same conditions (including sample concentration, lipid content, and measurement geometry). The problem of sample-detector geometry could be resolved by appropriate correction factors (8) or instrumentally, by using diaphragms (4), but doing so would considerably complicate the procedure.

Equation [3] can be rewritten in the following general form

[2] The intensity of transmitted light, I, is given by

$$I = I_0 \exp(-\alpha_S n \sigma l),$$

where α_S is scattering efficiency, n the concentration of particles, σ is their cross-sectional area, l the optical path length, and I_0 the intensity of the incident light. Turbidity, A, is

$$A = -\log(I/I_0) = 0.43\alpha_S n \sigma l.$$

The concentration, n, of unilamellar vesicles with bilayer thickness h and diameter D (assuming $h \ll D$), is given by

$$n = c/m_0 = cS_0N_A/2\pi MD^2,$$

where c is the weight concentration of lipid, m_0 the mass of individual vesicle, S_0 the area per lipid molecule in the bilayer, and M the molecular weight of lipid. Taking into account that $\sigma = \pi D^2/4$, one can obtain

$$A = 0.43\alpha_S(cS_0N_A/2\pi MD^2)(\pi D^2/4)l = 0.054\alpha_S cS_0N_A l/M.$$

$$A(D, \lambda) = f(D/\lambda)/\lambda^2. \quad [4]$$

The function f in the above equation can be obtained from the turbidity spectrum of a standard sample (known size) and then used to generate the size-turbidity relationship for a fixed wavelength. This consideration makes possible another mode of spectrophotometer calibration, utilizing only a single sample of known size.

1. Measure the turbidity spectrum (turbidity A as a function of wavelength) of a sample having a vesicle population of known size; i.e., obtain the function $A_0(\lambda) = A(D_0, \lambda) = f(D_0/\lambda)/\lambda^2$. As with procedure 1, the calibration sample can be produced by extrusion.
2. Calculate the size dependence of turbidity measured at some fixed wavelength λ_0, using the equation

$$\begin{aligned} A(D, \lambda_0) &= f(D/\lambda_0)/\lambda_0^2 = f(D_0/(\lambda_0 D_0/D))/\lambda_0^2 \\ &= f(D_0/\lambda^*)/\lambda_0^2 = \lambda^{*2} A_0(\lambda^*)/\lambda_0^2 \\ &= D_0^2 A_0(\lambda = \lambda_0 D_0/D)/D^2, \end{aligned} \quad [5]$$

where $\lambda^* = \lambda_0 D_0/D$.

It should be noted that this approach allows calibration only in a limited size range. Let us assume that a D_0 = 100-nm extruded sample is produced and the turbidity spectrum is obtained over the λ = 400–800 nm spectral range. Then, for λ_0 = 400 nm, the calibration can be used for sizes $D = \lambda_0 D_0/\lambda$ = 50–100 nm and, for λ_0 = 800 nm, $D = \lambda_0 D_0/\lambda$ = 100–200 nm. Naturally, this approach would benefit from any extension of spectral range.

Concluding Remarks

Turbidity and turbidity spectra measurements have been successfully used in the past to estimate the average size of dispersed particles (see Ref.7, pp. 325–343; 9, pp. 491–494). Interestingly, specific turbidity (i.e., turbidity normalized to concentration) for solid spheres at first increases with size, reaches a maximum, and then decreases for larger sizes. What accounts for the difference from the case of hollow spheres? If the scattering efficiency has a plateau because of interference of light scattered by different parts of the particle, this would seem to apply to solid spheres as well. Closer analysis reveals that a difference between shells and spheres is, in fact, expected. Equation [1] indicates that the only term which relates turbidity to size is the scattering efficiency of individual vesicles. In fact, turbidity is also proportional to the cross-sectional area of the particle (i.e., to D^2) and to the number of particles in a unit volume, which for vesicles (i.e., thin shells) is inversely proportional to D^2. Since these two dependencies mutually cancel, neither appears in Eq. [1]. The situation is different if particles can be represented as a solid sphere. In that case their cross-sectional area is given by the same expression, but the particle concentration is inversely proportional to D^3 (not D^2), thus causing a decrease of the turbidity as a function of size, as long as the scattering efficiency increase is not so large as to overwhelm the particle concentration effect.

The range of sizes available for the method is limited by the wavelength of incident light, thus giving the maximal measurable size of about 500–600 nm (can be slightly extended if proper equipment is available to take readings in the infrared range). Theory predicts that one can extend this range by reducing the acceptance angle of the light detector; however, even with a zero aperture, the turbidity changes by only about 15% when the vesicle diameter drops from two to one wavelength. The accuracy of the procedure could thus decrease, even with precautions to minimize the acceptance angle.

Chong and Colbow (4) previously described a method to obtain vesicle sizes using the turbidity spectrum. Their method did not involve use of any standards and, as a consequence, required determination of the refractive index spectrum of the lipid. Determination of the refractive index is tedious and requires specialized equipment (10). On the other hand, the introduction of extrusion methods (1, 2) has made it very easy to prepare vesicle dispersions of known size. Turbidity-based vesicle size measurement has thus become eminently practical. Because the method presented here has important advantages of speed, simplicity, and common availability of the necessary equipment, it should be useful in laboratories in which liposome research is done.

Acknowledgments. This work was supported by NIH Grants GM52329 and HL59586. L.M. was supported by the National Science Foundation through the Materials Research Internships for Minority Undergratuates Program, Materials Research Center, Northwestern University (DMR-9632472). We acknowledge the use of dynamic light scattering instrument in the Keck Biophysics Facility at Northwestern University.

REFERENCES

1. Hope, M. J., Bally, M. B., Webb, G., and Cullis, P. R. (1985) Production of large unilamellar vesicles by a rapid extrusion procedure—Characterization of size distribution, trapped volume and ability to maintain a membrane-potential. *Biochim. Biophys. Acta* **812,** 55–65.
2. MacDonald, R. C., MacDonald, R. I., Menco, B. P. M., Takeshita, K., Subbarao, N. K., and Hu, L. R. (1991) Small-volume extrusion apparatus for preparation of large, unilamellar vesicles. *Biochim. Biophys. Acta* **1061,** 297–303.
3. Koppel, D. E. (1972) Analysis of macromolecular polydispersity in intensity correlation spectroscopy: The method of cumulants. *J. Chem. Phys.* **57,** 4814–4820.

4. Chong, C. S., and Colbow, K. (1976) Light scattering and turbidity measurements on lipid vesicles. *Biochim. Biophys. Acta* **436**, 260–282.
5. Lord Rayleigh (1918) On the scattering of light by spherical shells, and by complete spheres of periodic structure, when the refractivity is small. *Proc. R. Soc. A* **94**, 296–300.
6. Tinker, D. O. (1972) Light scattering by phospholipid dispersions: Theory of light scattering by hollow spherical particles. *Chem. Phys. Lipids* **8**, 230–257.
7. Kerker, M. (1969) The Scattering of Light and Other Electromagnetic Radiation, Academic Press, New York.
8. Heirwegh, K. P. M. (1966) Errors in extinction measurements as due to scattering of light by solutions of relatively small particles. *J. Colloid Interface Sci.* **21**, 1–8.
9. Allen, T. (1990) Particle Size Measurement, 4th ed., Chapman & Hall, London.
10. Yi, P. N., and MacDonald, R. C. (1973) Temperature dependence of optical properties of aqueous dispersions of phosphatidylcholine. *Chem. Phys. Lipids* **11**, 114–134.

Concurrent Measurement of Promoter Activity and Transfection Efficiency Using a New Reporter Vector Containing both *Photinus pyralis* and *Renilla reniformis* Luciferase Genes

Jae B. Park[1]

Phytonutrients Laboratory, Building 307, Room 313, Beltsville Human Nutrition Research Center, Agricultural Research Service, USDA, Beltsville, Maryland 20705

Received October 6, 2000; published online February 26, 2001

Reporter vectors are essential for the quantitative analysis of gene elements that potentially regulate mammalian gene expression (1). These gene elements may be *cis*-acting, such as promoters and enhancers, or *trans*-acting, such as various DNA-binding factors (2). Several kinds of reporter vectors have been developed to study the promoter and/or enhancer activities of genes: chloramphenicol acetyltransferase (CAT)[2] reporter vector, β-galactosidase reporter vector, β-glucuronase, alkaline phosphatase reporter vector, green fluorescent protein reporter vector, and luciferase reporter vector (3–7). Currently, reporter vectors using chemiluminescence-based assays (β-galactosidase reporter vector, β-glucuronase, alkaline phosphatase reporter vector, and luciferase reporter vector) are commonly used in many quantitative analyses of gene elements (8), because the sensitivity of the assays is several orders of magnitude greater than that of conventional colorimetric- or fluorometric-based assays. Of them, luciferase reporter vectors are the most favored reporter vectors for functional analysis of promoters and enhancers of genes, due to their rapid, sensitive, and reproducible assay system (9). In the luciferase assay, luciferin and other components are added to cell extracts, and the production of light from both cell extracts expressing the luciferase gene is measured conveniently by a luminometer or scintillation counter (10).

Although luciferase reporter vectors have been commonly employed in numerous studies, the transfection of only luciferase vector cannot provide normalized values of the activities of gene elements without simultaneous transfection of a second reporter vector to measure the efficiency (11). In this paper, a novel report vector ($pJDL_{cmv}$) was constructed to contain two luciferase genes, *Photinus pyralis* and *Renilla reniformis* luciferases, regulated by two different promoters for the first time, in order to measure simultaneously promoter activity and transfection efficiency. Two promoters of human glutaredoxin and ribonucleotide reductase R2 gene were investigated with this novel reporter vector to verify its appropriateness for simultaneous measurement of promoter activity and transfection efficiency.

Materials and Methods

T4 DNA ligase and restriction enzymes were purchased from Promega (Madison, WI), Chameleon double-stranded site directed mutagenesis kit was from Stratagene (La Jolla, CA), and *Taq* polymerase and deoxynucleotides were from Perkin-Elmer (Norwalk, CT). Bio-Rad protein assay kit (Bio-Rad, Hercules, CA) was used to determine the amount of protein.

Cell culture conditions. HeLa and NT cells were cultured in DMEM supplemented with 10% fetal bovine serum. The cells were grown to 60% confluence for the transfection experiments.

PCR cloning of P. pyralis and R. reniformis luciferase genes. P. pyralis and *R. reniformis* luciferase genes were amplified from pGL and pRL vectors (Promega), respectively, by PCR using respective forward and backward primers corresponding to two genes: 5′-TGCTTGGCATTCCGGTACTGTTGG-3′ and 5′-TTTACAATTTGGACTTTCCGCCCTTCTT-3′ for the *Photinus* gene; 5′-CTGCAGAAGTTGGTCGTGAGGCAC-3′ and 5′-TTGTTCATTTTTGAGAACAGC-3′ for the *Renilla* gene (12).

PCR cloning of two DNA fragments containing poly(A) signal for P. pyralis and R. reniformis luciferase genes. Two DNA fragments containing SV40 early and late poly(A) signals were respectively amplified from pEGFP (Clontech) and pRL (Promega) by PCR using forward and

[1] Fax: (301) 504-9456. E-mail: Park@307.bhnrc.usda.gov.

[2] Abbreviations used: CAT, chloramphenicol acetyltransferase; DMEM, Dulbecco's modified Eagle's medium; PCR, polymerase chain reaction; CMV, *cytomegalovirus;* poly(A), polyadenylation.

Analytical Biochemistry **291**, 162–166 (2001)
doi:10.1006/abio.2001.5003
0003-2697/01 $35.00

C11

THE MERCK INDEX

AN ENCYCLOPEDIA OF CHEMICALS, DRUGS, AND BIOLOGICALS

FOURTEENTH EDITION

Maryadele J. O'Neil, *Editor*
Patricia E. Heckelman, *Senior Associate Editor*
Cherie B. Koch, *Associate Editor*
Kristin J. Roman, *Assistant Editor*

Catherine M. Kenny, *Editorial Assistant*
Maryann R. D'Arecca, *Administrative Associate*

Published by
Merck Research Laboratories
Division of
MERCK & CO., INC.
Whitehouse Station, NJ, USA

2006

thesis: M. Tomita, Y. Sendju, *Z. Physiol. Chem.* 169, 263 (1927); R. Voeffray *et al.*, *Helv. Chim. Acta* 70, 2058 (1987). Enantioselective synthesis from glycerol: M. Marzi *et al.*, *J. Org. Chem.* 65, 6766 (2000). Biosynthesis: G. Wolf, C. R. A. Berger, *Arch. Biochem. Biophys.* 92, 360 (1961). Absolute configuration: T. Kaneko, R. Yoshida, *Bull. Chem. Soc. Jpn.* 35, 1153 (1962). Metabolism in humans: M. E. Mitchell, *Am. J. Clin. Nutr.* 31, 293 (1978). Historical review: G. Fraenkel, S. Friedman, *Vitam. Horm.* XV, 73-118 (1957). Review of physiological significance and deficiency syndromes: C. J. Rebouche, D. J. Paulson, *Annu. Rev. Nutr.* 6, 41-66 (1986); of clinical pharmacology: J. J. Bahl, R. Bressler, *Annu. Rev. Pharmacol. Toxicol.* 27, 257-277 (1987); of biosynthesis in mammals: F. M. Vaz, R. J. A. Wanders, *Biochem. J.* 361, 417-429 (2002). Review of effect on myocardial metabolism and clinical experience in ischemic heart disease: R. Lango *et al.*, *Cardiovasc. Res.* 51, 21-29 (2001); of use as dietary supplement in athletes: H. Karlic, A. Lohninger, *Nutrition* 20, 709-715 (2004). Symposium on physiology, pharmacology and therapeutic potential: *Ann. N.Y. Acad. Sci.* 1033, 1-197 (2004).

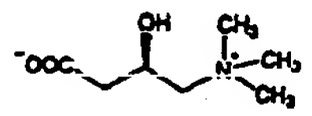

Crystals from anhydrous ethanol + acetone, dec 196-198° (Carter, Bhattacharyya); also reported as crystals from isopropanol, mp 200° (dec) (Marzi). Very hygroscopic solid. $[\alpha]_D^{25}$ −31.3° (c = 10 in water); $[\alpha]_{546}^{25}$ −37.0° (c = 10 in water). Sol in water, hot alcohol. Practically insol in acetone, ether, benzene.

Hydrochloride. [6645-46-1] Levocarnitine chloride; Flatistine. $C_7H_{15}NO_3.HCl$; mol wt 197.66. Crystals, dec 142°.

DL-Form. [406-76-8] γ-Amino-β-hydroxybutyric acid trimethylbetaine; γ-trimethyl-β-hydroxybutyrobetaine. Synthesis: E. Strack *et al.*, *Ber.* 86, 525 (1953); H. E. Carter, P. K. Bhattacharyya, *J. Am. Chem. Soc.* 75, 2503 (1953). Hygroscopic crystalline solid, dec 195-197°. Sol in water, ethanol.

DL-Form hydrochloride. [461-05-2] Needles from ethanol, mp 196° (dec). Very sol in water; sol in hot ethanol; slightly sol in cold ethanol. Practically insol in acetone, ether.

D-Form. [541-14-0] Prepn: S. Friedman *et al.*, *Arch. Biochem. Biophys.* 66, 10 (1957). Crystals, dec 210-212°. $[\alpha]_D$ +30.9°. Very sol in water and alcohol. Practically insol in acetone and ether.

D-Form hydrochloride. [10017-44-4] Crystals, dec 142°.

THERAP CAT: Vitamin (enzyme cofactor).

1850. Carnosine. [305-84-0] β-Alanyl-L-histidine; Ignotine. $C_9H_{14}N_4O_3$; mol wt 226.23. C 47.78%, H 6.24%, N 24.77%, O 21.22%. Naturally occurring dipeptide found in large amounts in skeletal muscle. Also present in other tissues such as brain, cardiac muscle, kidney. Water soluble antioxidant; functions as a free-radical scavenger. Isoln: Gulewitsch, Amiradzibi, *Ber.* 33, 1902 (1900); Wolff, Wilson, *J. Biol. Chem.* 95, 495 (1932); 109, 565 (1935). Synthesis from histidine and β-iodo- or β-nitropropionyl chloride: Baumann, Ingvaldsen, *Ibid.* 35, 271 (1918); Barger, Tutin, *Biochem. J.* 12, 406 (1918). Later syntheses: Sifford, du Vigneaud, *J. Biol. Chem.* 108, 753 (1935); R. A. Turner, *J. Am. Chem. Soc.* 75, 2388 (1953); F. J. Vinick, S. Jung, *J. Org. Chem.* 48, 392 (1983). Crystal structure: H. Itoh *et al.*, *Acta Crystallogr.* 33B, 2959 (1977). Possible role in wound healing: D. E. Fischer *et al.*, *Proc. Soc. Exp. Biol. Med.* 158, 402 (1978). Review of physiological properties and therapeutic potential: S. E. Gariballa, A. J. Sinclair, *Age Ageing* 29, 207-210 (2000).

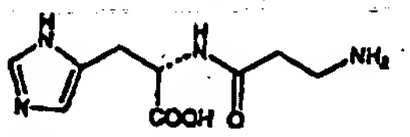

Crystals from aqueous ethanol, mp 262° (dec) (Vinick, Jung); also reported as mp 260° (capillary tube) and as mp 308-309° (Dennis bar) (Sifford, du Vigneaud). $[\alpha]_D^{25}$ +21.0° (c = 1.5 in water). pK_1 2.64; pK_2 6.83; pK_3 9.51. Alkaline reaction. One gram dissolves in 3.1 ml water at 25°.

Nitrate. [5852-98-2] $C_9H_{15}N_5O_6$. Crystals, dec 222°. $[\alpha]_D^{20}$ +24.1° (c = 1.5 in water). Very sol in water.

Hydrochloride. [5852-99-3] $C_9H_{15}ClN_4O_3$. Crystals, dec 245°. Very sol in water.

D-Form. [5853-00-9] Crystals, mp 260°. $(\alpha)_D^{25}$ −20.4° (c = 1.5).

1851. Caro's Acid. [7722-86-3] Peroxymonosulfuric acid; sulfomonoperacid; persulfuric acid. H_2O_5S; mol wt 114.08. H 1.77%, O 70.12%, S 28.11%. Dry reagent is prepd by stirring 10 g potassium persulfate into 11 g concd H_2SO_4 for 10 min and adding 30 g finely powdered potassium sulfate; liquid reagent is obtained by triturating potassium persulfate with three times as much (by weight) of H_2SO_4; dil reagent is prepd by stirring 10 g potassium persulfate into 11 g concd H_2SO_4 and adding 50 cc ice: Baeyer, Villiger, *Ber.* 32, 3625 (1899); another prepn by reacting 90% H_2O_2 with chlorosulfonic acid at −40 to −50°: Ball, Edwards, *J. Am. Chem. Soc.* 78, 1125 (1956).

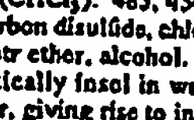

The product is a syrupy liquid consisting of about equal amounts of Caro's acid and H_2SO_4. pK_2 of Caro's acid 9.4 ± 0.1. Oxygen is evolved at room temp; should be stored at dry ice temp.

Caution: Can be dangerously unstable, like most peroxides. Description of explosion at Brown University: J. O. Edwards, *Chem. Eng. News* 33, 3336 (1955). Explosion at Sun Oil, *Ibid.* 38, 59 (Nov. 21, 1960). May be highly irritating to skin, eyes, mucous membranes.

USE: In prepn of dyes; oxidation of olefins to α-glycols; oxidation of ketones to lactones or esters; treating woolens to prevent felting and shrinking; in bleaching compositions.

1852. α-Carotene. [7488-99-5] $C_{40}H_{56}$; mol wt 536.87. C 89.49%, H 10.51%. About as widely distributed as its β-isomer, but in smaller amounts. Best sources for both the α- and β-isomers are carrots, palm-oil, and green leaves of various species. As a provitamin A it is half as active as β-carotene. Found in the mother liquors after crystallizing β-carotene. Isoln by chromatography: Karrer, Walker, *Helv. Chim. Acta* 16, 641 (1933). Structure: Kuhn, Lederer, *Ber.* 64, 1349 (1931); Karrer *et al.*, *Helv. Chim. Acta* 14, 614 (1931); 16, 975 (1933). Natural (+)-α-carotene has 6'R configuration: Eugster *et al.*, *Ibid.* 52, 1729 (1969). Synthesis of *dl*-α-carotene: Eugster, Karrer, *Ibid.* 38, 610 (1955); Tschamer *et al.*, *Ibid.* 40, 1676 (1957); Ruegg *et al.*, *Ibid.* 44, 985 (1961).

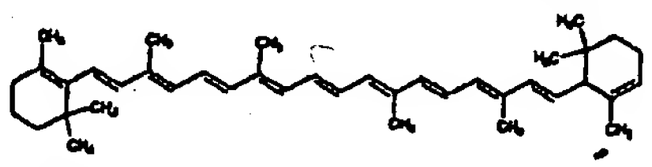

Deep purple prisms, polyhedra from petr ether or from benzene + methanol, mp 187.5° (evacuated tube). $[\alpha]_{443}^{15}$ +385° (c = 0.08 in benzene). Absorption max ($CHCl_3$): 485, 454 nm. More sol than β-carotene. Freely sol in carbon disulfide, chloroform; sol in ether, benzene. Slightly sol in petr ether, alcohol. 100 ml hexane dissolves 294 mg at 0°. Practically insol in water, acids, alkalies. Absorbs oxygen from the air, giving rise to inactive colorless oxidation products. The oxidation in light is autocatalytic. *Store in darkness in sealed ampoules and at low temp (−20°C).*

THERAP CAT: Vitamin A precursor.

THERAP CAT (VET): Vitamin A precursor for all species except cats.

1853. β-Carotene. [7235-40-7] β,β-Carotene; Carotaben; Provatene; Solatene. $C_{40}H_{56}$; mol wt 536.87. C 89.49%, H 10.51%. Most important of the provitamins A. Widely distributed in the plant and animal kingdom. In plants it occurs almost always together with chlorophyll. Isoln from carrots: Willstätter, Escher, *Z. Physiol. Chem.* 64, 47 (1910); Kuhn, Lederer, *Ber.* 64, 1349 (1931); Barnett *et al.*, US 2848508 (1958). Chromatography: Karrer, Walker, *Helv. Chim. Acta* 16, 641 (1933). Structure: Willstätter, Mieg, *Ann.* 355, 1 (1907); Zechmeister *et al.*, *Ber.* 61, 566 (1928); 66, 123 (1933); Karrer *et al.*, *Helv. Chim. Acta* 12, 1142 (1929); 13, 1084 (1930); 14, 1033 (1931); Kuhn, Brockmann, *Ber.* 65, 894 (1932); 66, 1319 (1933); 67, 1408 (1934); *Ann.* 516, 95 (1935). Crystal structure: Sterling, *Acta Crystallogr.* 17, 1224 (1964). Synthesis: Milas *et al.*, *J. Am. Chem. Soc.* 72, 4844

(1950); Karrer, Eugster, *Compt. Rend.* 250, 1920 (1950); Inhoffen *et al., Chem. Ztg.* 74, 285, 309 (1950); Surmatis, Ofner, *J. Org. Chem.* 26, 1171 (1961); Rüegg *et al., Helv. Chim. Acta* 44, 985 (1961); Bestmann *et al., Ann.* 1973, 760; Fischli, Mayer, *Helv. Chim. Acta* 58, 1584 (1975). Industrial mfg procedure: Isler *et al., Helv. Chim. Acta* 39, 249 (1956); Isler *et al.*, US 2917539 (1959 to Hoffmann-La Roche). Microbial production by *Choanephora trispora:* Zajic, US 2959521; US 2959522 and US 3128236 (1960, 1960 and 1964, all to Grain Processing); Miescher, US 3001912 (1961 to C.S.C.). *Review:* Fleming, *Selected Organic Syntheses* (John Wiley, London, 1973) pp 70-74.

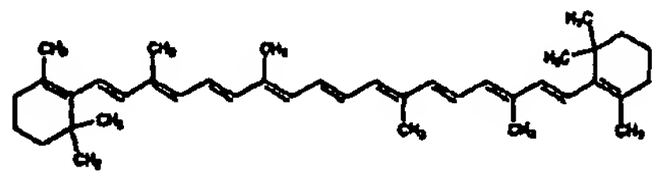

Deep-purple, hexagonal prisms from benzene + methanol. Red, rhombic, almost square leaflets from petr ether. mp 183° (evacuated tube). Absorption max (chloroform): 497, 466 nm. Less sol than α-carotene. Sol in CS_2, benzene, chloroform. Moderately sol in ether, petr ether, oils. 100 ml hexane dissolve 109 mg at 0°. Very sparingly sol in methanol and ethanol. Practically insol in water, acids, alkalies. Dil solns are yellow. Absorbs oxygen from the air giving rise to inactive, colorless oxidation products. *Keep tightly closed and protected from light. Store at low temp (−20°C).* Commercial crystalline β-carotene has a vitamin A activity of 1.67 million U.S.P. units per gram. The I.U. of 0.6 μg β-carotene is almost exactly equivalent to 0.3 μg vitamin A.

USE: Yellow coloring agent for foods.

THERAP CAT: Vitamin A precursor. Ultraviolet screen.

THERAP CAT (VET): Vitamin A precursor for all species except cats.

1854. γ-Carotene. [472-93-5] $C_{40}H_{56}$; mol wt 536.87. C 89.49%, H 10.51%. A rare carotenoid. Has provitamin A activity. Best source is *Penicillium sclerotiorum:* Mase *et al., Arch. Biochem. Biophys.* 68, 150 (1957). Also present in small proportions in many plant materials, esp fruits containing β-carotene. Chromatographic isoln from crude carotenes: Kuhn, Brockmann, *Ber.* 66, 407 (1933); Winterstein, *Z. Physiol. Chem.* 219, 249 (1933). Structure: Kuhn, Brockmann, *loc. cit.; Naturwissenschaften* 21, 44 (1933). Synthesis: Garbers *et al., Helv. Chim. Acta* 36, 1783 (1953); Ruegg *et al., ibid.* 44, 985 (1961).

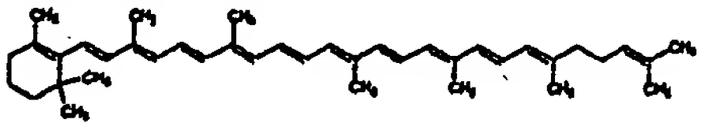

Probably crystallizes in polymorphous forms. Synthetic form: red plates, mp 152-153.5°. Absorption max (petr ether): 437, 462, 494 nm ($E^{1\%}_{1cm}$ 2055, 3100, 2720). Natural form: minute, deep-red prisms with bluish luster from benzene + methanol. mp 177.5°. Absorption max (chloroform): 508.5, 475, 446 nm. Somewhat less sol than β-carotene. *Store in darkness in sealed ampoules at low temps (0°C).*

THERAP CAT: Vitamin A precursor.

THERAP CAT (VET): Vitamin A precursor for all species except cats.

1855. δ-Carotene. [472-92-4] ε,ψ-Carotene. $C_{40}H_{56}$; mol wt 536.87. C 89.49%, H 10.51%. Extracted from the fruit of *Gonocaryum pyriforme* Mig., *Icacinaceae:* Winterstein, *Z. Physiol. Chem.* 219, 249 (1933). Occurs also in carrots and certain varieties of tomatoes. Isoln from tomato mutants: Porter, Murphey, *Arch. Biochem. Biophys.* 32, 21 (1951). Structure: Karrer, Quackenbush, *ibid.* 88, 59 (1960). Synthesis: Manchand *et al., J. Chem. Soc.* 1965, 2019. Absolute configuration: Buchecker, Eugster, *Helv. Chim. Acta* 54, 327 (1971).

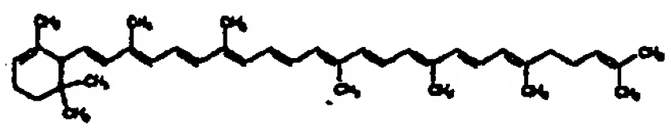

Long orange-red needles from CS_2 + hexane [illegible] 140.5°. $[\alpha]_{Cd}$ +317°; $[\alpha]_D^{25}$ +352° ±16% (hexane) [illegible] spectrum: Karrer, Quackenbush, *loc. cit.*

1856. β-Carotol. [465-28-1] (3*R*-(3aα,3bα,8aα)-[illegible]-Hexahydro-6,8a-dimethyl-3-(1-methylethyl)-3a(1*H*)-[illegible]-4,5,8,8a-hexahydro-3-isopropyl-6,8a-dimethyl-3a[illegible] $C_{15}H_{24}O$; mol wt 222.37. C 81.02%, H 11.79%, O [illegible] oil of carrot seeds, *Daucus carota* L., *Umbelliferae:* Tsukamoto, *J. Pharm. Soc. Jpn.* 525, 961 (1925); [illegible] (1926); Sorm *et al., Collect. Czech. Chem. Commun.* [illegible] Pigulevskii, Kovaleva, *Zh. Prikl. Khim.* 32, 2703 (19[illegible] Sykora *et al., Collect. Czech. Chem. Commun.* 26[illegible] Zalkow *et al., J. Org. Chem.* 26, 981 (1961). Ste[illegible] Levisalles, Rudler, *Bull. Soc. Chim. Fr.* 1964, 2020 [illegible] Synthesis of (+)-form: DeBraissia *et al., ibid.* 1972, [illegible] *Chem. Commun.* 1972, 855.

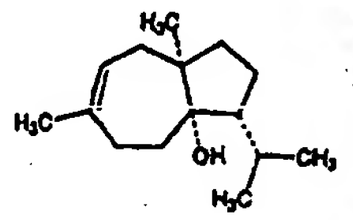

(+) - Carotol

Liquid. $bp_{2.5}$ 126°. $[\alpha]_D^{20}$ +30.4°. n_D^{20} 1.4964. d^{20} [illegible]

1857. Caroverine. [23465-76-1] 1-[2-(Die[illegible] yl]-3-[(4-methoxyphenyl)methyl]-2(1*H*)-quinoxalinon[illegible] aminoethyl)-3-(*p*-methoxybenzyl)dihydro-2-quinox[illegible] mium. $C_{22}H_{27}N_3O_2$; mol wt 365.47. C 72.30%, [illegible] 11.50%, O 8.76%. Prepn: Zellner *et al.*, US 302[illegible] Donau-Pharm.). Polarographic study: P. Pflegel, *[illegible]* 667 (1969). Pharmacological study: P. Hahn *et al.*, *Pharmacodyn. Ther.* 199, 108 (1972).

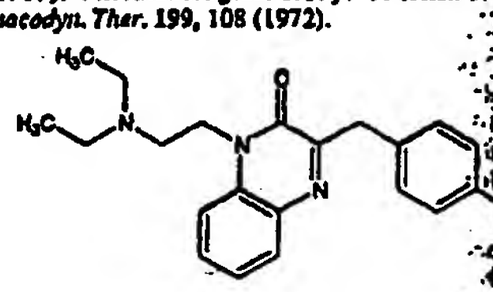

Crystals from isopropyl alcohol. mp 69°. $bp_{0.01}$ [illegible] Hydrochloride. Dec 188°.

THERAP CAT: Antispasmodic.

1858. Carpaine. [3463-92-1] $C_{28}H_{50}N_2O_4$; [illegible] C 70.25%, H 10.53%, N 5.85%, O 13.37%. Found [illegible] *papaya* L. and in *Vasconcellosia hastata* Carriel, *Caric[illegible]* from papaya leaves: Greshoff, *Mededeel. uit's Lands [illegible] tenzorg.* No. 7, 5 (1890); Rapoport, Baldridge, *J. Am. C[illegible]* 343 (1951). Reportedly causes bradycardia, CNS de[illegible] kowski, *Arch. Int. Pharm.* 15, 84 (1905). Structure and [illegible] istry: Govindachari *et al., Tetrahedron Lett.* 1965, [illegible] configuration: Coke, Rice, *J. Org. Chem.* 30, 3420 (1[illegible] of structural studies: Govindachari, *J. Indian Chem.* [illegible] (1968).

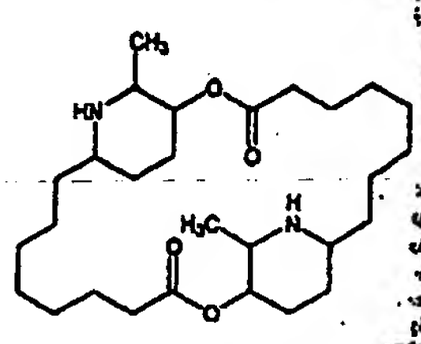

Monoclinic prisms from acetone. mp 119-120° a[illegible] 120° under 0.05 mm pressure. $[\alpha]_D^{27}$ +24.7° (c = 1.0[illegible] Slightly sol in water. Sol in most organic solvents exc[illegible]

[illegible]859. Carpetimycins. Carba[illegible] [illegible]emycin and olivanic acids, q.v.[illegible] [illegible]are known. Prodn of A and B b[illegible] [illegible]193, now named *Streptomyces g*[illegible] [illegible]ibacterial properties: NL 80[illegible] [illegible]58529 (1980, 1985 to Takeda); A[illegible] [illegible]47 (1980); by *Streptomyces* strain [illegible] [illegible]. 1388. Structure and abs config[illegible] [illegible]1425 (1980); M. Nakayama *et al.*[illegible] [illegible]ppo study: Y. Nozaki *et al.*, *ibid.*[illegible] [illegible]petimycin A: H. Natsugari *et al.*[illegible] [illegible]3, 403; M. Ihara *et al.*, *Heterc.*[illegible] [illegible]ynak, M. N. Roo, *J. Org. Chem.*[illegible] [illegible]-carpetimycin A: T. Iimori *et a*[illegible] [illegible]43); M. Aratani *et al.*, *Tetrahe*[illegible] [illegible]basaki *et al.*, *ibid.* 2217.

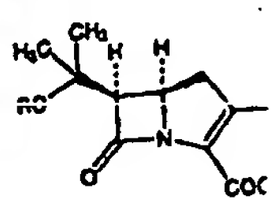

Carpetimycin A:
Carpetimycin B

[illegible]Carpetimycin A. [76025-73-[illegible] [illegible]dino)ethenyl]sulfinyl)-6-(1-[illegible] [illegible]bicyclo[3.2.0]hept-2-ene-2-c[illegible] [illegible]ntibiotic C-19393-H_3; antibioti[illegible] [illegible]$_6N_2O_4S$; mol wt 342.37. Col[illegible] [illegible]27° (c = 1.7 in water). uv ma[illegible] [illegible]0) (Nakayama, 1980).

[illegible]Carpetimycin B. [76094-36-[illegible] [illegible]e KA-6643-B; C-19393-S_2-[illegible] [illegible]olorless solid melting above [illegible] [illegible]ter). uv max (water): 240, 2[illegible] [illegible]80).

[illegible]1860. Carphenazine. [2([illegible] [illegible]nyl)-1-piperazinyl]propyl]-10[illegible] [illegible]10-[3-[4-(2-hydroxyethyl)-1-[illegible] [illegible]henothiazine; 2-propionyl-10[illegible] [illegible]ppyl]phenothiazine; Prok[illegible] [illegible]25.59. C 67.73%, H 7.34%, [illegible] [illegible]rt, Sherlock, N. Sperber, U[illegible] [illegible]low *et al.*, US 3023146 (19[illegible]

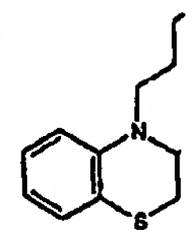

[illegible]maleate. [2975-34-0] [illegible]ates from isopropanol, [illegible] [illegible]ystals from methanol, m[illegible] [illegible]RAP CAT: Antipsycho[illegible] [illegible]ine.

[illegible]1862. Carpipramine. [illegible]benz[b,f]azepin-5-yl)[illegible] [illegible]4-[3-(4-piperidino-4[illegible] [illegible]5H-dibenz[b,f]azepi[illegible] [illegible]3] mol wt 446.63. C[illegible] [illegible]984; Nakanishi, T.[illegible] [illegible]ld *et al.*, US 33296[illegible]

mechanism of action: H. Ito, *Expert Opin. Ther. Targets* 8, 287-294 (2004).

THERAP CAT: Anti-inflammatory.

9494. Tocol. [119-98-2] 3,4-Dihydro-2-methyl-2-(4,8,12-trimethyltridecyl)-2*H*-1-benzopyran-6-ol; 2-methyl-2-(4,8,12-trimethyltridecyl)-6-chromanol; 2-methyl-2-phytyl-6-chromanol; 6-hydroxy-2-methyl-2-phytylchroman; 2-methyl-2-phytyl-6-hydroxychroman. $C_{26}H_{44}O_2$; mol wt 388.63. C 80.35%, H 11.41%, O 8.23%. Synthesis by the condensation of hydroquinone and phytol in the presence of anhydr formic acid: Pendse, Karrer, *Helv. Chim. Acta* 40, 1837 (1957). Antioxidant activity of tocol and its methyl derivs: Olcott, van der Veen, *Lipids* 3, 331 (1968).

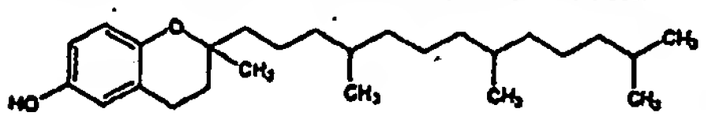

Colorless, viscous oil. $bp_{0.05}$ 165-175°.
Acetate. $C_{28}H_{46}O_3$. Viscous oil. $bp_{0.05}$ 180-185°.
USE: Antioxidant.

9495. α-Tocopherol. [59-02-9] (2*R*)-3,4-Dihydro-2,5,7,8-tetramethyl-2-[(4*R*,8*R*)-4,8,12-trimethyltridecyl]-2*H*-1-benzopyran-6-ol; (+)-2,5,7,8-tetramethyl-2-(4',8',12'-trimethyltridecyl)-6-chromanol; *R,R,R*-α-tocopherol; *d*-α-tocopherol; 5,7,8-trimethyltocol; Optovit; Tocovital. $C_{29}H_{50}O_2$; mol wt 430.71. C 80.87%, H 11.70%, O 7.43%. Most bioactive of the naturally occurring forms of vitamin E, *q.v.* Richest sources are green vegetables, grains, and oils, particularly palm, safflower and sunflower oils. Isoln from wheat germ: H. M. Evans *et al., J. Biol. Chem.* 113, 319 (1936). Structure: E. Fernholz, *J. Am. Chem. Soc.* 59, 1154 (1937); 60, 700 (1938). Synthesis of *dl*-form: P. Karrer *et al., Helv. Chim. Acta* 21, 520, 820 (1938); F. Bergel *et al., J. Chem. Soc.* 1938, 1382. Distillation from vegetable oils and prepn of esters: J. G. Baxter *et al., J. Am. Chem. Soc.* 918 (1943). Prepn of crystalline natural form: C. D. Robeson, *ibid.* 1660; of crystalline acetate: *idem, ibid.* 64, 1487 (1942). Abs config of natural α-tocopherol: H. Mayer *et al., Helv. Chim. Acta* 46, 963 (1963). Stereoselective synthesis: K.-K. Chan *et al., J. Org. Chem.* 43, 3435 (1978). Total synthesis of all 8 stereoisomers: N. Cohen *et al., Helv. Chim. Acta* 64, 1158 (1981). Clinical trial in Alzheimer's disease: M. Sano *et al., N. Engl. J. Med.* 336, 1216 (1997); to improve immune function in healthy elderly: S. N. Meydani *et al., J. Am. Med. Assoc.* 277, 1380 (1997). Review of bioavailability from vitamin E supplements: M. G. Traber, *BioFactors* 10, 115-120 (1999). Review of clinical trials in heart disease: W. A. Pryor, *Free Radical Biol. Med.* 28, 141-164 (2000).

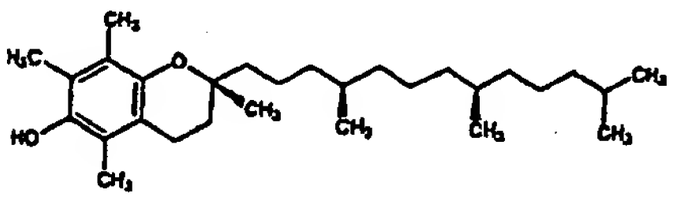

Transparent needles, mp 2.5-3.5°. $[\alpha]_{546.1}^{25}$ −3.0° (benzene); $[\alpha]_{546.1}^{25}$ +0.32° (ethanol).
Acetate. [58-95-7] Spondyvit. $C_{31}H_{52}O_3$; mol wt 472.74. Light yellow oil. Crystallized at −30° as needle-like crystals, mp 26.5-27.5°. $[\alpha]_D^{25}$ +0.25° (c = 10 in chloroform); $[\alpha]_D^{25}$ +3.2° (in ethanol).
Succinate. [4345-03-3] *d*-α-Tocopheryl acid succinate; Tocovite. Needles from pet ether, mp 76-77°. uv max (ethanol): 286 nm ($E_{1cm}^{1\%}$ 38.5). Practically insol in water.
dl-α-Tocopherol. [10191-41-0] *all-rac*-α-Tocopherol. Equimolar mixture of all four racemates. Slightly viscous, pale yellow oil. d^{25} 0.950; $bp_{0.1}$ 200-220°; n_D^{25} 1.5045. uv max: 294 nm ($E_{1cm}^{1\%}$ 71). Practically insol in water. Freely sol in oils, fats, acetone, alcohol, chloroform, ether, other fat solvents. Stable to heat and alkalies in the absence of oxygen. Not affected by acids up to 100°. Slowly oxidized by atm oxygen, rapidly by ferric and silver salts. Gradually darkens on exposure to light.
dl-α-Tocopherol acetate. [52225-20-4] *dl*-α-Tocopheryl acetate; Detulin; Ephynal; Eusovit; Evion. Comprehensive description: B. C. Rudy, B. Z. Senkowski, *Anal. Profiles Drug Subs* 111-126 (1974). Pale yellow, viscous liquid. mp −27.5°; d 0.9533. $bp_{0.01}$ 184°; $bp_{0.015}$ 194°; $bp_{0.3}$ 224°. n_D^{20} 1.4950-1.49 uv max (cyclohexane): 285.5 nm. Practically insol in wa Freely sol in acetone, chloroform, ether. Less readily sol in alc.
USE: As an antioxidant in vegetable oils and shortening.
THERAP CAT: Vitamin E supplement.
THERAP CAT (VET): Vitamin E supplement.

9496. β-Tocopherol. [16698-35-4]; [148-03-8] (*dl*-form (2*R*)-3,4-Dihydro-2,5,8-trimethyl-2-[(4*R*,8*R*)-4,8,12-trimethyldecyl]-2*H*-1-benzopyran-6-ol; (+)-2,5,8-trimethyl-2-(4,8,1 methyltridecyl)-6-chromanol; 5,8-dimethyltocol; cumotocopher neotocopherol; *p*-xylotocopherol. $C_{28}H_{48}O_2$; mol wt 416.68 80.71%, H 11.61%, O 7.68%. One of the naturally occurring fo of vitamin E, *q.v.* Is biologically less active than α-tocopher May be separated by fractional crystn: Emerson *et al., Scie* 83, 421 (1936); *J. Biol. Chem.* 113, 319 (1936); Baxter *et al., J Chem. Soc.* 65, 918 (1943).

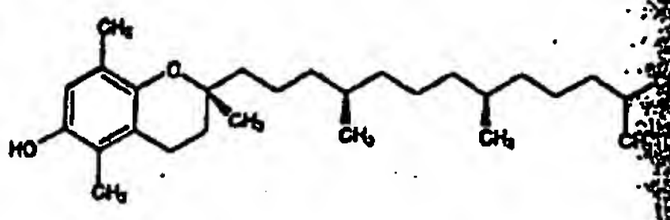

Pale yellow, viscous oil. $bp_{0.1}$ 200-210°. $[\alpha]_{546.1}^{25}$ +2.9° (c in ethanol). uv max: 297 nm ($E_{1cm}^{1\%}$ 87.6). Insol in water. Fr sol in oils, fats, acetone, alcohol, chloroform, ether, other fat vents. Very stable to heat and alkalies. Slowly oxidized by at pheric oxygen, rapidly by ferric and silver salts. Gradually dar on exposure to light.

9497. γ-Tocopherol. [54-28-4]; [7616-22-0] (*dl*-form (2*R*)-3,4-Dihydro-2,7,8-trimethyl-2-[(4*R*,8*R*)-4,8,12-trimethyldecyl]-2*H*-1-benzopyran-6-ol; (+)-2,7,8-trimethyl-2-(4,8,1 methyltridecyl)-6-chromanol; (*R,R,R*)-γ-tocopherol; 7,8-dimeth tocol; α-xylotocopherol. $C_{28}H_{48}O_2$; mol wt 416.68. C 80. H 11.61%, O 7.68%. One of the naturally occurring fo vitamin E, *q.v.* Most abundant tocopherol in soybean a oils. Isoln by fractional crystn: Emerson *et al., Science* (1936); *J. Biol. Chem.* 113, 319 (1936); J. G. Baxter *et al.*, *Chem. Soc.* 65, 918 (1943). Prepn of crystalline natural fo D. Robeson, *J. Am. Chem. Soc.* 65, 1660 (1943). Comp bioactivity with α-tocopherol, *q.v.*: J. G. Bieri, R. P. Evarts, 104, 850 (1974). Protective effects vs reactive nitrogen ox cies: R. V. Cooney *et al., Proc. Natl. Acad. Sci. USA* (1993); S. Christen *et al., ibid.* 94, 3217 (1997). HPLC d serum: A. Sobczak *et al., J. Chromatogr. B* 730, 265 Review of bioavailability, metabolism, and activity: Q. *al., Am. J. Clin. Nutr.* 74, 714-722 (2001).

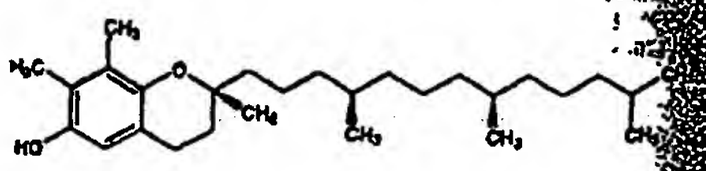

Pale yellow, viscous oil. Has been crystallized as trans needles, mp −3 to −2°. $bp_{0.1}$ 200-210°. $[\alpha]_{546.1}^{25}$ −2.4° (c in benzene); $[\alpha]_{546.1}^{25}$ +2.2° (c = 9.32 in ethanol). uv max: 2 ($E_{1cm}^{1\%}$ 92.8). Insol in water. Freely sol in oils, fats, acetone hol, chloroform, ether, other fat solvents. Very stable to h alkalies. Slowly oxidized by atmospheric oxygen, rapidly b and silver salts. Gradually darkens on exposure to light.

9498. δ-Tocopherol. [119-13-1] (2*R*)-3,4-Dihydr methyl-2-[(4*R*,8*R*)-4,8,12-trimethyltridecyl]-2*H*-1-benzop ol; 8-methyltocol. $C_{27}H_{46}O_2$; mol wt 402.65. C 80. 11.52%, O 7.95%. One of the naturally occurring forms E, *q.v.* Isoln from soybean oil: Stern *et al., J. Am. Chem* 869 (1947). Synthesis: Groen *et al., J. Chem. Soc.* 1959, 3 900085 (1961 to Hoffmann-La Roche).

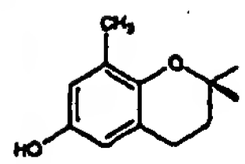

Pale yellow, viscou +1.1° (c = 10.9 in benz

9499. Tocoretin 3,4-dihydro-2,5,7,8-t tridecyl]-2*H*-1-benzop yl-2-[(4*R**,8*R**)-4,8,1 tretinoin tocoferil; Dr non. $C_{49}H_{76}O_3$; mol Wound healing agent fibroblasts. Prepn: H. *idem*, US 3878202 (1 Pharmacology: K. Sai 116, 228223z (1992). 205. *C.A.* 117, 19823 Kawamura *et al., Dig.* tion in skin ulcers: T. *et al., ibid.* 209. Acute 43, 227 (1992). *C.A.* 11

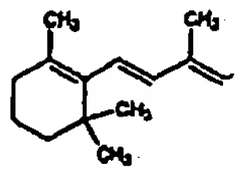

Light yellow oil. u in mice (mg/kg): >100 THERAP CAT: Vulne

9500. α-Tocotrie stereo). (2*R*)-3,4-Dihy trimethyl-3,7,11-tride tetramethyl-2-(4,8,12-t ζ1-tocopherol. $C_{28}H_{44}$ O 7.54%. One of the isoln from wheat bran (1955); Green *et al.*, Green *et al., J. Chem* McHale *et al., ibid.* 19 icochemical Propertie Harris, I. G. Wood, *Vi* of all-*trans*-form: Schu

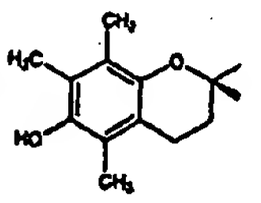

uv max (ethanol): 29

9501. β-Tocotri trimethyl-2-[(3*E*,7*E*)-4, benzopyran-6-ol; 2,5,8 trienyl)chroman-6-ol; 5 wt 410.63. C 81.90%, occurring forms of vit from bran: Eggitt, War Norris, *Ibid.* 6, 689 (19 *J. Chem. Soc.* 1959, 33 *al., J. Chem. Soc.* 1963, *Acta* 46, 2517 (1963).

Consult the Name Index before using this section.

C12

International Journal of Food Science and Technology 2002, 37, 263–269

Formation of sunflower oil emulsions stabilized by whey proteins with high-pressure homogenization (up to 350 MPa): effect of pressure on emulsion characteristics

Anne Desrumaux* & Julie Marcand

Département de Génie des Procédés Alimentaires, ENITIAA GPA, BP82225-44322 Nantes Cedex 03, France

(Received 9 August 2000; Accepted in revised form 6 February 2001)

Summary A new ultra-high-pressure homogenizer was used to make very fine oil in water emulsions. The effect of pressures up to 350 MPa on sunflower oil (20%) in water emulsions was studied. The emulsifier used was whey protein concentrate (1.5%). The properties of the emulsions were characterized by laser light scattering (droplet size distribution) and coaxial cylinders rheometry (rheological behaviour). The protein adsorption fraction was obtained by a spectrophotometric method using bicinchoninic acid reagent.

Significant modifications in the structure and the texture of the emulsions were observed as the pressure increased. No change was revealed by polyacrylamide gel electrophoresis of the whey protein within the pressure range studied. Microdifferential scanning calorimetry scans indicated that the changes of the structural and textural properties may be because of changes in the protein conformation.

Keywords Droplet size, emulsification, microdifferential scanning calorimetry, protein adsorption, viscosity.

Introduction

A large variety of foods are emulsions, from the more natural, e.g. milk, to the more sophisticated, e.g. sausages, mayonnaises. Emulsions are dispersions of liquid droplets in a liquid continuous phase. As the two liquids are immiscible, emulsions are very unstable. In order to stabilize emulsions, there must be surface active molecules at the interface of the droplet to prevent instantaneous coalescence.

Food emulsions are commonly produced in high-pressure homogenizers, in colloid mills or in batch reactors with high-speed blenders. Initially built for the homogenization of milk, high-pressure homogenizers are the most often used, as they give fine emulsions with precise texture properties (creams, ice creams) and higher degrees of stability. The principle of high-pressure homogenization is simple: a coarse emulsion produced with a high-speed blender is forced under pressure through a narrow valve. The combination of the intense shear, cavitation and turbulent flow conditions in this valve leads to the disruption of fat globules (Walstra & Smulders, 1997; McClement, 1999). The decrease of the average size of the fat globules reduces the creaming velocity (Stokes law) and increases the stability of the emulsion. Food homogenizers usually go up to 60 MPa and the gap of the valves is typically between 15 and 300 μm. Increasing the pressure and decreasing the gap size cause a greater degree of breakdown of droplets. Despite the large use of high-pressure homogenizers, few studies deal with the effect of very high pressures on the emulsions properties. Moreover, the studies are limited in the pressure range. According to Mulder & Walstra (1974) and Phipps (1975), the average fat globule diameter (d) decreases with emulsification pressure (P) in a relation $d\alpha P^{-0.6}$, for pressures between 0.25 and 40.5 MPa. Davies (1985) described the breakdown of fat droplets with the Kolmogoroff theory and found a relation between the maximal droplet size

*Correspondent: Fax: +33 251785467;
e-mail: desrumau@enitiaa-nantes.fr

and $P^{0.4}$. According to Tornberg (1980), for pressures over 40 MPa and for a mass oil fraction of 12%, a phenomenon called 'overprocessing' occurs: the average droplet size increases with pressure. Robin *et al.* (1992) processed butter oil in water emulsions, with sodium caseinate as emulsifier, from 7.8 to 76.3 MPa in a microfluidizer. In the microfluidizer, two microsteams were projected under pressure against one another. They showed that the average size of fat globules decreased with pressure and reached a minimum around 60 MPa. Until now, no study has related the effect of 'dynamic' high pressures over 100 MPa on food emulsion formation. The effects of isostatic pressure on emulsions has been studied as a means of preservation. It has been shown that its influence on the already formed emulsions depends on the emulsifiers used (Dumay *et al.*, 1996).

Thus, the purpose of this work was to test the hypothesis that ultra-high-pressure homogenization (from about 50 to 350 MPa) significantly alters properties of oil-in-water emulsions when compared with more traditional pressure treatments.

Material and methods

Ingredients

Whey protein concentrate 'PS85' (85% protein), obtained by ultrafiltration of casein serum, was supplied by Eurial Poitou Touraine (Herbignac, France). The reported composition of this product is: $N \times 6.38$: 85%; fat: 3%; mineral salts: 4%; water content: 4%; pH 6.5 ± 0.2. The proteins are soluble over the complete pH range, and are good emulsifiers at pH < 7.

Sunflower oil was purchased from Lesieur (Neuilly-sur-Seine, France). Distilled water was filtered through a 0.2-μm filter before use. Solutions of whey proteins (1.5%) were prepared using a ultraturrax rotor–stator system (Ika Larbortechnik, Staufen, Germany) and stored at 4 °C.

Ultra-high-pressure homogenizer

Coarse emulsions containing 20%, by mass, of sunflower oil and 80% of the whey protein concentrate aqueous solution were prepared at 4 °C, using an ultraturrax rotor–stator system and then passed through a homogenizer operating from 20 to 350 MPa (Stansted Fluid Power Ltd, Essex, UK). Emulsions were homogenized at different pressures in the range of 50–350 MPa. The homogenizing chamber was cooled with a cooling jacket containing cold water at 5 °C, in order to slow down the rise of temperature. Each emulsion was carefully collected and stored at 4 °C before analysing. This procedure was used to prevent any change in the size distribution of the fat globules because of churning. The experiments were duplicated.

The reproducibility of the high-pressure homogenization was tested by repeating an experimental point (20% oil, 150 MPa) four times.

Light scattering measurements

The size distributions of the oil droplets were determined by the laser light scattering method. The diffractometer model used was the Mastersizer S (Malvern Instruments, Malvern, UK) equipped with a 300 reverse Fourier lens and a He–Ne laser ($\lambda = 633$ nm). The emulsion was measured 5 min after ultra-high-pressure homogenization to cancel any creaming effect, and diluted to about 1/1000 with distilled water in the diffractometer cell, whilst stirring. Size distribution was presented as volume percentage vs. droplet diameter. The volume size distribution was calculated from the intensity of the light diffracted at each angle using Mie theory. The analysis requires a parameter known as the presentation value, a combination of the ratio of the relative refractive indices of the dispersed phase and water and the absorbance of the dispersed phase. The 3NAD presentation was used: oil (1.4564, 0.0000) in water (1.33), for which the absorbance value was selected after consultation with Malvern Instruments and verified using a carefully diluted emulsion of known concentration. The full size distribution was obtained using a polydisperse analysis, which allowed the calculation of the mean droplet diameter d_{32} (Sauter mean diameter) and a dispersion index called 'span', defined as

$$\text{span} = \frac{d[90] - d[10]}{d[50]}$$

where $d[x]$ is the average droplet size in a volume in which $[x]$% of the total sample weight remains constant. Measurements were repeated three times for each sample.

Rheology measurements

Dynamic shear stress measurements were done at 20 °C with an AR 1000 Rheometer (TA Instruments, Waters Corporation, USA), equipped with a coaxial system (medium concentric cylinder with a conical end; R1 = 13.83 mm, R2 = 15.0 mm). Flow curves (shear stress vs. shear rate) were determined at increasing shear rates: 0–1200 s^{-1} in 2 min (up and down flow curves).

Protein surface concentration

Emulsion samples were centrifuged at 13 000 *g* for 30 min to separate the droplets from the aqueous serum phase. The supernatant (the cream) was carefully removed from the aqueous phase using a syringe. The cream layer was resuspended in ultrapure water to wash away any protein trapped between droplets, and the resulting emulsion was centrifuged again at 13 000 *g* for 30 min. The protein concentration of the two serums was determined by the Sigma Pierce spectrophotometric method using bicinchoninic acid reagent (BCA, Sigma procedure TPRO-562). This spectrophotometric method is based on the reduction of Cu^{2+} to Cu^{+} by the proteins (Biuret reaction). Cu^{+} reacts with the BCA and an intense purple complex is formed. This complex produces an absorbance maximum at 562 nm, which is directly proportional to the protein concentration (Smith *et al.*, 1985). A calibration curve was generated using bovine serum albumin (BSA) standard solution (Sigma, St Louis, USA), with a determination coefficient $r^2 = 0.99$ (15 different concentrations used). The quantity of whey proteins absorbed was expressed in equivalent BSA and was calculated from the difference in the serum concentration prior to and after emulsification. The surface concentration of the absorbed protein was calculated from the known surface area per unit volume of emulsion and the difference in the amount of protein measured in the serum phase and the amount used to make the original emulsion, making allowance for any dilution.

Electrophoresis (SDS-PAGE)

The protein fractions were determined by sodium dodecyl sulphate-polyacrylamide gel electrophoresis (SDS-PAGE), following the procedure described by Arrese *et al.* (1991). Gel slabs were fixed and stained simultaneously in aqueous solution containing 40% v/v ethanol, 7% v/v acetic acid and 0.025% coomassie brilliant blue R250. Proteins were denaturated with a treatment buffer containing 0.125 M Tris, 4% SDS v/v Glycerol, 0.2 M dithiotreitol, 0.02% bromophenol blue. About 50 µg of protein was applied to each gel slot. Molecular weights of the protein bands were estimated by means of the SDS-70L kit (Sigma Chemical Co., St Louis, USA).

Microdifferential scanning calorimetry

Microdifferential scanning calorimetry (µDSC) was used to assess the degree of denaturation of the whey protein by the pressure of homogenization. µDSC thermographs of aqueous solutions of whey proteins before and after a single run in the homogenizer were prepared by using a Setaram 3 calorimeter (Calluire, France). Samples (700 mg) of 2% dispersions of whey proteins (pH 6.7) in distilled water were hermetically sealed in hastelloy C276 pans (volume = 1 cm^3). A closed pan filled with distilled water was used as the reference. The heating rate was fixed at 0.5 °C min^{-1} from 20 to 110 °C. Triplicate samples were analysed by µDSC.

Results and discussion

Whey protein composition

Electrophoresis measurements indicated that the whey proteins were mainly composed of β-lactoglobulin (18 600 Da), α-lactalbumin (14 200 Da), and serum albumin (66 000 Da) (Fig. 1). Examination of the µDSC curves showed three endothermic phenomena (Fig. 2): the first around 40–45 °C, the second between 60 and 65 °C and the third between 70 and 75 °C. These endothermic phenomena in whey proteins are explained by the behaviour of β-lactoglobulin and α-lactalbumin, which are the predominant proteins (Paulsson *et al.*, 1985). The dimer form of β-lactoglobulin exits at 5.2 < pH < 7.5 as in our case (pH 6.7). Thus, according to McKenzie (1971) the first endothermic peak could be a dissociation of the dimers of β-lactoglobulin. The

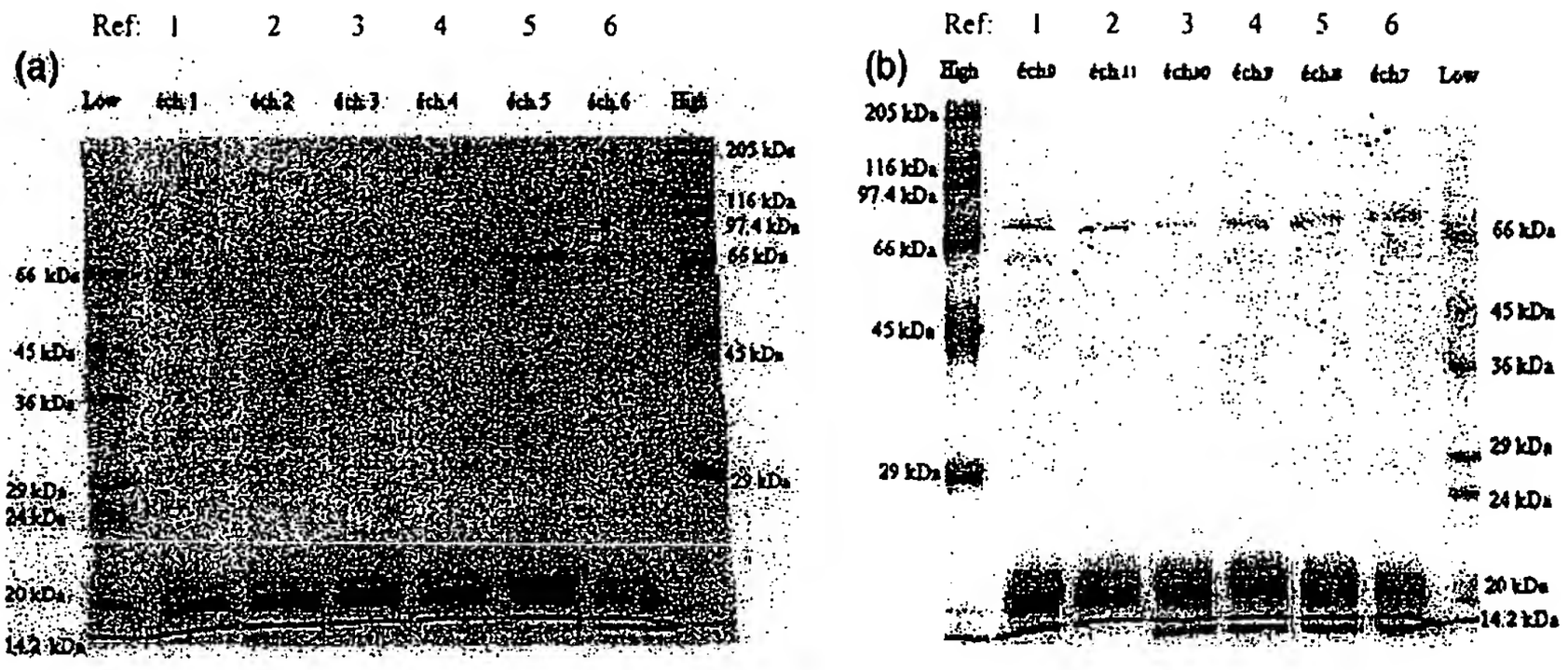

Figure 1 (a) SDS-PAGE of proteins before and after a single run in the homogenizer. Ref: α-lactalbumin (14.2 kDa), tripsin (20 kDa), egg albumin (45 kDa), serum albumin (66 kDa). Column 1: before homogenization. Columns 2–6: after a single run in the homogenizer at 2: 30 MPa; 3: 60 MPa; 4: 90 MPa; 5: 120 MPa; 6: 150 MPa. (b) SDS-PAGE of protein after one run in the homogenizer. Ref: see (a). Column 1: 180 MPa; 2: 210 MPa; 3: 240 MPa; 4: 270 MPa; 5: 300 MPa; 6: 350 MPa.

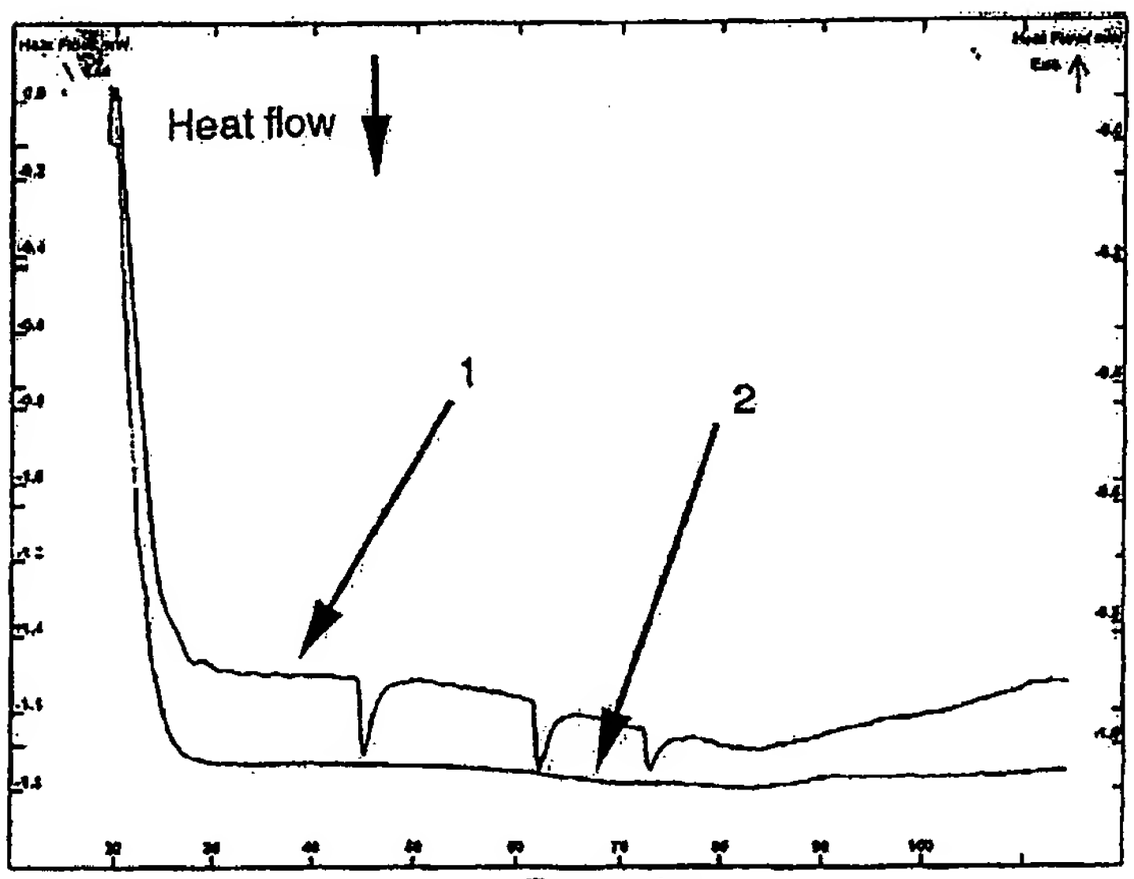

Figure 2 Micro-DSC graph of whey protein aqueous solutions (1.5%) before (1) and after (2) treatment at 300 MPa in the high-pressure homogenizer.

second endothermic peak at 60–65 °C corresponds at pH around 7 to the denaturation of the α-lactalbumin, and the last endothermic peak around 70–75 °C corresponds to the denaturation of the β-lactoglobulin.

Reproducibility of the experiments

The reproducibility of the high-pressure homogenization after testing with an experimental point (20% oil, 150 MPa) and repeated four times on four different days is shown in Table 1. According to the s.d. obtained, the reproducibility was satisfactory.

Evolution of temperature during the experiments

Despite the use of the cooling jacket, the temperature of the emulsion at the exit of the valve increased linearly with the pressure in the valve

Table 1 Reproducibility of the point 150 MPa, 20% oil

Temperature at the exit of the homogenizer	Sauter diameter d_{32} (μm)	Size dispersion coefficient	Viscosity (Pa s)	Fraction of adsorbed proteins (mg m^{-2})
40 °C (1)	0.68 (0.02)	3.75 (0.6)	0.009 (0.001)	0.77 (0.1)

Values within parentheses are standard deviations.

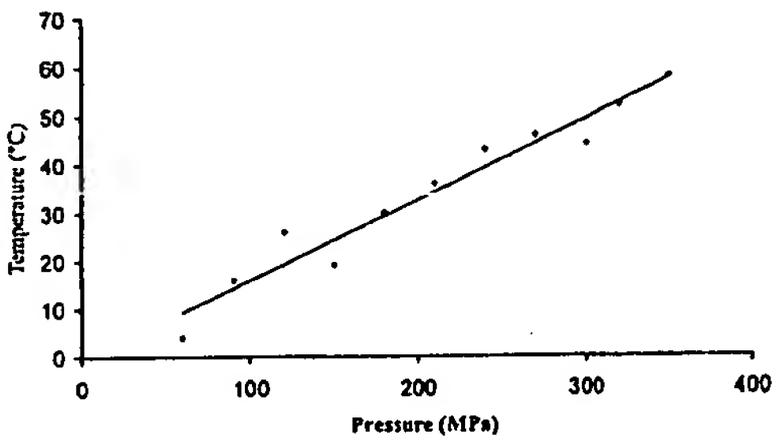

Figure 3 Effect of pressure on the temperature at the exit of the homogenizer.

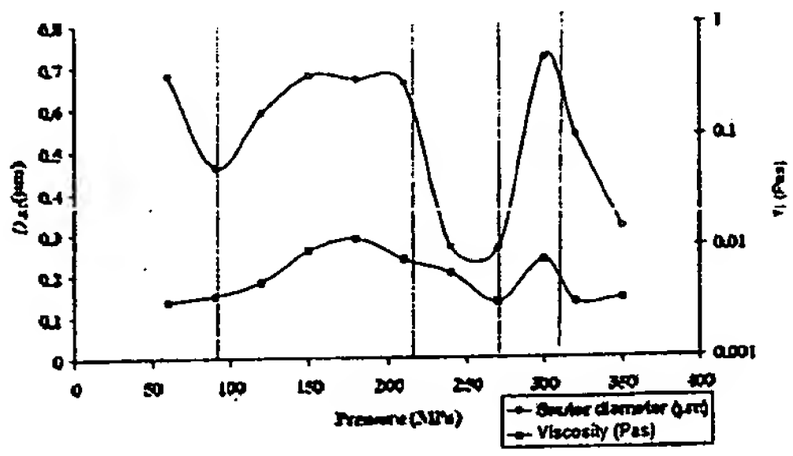

Figure 4 Effect of the pressure of homogenization on the Sauter diameter d_{32} and the viscosity η of the emulsions.

(Fig. 3). Above 300 MPa, the temperature of the emulsion at the exit is close to the temperatures of the peaks observed by μDSC.

Effect of high pressure on emulsion properties

The Sauter diameter before homogenization was around 30 μm. Homogenization reduced the Sauter diameter appreciably, the reduction increasing with treatment pressure from 50 to 90 MPa (Fig. 4). This result agrees with the study of Robin *et al.* (1992), who observed a decrease in the droplet average size between 7.8 and 76.3 MPa. Above 90 MPa, d_{32} increased with pressure (Fig. 4) and then stabilized approaching 200 MPa. Robin *et al.* (1992) observed a similar plateau of the droplet size diameter, but between 60 and 76.3 MPa. This phenomenon can be referred to as 'overprocessing,' as stated by Tornberg (1980): the average droplet size is stable over a certain range of pressure, and increases at higher pressures. The density of energy (up to 10^{12} W m^{-3}) is estimated by knowing the flow rate and the pressure drop inside the valve, and is partially dissipated as heat (Fig. 3), which can lead to an increase of the Sauter diameter: the Brownian motion increases and so also the probability of collision and coalescence.

Above 200 MPa, d_{32} decreased and then increased again at around 250 MPa. However, there was a final decrease of d_{32} above about 300 MPa. This final decrease could be explained by the increased probability of rupture. At this level of pressure, the shear rate inside the valve is enormous, the probability of rupture again becomes higher than the probability of coalescence and d_{32} decreases.

The effects of high-pressure homogenization on the sizes dispersion coefficient are interesting: above 90 MPa, as the pressure increased, the dispersion coefficient strongly decreased (sevenfold) (Fig. 5). Also, the droplet size distribution was bimodal for the lower pressures, but at higher

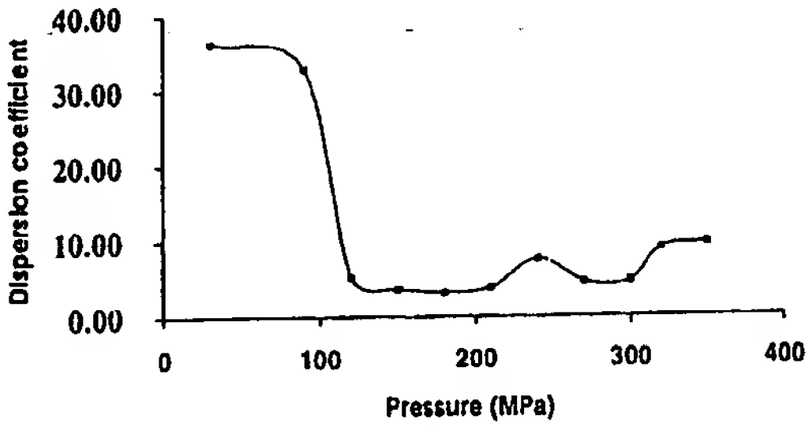

Figure 5 Effect of pressure of homogenization on the size dispersion coefficient of the droplet.

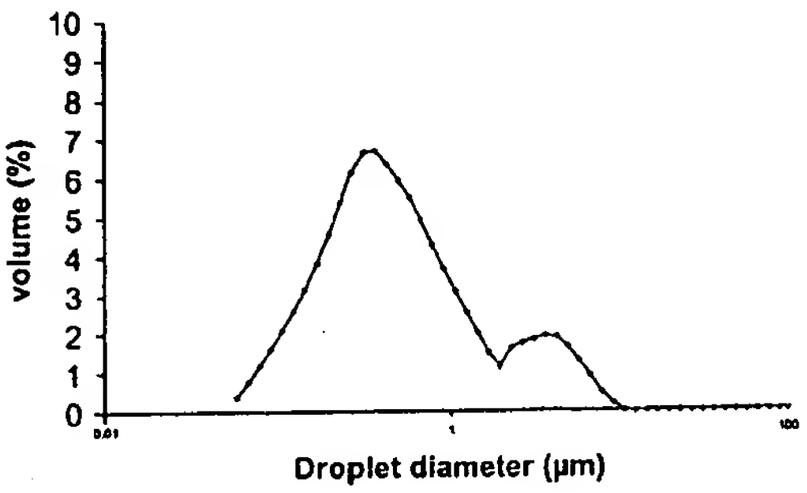

Figure 6 Size distribution of the oil droplet of the emulsion after a single run in the homogenizer at 300 MPa.

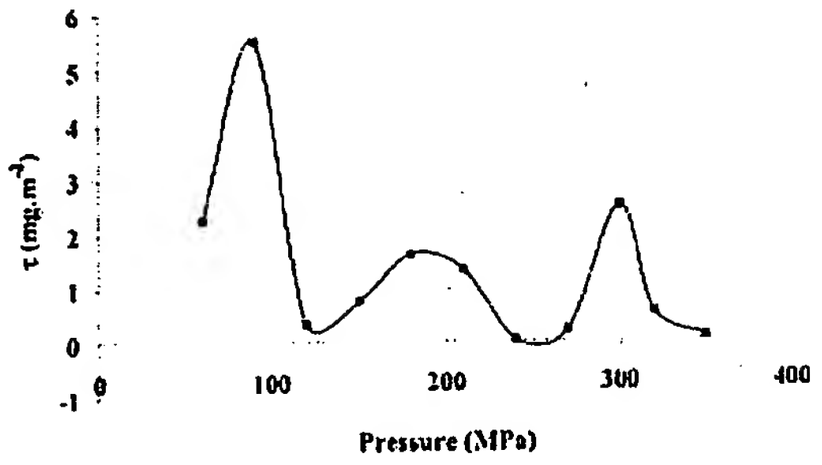

Figure 7 Effect of pressure of homogenization on the fraction of absorbed proteins.

pressures the second peak decreased (Fig. 6). Thus, the coalescence rate of the droplets is reduced because a large dispersion favours rapid coalescence. Above 90 MPa, the main effect of high-pressure homogenization on the size properties is the decrease in the dispersion coefficient of size.

Examination of the rheological properties of the emulsions showed a Newtonian behaviour in all cases, agreeing with previous studies (Desrumaux & Della Valle, 1999). However, the viscosity changed with the pressure in the valve (Fig. 4).

It is interesting to see the similarity of behaviour between the curves for the viscosity η and the Sauter diameter d_{32} (Fig. 4). Both show a complicated behaviour, with four zones, although differences exist in the limits of the zones. In the first zone, up to 90–100 MPa, the Sauter diameter decreased and viscosity increased slowly (Fig. 4). At the same time, the amount of adsorbed protein increased (Fig. 7), as expected, since, as the average droplet size decreases, the specific area increases, which leads to an increase of the fraction of adsorbed proteins. Above 100 and up to ≈210 MPa, d_{32} increased and reached a plateau (Fig. 4), which can be attributed to the 'overprocessing' phenomenon. Simultaneously, the fraction of adsorbed proteins decreased strongly and then increased (Fig. 7). Viscosity followed the same behaviour as d_{32} (Fig. 4). Above 200–210 MPa the behaviour of the structural and textural properties was complicated and, is probably explained, by the effect of the high pressure on the protein conformation. Indeed, studies on isostatic high-pressure treatment of proteins have shown that pressure has a huge effect on food protein functionality (Messens *et al.*, 1997). High-pressure effects on proteins are primarily related to the rupture of noncovalent interactions within protein molecules and to the subsequent re-formation of intra- and intermolecular bonds within or between protein molecules (Smith *et al.*, 2000). As extensively described by Messens *et al.* (1997), the whey proteins, particularly the β-lactoglobulin, are far more sensitive to isostatic pressure than other proteins such as BSA. In our case the treatment at high pressure was very short, estimated at 10^{-4} s from the flow rate and the size of the gap (≈1 µm), but was associated with a significant rise in temperature (Fig. 3). The complicated effects of pressure on emulsions properties could be explained by a change of conformation of the emulsifying whey proteins during the emulsification process. Only a small part of the whey protein is likely to be absorbed at the water/oil interface in the coarse emulsion, because the kinetics of absorption requires a much longer time than that for emulsification. Thus, a large part of the whey protein was in the aqueous phase during the homogenization and the absorption of the whey protein at the interface occurred after homogenization. In order to understand the possible change of the whey protein, we tested aqueous whey protein solutions (1.5%) before and after a single run in the homogenizer at 300 MPa (Fig. 2). Comparing the µDSC graph with the µDSC graph obtained before treatment in the high-pressure homogenizer (Fig. 2), it can be seen that the endothermic peaks disappeared, indicating that the proteins had probably denatured. This phenomenon is because of the combined

effects of the high shear rate inside the gap (velocity at 300 MPa estimated at 500 m s^{-1}) and the rise of temperature observed. At such a high pressure, it was impossible to slow down the rise of temperature inside the valve, the temperature at the exit being directly proportional to the pressure of homogenization. Electrophoresis measurements of extracted proteins after treatment in the high-pressure homogenizer did not show any significant change in the molecular weights (Fig. 1b): the proteins were not broken down into smaller entities during the homogenization, the time of treatment (estimated at 10^{-4} s) probably being too short.

Over 200–210 MPa, the proteins were denatured and had probably partially lost their emulsifying activity (Fig. 4). The effect of the high-pressure homogenization could be protein aggregation; however, the electrophoresis experiments in the presence of SDS prevents observation of protein aggregation.

Conclusions

The effects of high-pressure homogenization on oil in water emulsions are complicated. From 20 to 100 MPa, the Sauter diameter decreased, confirming the results of Davies (1985) and Robin *et al.* (1992). Over 100 MPa, d_{32}, viscosity and the fraction of adsorbed protein displayed up to four zones of behaviour: from 100 to 210 MPa, the Sauter diameter and viscosity increased up to a maximum. This behaviour could be because of the 'overprocessing' phenomenon. Over 210 MPa, μDSC graphs on whey proteins before and after a single run at 300 MPa in the homogenizer confirmed changes in protein conformation, probably because of the combined effects of high-pressure treatment and the rise in temperature observed. This change in the conformation of proteins probably modifies the emulsifying properties of the whey proteins. There is a strong correlation between the formulation of emulsion and the range of pressure used in homogenization. For sunflower oil in water emulsion (20% oil) stabilized with whey proteins, the optimum pressure of homogenization according to the light scattering measurements is ≈100 MPa. At this pressure the d_{32} and the size dispersion coefficient reach a minimum.

Acknowledgments

The authors wish to thank Pierre Cantoni for his technical assistance.

References

Arrese, E.L., Sorgentini, D.A., Wagner, J.R. & Anon, M.C. (1991). Electrophoretic, solubility, and functional properties of commercial soy protein isolate. *Journal of Agricultural Food Chemistry*, 39, 1029–1032.

Davies, J.T. (1985). Drop sizes of emulsions related to turbulent energy dissipation rates. *Chemical Engineering Science*, 40, 839–842.

Desrumaux, A. & Della Valle, D. (1999). Rhéologie d'émulsions huile dans eau: influence du procédé. *Les Cahiers de Rhéologie*, 16, 358–363.

Dumay, E., Lambert, C., Funtenberger, S. & Cheftel, J.C. (1996). Effects of high pressures on the physicochemical characteristics of dairy creams and model oil in water emulsions. *Lebensmittelwissenchaft und Technologie*, 29, 606–625.

McClement, D.J. (1999). *Food Emulsions: Principles, Practice and Techniques*. Pp. 161–183, Boca Raton, FL: CRC Press.

McKenzie, H.A. (1971). β-Lactoglobulins. In: *Milk Proteins 2*. Pp. 257–330. New York: Academic Press.

Messens, W., Van Camp, J. & Huyghebaert, A. (1997). The use of high pressure to modify the functionality of food proteins. *Trends in Food Science and Technology*, 8, 107–112.

Mulder, H. & Walstra, P. (1974). *The Milk Fat Globule, Emulsion Science as Applied to Milk Products and Comparable Foods*. Pp. 163–192, UK: CABI.

Paulsson, M., Hegg, P.O. & Castberg, H.B. (1985). Thermal stability of whey proteins studied by differential scanning calorimetry. *Thermochemica Acta*, 95, 435–440.

Phipps, L.W. (1975). The fragmentation of oil drops in emulsions by a high-pressure homogenizer. *Journal of Physics D: Applied Physics*, 8, 448–462.

Robin, O., Blanchot, V., Vuillemard, J.C. & Paquin, P. (1992). Microfluidization of dairy model emulsions. I. Preparation of emulsions and influence of processing on the size distribution of milk fat globules. *Lait*, 72, 511–550.

Smith, P.K., Krohn, R.I., Hermanson, G.T. & Mallia, A.K. (1985). Measurement of protein using bicinchoninic acid. *Analytical Biochemistry*, 150, 76–85.

Smith, D., Galazka, V.B., Wellner, N. & Sumner, I.G. (2000). High pressure unfolding of ovalbumin. *International Journal of Food Science and Technology*, 35, 361–371.

Tornberg, E. (1980). Functional characteristics of protein stabilized emulsions: emulsifying behavior of proteins in a sonifier. *Journal of Food Science.*, 45, 1662–1668.

Walstra, P. & Smulders, P. (1997). Formation of emulsions. In: *Proceedings of the Second World Congress on Emulsion*, Vol 1. Paris: Lavoisier Press.